

Carbon dioxide release from disturbed wetland soils of the Mpumalanga Highveld

by

GARTH VAN ROOYEN

**Submitted in fulfilment of the requirements for the degree
M.Sc. Soil Science**

**In the Department of Plant Production and Soil Science
University of Pretoria**

**Supervisor: Mr. P.C. de Jager
Co-Supervisor: Steve Mitchell**

2018

DECLARATION

I, Garth van Rooyen declare that the dissertation, which I hereby submit for the degree MSc. Soil Science at the University of Pretoria, is my own work and has not previously been submitted by me for a degree at this or any other tertiary institution.

Signature:  _____ Date: ____ December-2018 _____

ABSTRACT

The release of carbon dioxide from wetland soils is a phenomenon which involves several biochemical processes and environmental conditions. Heterotrophic respiration through the metabolisation of organic material by heterotrophic organisms is one such process. The oxidation of methane to carbon dioxide is another important source of carbon dioxide. The oxidation of methane transforms methane into carbon dioxide, joining the oxidation of carbon with the reduction (electron acceptor) of sulphate and/or nitrate.

Acid Mine Drainage (AMD) is an increasing threat to environmental resources in South Africa. AMD originates from sulfide bearing minerals such as pyrite (FeS_2) being exposed and reacting with oxygen-bearing water to produce an acidic medium which is increasingly entering natural watercourses such as wetlands. The addition of an acidic solution into wetlands causes, amongst others, a change in pH, change in Electrical Conductivity (EC) as well as a change in redox chemistry. AMD can also cause a change in salinity within wetlands. The salinity that is generated during AMD neutralisation can be the greater long-term problem. The study aims to develop a field method of measuring carbon dioxide emissions from wetlands in the field, as well as to investigate the influence of AMD on the carbon dioxide release of wetland soils, focusing on the low organic carbon soils and high organic carbon wetland soils.

The field studies were conducted on three wetland study sites, in which field measurements were taken for pH, Electrical Conductivity (EC), redox potential and CO_2 emissions. For each study site, soil classification was done to delineate the different wetland zones. The results indicated that in a low carbon mineral wetland, the permanent zone contained the highest carbon dioxide emission measurements, where the outer terrestrial zone contained the lowest measurements. In the high carbon organic wetland, low carbon dioxide emissions were measured in the permanent zone. The depletion of oxygen due to prolonged saturation and stagnation, results in low oxygen levels which are not enough to sustain respiration of organic matter. The

organic wetland is storing its carbon rather than releasing its carbon, thus resulting in an organic wetland.

The introduction of synthetic AMD into wetland soils resulted in a short term, rapid increase in the amount of carbon dioxide released. Changes in the soil before and after the addition of AMD were highly significant with respect to pH, EC, CO₂ increase and redox potential for both the organic and mineral soil. Upon the addition of AMD, the organic soil increased its original CO₂ emissions by 385.6%, with the mineral soil increasing by 5.28%. The “Birch Effect” was proven to be relevant in saturated soils, rather than only in unsaturated soils. This proves that soils with high levels of organic matter and thus a high carbon percentage, pose a greater risk to increased carbon dioxide emissions upon the addition of AMD. These high carbon percentage soils are particularly common in wetland systems, most notably in the permanent zone of the wetland.

The introduction of AMD into wetlands has been proved to enhance the “source” component, disrupting the carbon balance and at the same time enhancing atmospheric CO₂ concentrations. The results confirmed that AMD contamination to wetlands does not only affect the system directly, but also the larger environment as the carbon stock of the wetland will ultimately decrease, and transfer to another system.

TABLE OF CONTENTS

CHAPTER ONE: Introduction and literature review	1
1. Introduction	1
1.1 Wetlands	2
1.2 Carbon in wetlands	3
1.3 Redox potential	5
1.4 Wetland methane production	8
1.5 Wetland carbon dioxide production	10
1.6 Measurement of carbon dioxide emissions	12
1.7. Acid mine drainage from Mpumalanga Highveld coal mines	15
1.7.1 Coal producing regions	15
1.7.2 Acid mine drainage	16
1.7.3 Lime-treated acid mine drainage for agricultural use	18
CHAPTER TWO: Carbon dioxide emissions in mine affected environments	20
2. Introduction	20
2.1 Field method of measuring carbon dioxide emissions	21
2.2 Carbon dioxide emissions from the Rietvlei wetland	24
2.3 Mpumalanga Highveld wetlands: study area and location	28
2.3.1 Geology	31
2.4 Field study	34
2.5 Wetland A field study	35
2.5.1 Soil classification	36
2.5.2 Carbon dioxide emissions for Wetland A	38
2.5.3 Spatial pH, EC and redox potential distribution for Wetland A	41

2.6	Wetland B field study.....	44
2.6.1	Carbon dioxide emissions for Wetland B	46
2.6.2	Spatial distribution of pH, EC and redox potential for Wetland B	50
2.7	Wetland C field study.....	53
2.7.1	Carbon dioxide emissions for Wetland C	56
2.7.2	Spatial distribution of pH, EC and redox potential data	57
2.8	Statistical analysis	61
2.8.1	Redox potential vs. pH	62
2.8.2	Measured CO ₂ vs Electrical Conductivity	63
2.8.3	Measured CO ₂ vs redox potential	65
2.8.4	Measured CO ₂ vs pH	66
CHAPTER THREE: Initial response of organic and mineral soils to acid mine drainage (AMD).....		70
3.1	Introduction.....	70
3.2	Synthetic acid mine drainage	71
3.3	Column experiments.....	72
3.3.1	Methods and materials	73
3.4	Results	76
3.4.1	Organic soil	76
3.4.2	Mineral soil.....	80
3.5	Chemical data analysis and carbon mass	82
3.5.1	Carbon mass balances	88
3.6	Significance of results	89
CHAPTER FOUR: Synthesis		92



REFERENCES.....	94
APPENDIX.....	104

LIST OF FIGURES

Figure 1.1: Carbon cycle (Kayranli <i>et al</i> 2010)	3
Figure 1.2: Nernst equation (Reddy <i>et al</i> 2000)	6
Figure 1.3: Methanogenic bacteria products (Jardine <i>et al</i> 2002)	10
Figure 1.4: Major transformations of the carbon cycle (Vepraskas 2016)	11
Figure 1.5: Photosynthesis reaction	11
Figure 1.6: NDIR principle (Seitz and Tong 2013).....	13
Figure 1.7: Gas chamber in the field (Sattazahn 2012).....	14
Figure 1.8: Ideal Gas Law for conversion of volumetric to mass (Collier <i>et al</i> 2014).....	14
Figure 1.9: General procedure: a) static gas chambers. b) gas extraction by syringe. c) transfer of gas from syringe to collection vial. d) labeling of vials. e) gas chromatography (adapted from Arias-Navarro <i>et al</i> 2013).....	15
Figure 1.10: Location of the coal producing regions of eastern South Africa (McCarthy and Pretorius 2009).....	16
Figure 2.1 Satellite imagery from 2004 and the latest satellite imagery from 2016	22
Figure 2.2 Soil forms and wetland zones	23
Figure 2.3 NDIR carbon dioxide sensor field experiment setup	25
Figure 2.4 Interpolated carbon dioxide emissions for the Rietvlei wetland.....	27
Figure 2.5 Locality map.....	29
Figure 2.6 Detailed locality map	31
Figure 2.7 Geology map (Council for Geoscience 2017).....	32
Figure 2.8 Hydrology of study area	33
Figure 2.9 Wetland A sample points.....	36
Figure 2.10: Delineation and Soil map for Wetland A.....	37
Figure 2.11 Carbon dioxide emissions for Wetland A	39

Figure 2.12: Wetland A spatial pH distribution	41
Figure 2.13 Wetland A spatial EC distribution	42
Figure 2.14 Wetland A spatial redox potential distribution.....	43
Figure 2.15 Wetland B soil forms	45
Figure 2.16 Carbon dioxide emissions for Wetland B	47
Figure 2.17 Carbon storage and organic matter accumulation after wetland restoration (Moreno-Mateos <i>et al</i> 2012) The 'zero value' dashed line represents reference wetlands.....	49
Figure 2.18 Wetland B spatial distribution of pH data	51
Figure 2.19 Wetland B spatial distribution of EC data	52
Figure 2.20 Wetland B spatial distribution of redox potential data.....	53
Figure 2.22 O horizon sample at 400 mm depth	55
Figure 2.23 Carbon dioxide emissions for Wetland C	56
Figure 2.24 Wetland C spatial distribution of pH data	58
Figure 2.25 Wetland C spatial distribution of EC data	59
Figure 2.26 Wetland C spatial distribution of redox potential data	60
Figure 2.27 a) Redox potential vs pH for Wetland A. b) Redox potential vs pH for Wetland B. c) Redox potential vs pH for Wetland C.....	62
Figure 2.28 a) CO ₂ vs Electrical Conductivity for Wetland A. b) CO ₂ vs Electrical Conductivity for Wetland B. c) CO ₂ vs Electrical Conductivity for Wetland C	63
Figure 2.29 a) CO ₂ vs Redox potential for Wetland A. b) CO ₂ vs Redox potential for Wetland B. c) CO ₂ vs Redox potential for Wetland C.....	65
Figure 2.30 a) CO ₂ vs pH for Wetland A. b) CO ₂ vs pH for Wetland B. c) CO ₂ vs pH for Wetland C	66
Figure 3.1 Directly affected watercourses (NFEPA).....	75

Figure 3.2 Soil column experiment setup 76

Figure 3.3 Carbon dioxide release in response to AMD for peat 77

Figure 3.4 Second order reaction ($1/\text{CO}_2$ vs time) for organic soil 79

Figure 3.5 Carbon dioxide release in response to AMD for mineral soil 80

Figure 3.6 Second order reaction ($1/\text{CO}_2$ vs time) for mineral soils 81

Figure 3.7: Second order reaction ($1/\text{CO}_2$ vs time) for saturated CaCO_3 87

Figure 3.8: High risk areas susceptible to acid mine drainage effects in the greater Emalahleni area 87

LIST OF TABLES

Table 2.1 Correlation coefficients.....	67
Table 2.2 Mean CO ₂ release by soil form (descending order).....	69
Table 3.1 Synthetic AMD ion concentrations.....	72
Table 3.2 Soil physical properties	72
Table 3.3 Variables for experiment.....	73
Table 3.4 Average coefficient of determination (R ²) test for each reaction order	78
Table 3.5 Second order average values for organic soil.....	79
Table 3.6 Average coefficient of determination (R ²) test for each reaction order	80
Table 3.7 Second order average values for mineral soil	81
Table 3.8 Average data for organic/mineral soils before and after addition of AMD.....	82
Table 3.9 Significance of differences (p-values).....	82
Table 3.10 ICP results for the major ions for the organic and mineral soil.	85
Table 3.11 Statistical inference of concentration changes of major ions	85
Table 3.12 CaCO ₃ reaction	87
Table 3.13 Average carbon mass before and after AMD	89

CHAPTER ONE: Introduction and literature review

1. Introduction

Acid Mine Drainage (AMD) and wetlands have been the centre of many research topics. Large emphasis has been placed on the conservation of wetlands and as such, organisations such as Working For Wetlands, WWF Mondi Wetlands Programme and Ramsar have been established in order to assist in the conservation of wetlands. AMD on the other hand, is an acidic, often also saline solution originating from mining activities which are increasingly threatening our natural watercourses. The link between AMD and natural watercourses is therefore highly relevant, and one which involves many different chemical and physical processes. The Mpumalanga Highveld contains a high abundance of wetlands which are located in a predominantly coal mining environment. A high probability exists that wetlands in this area are recipients of AMD discharge, or are at risk of receiving AMD in the future.

The hypothesis for this study is that the introduction of AMD into wetland soils will increase the amount of carbon dioxide released: Chapter one will focus on the literature of wetlands, methane and carbon dioxide production, as well as the origin of AMD. Chapter two investigates the carbon dioxide (CO₂) release of several wetlands surrounded by coal mining activities in the Mpumalanga Highveld, as well as a control site not directly affected by coal mining. The purpose (aim) of the approach of Chapter two was to investigate field-scale correlations between carbon emission and basic soil properties. Chapter three was aimed to investigate the response of Wetlands soils to AMD and to establish direct causality, between CO₂ emission and changes in various chemical properties. Chapter three investigates the effect of AMD on the carbon dioxide release of an organic soil (>10% organic carbon) and a mineral (low organic carbon) soil. Chapter three involves controlled laboratory experiments isolating certain variables in order to monitor the effects of AMD on the release of carbon dioxide.

1.1 Wetlands

Wetlands are areas of saturated soil and can include a wide variety of natural features such as lakes, rivers, floodplains and marshes. Wetlands occupy a small portion of the Earth's surface, anywhere from 2% to 6% depending on the definition of wetlands (Schlesinger 1991).

Definitions of wetlands vary greatly, although the accepted global definition is that from the Ramsar Convention. The Ramsar Convention is a worldwide intergovernmental treaty that focuses on the global conservation of wetlands. The definition of a wetland from the Ramsar Convention is as follows:

“Areas of marsh, fen, peatland or water, whether natural or artificial, permanent or temporary, with water that is static or flowing, fresh, brackish or salt, including areas of marine water to the depth of which at low tide does not exceed six metres.”-Ramsar Convention definition (Ramsar 1993).

In South Africa the definition of a wetland is as follows, as defined by the National Water Act:

“Land which is transitional between terrestrial and aquatic systems where the water table is usually at or near the surface, or the land is periodically covered with shallow water, and which land in normal circumstances supports or would support vegetation typically adapted to life in saturated soil.”- National Water Act of South Africa (DWAF 2005).

Wetlands provide a huge economic worth that makes significant contributions to national economies. According to the scientific journal *Nature* (1997 vol. 387, p. 253) wetlands are worth 14 trillion US dollars per year (DWAF 2005). Wetlands control the runoff of water, and act like large sponges. It is estimated that by the year 2030, the available water in South Africa will reach critical levels (DWAF 2005) and wetlands will become very valuable commodities. With that being said, wetlands will degrade as water levels decrease. Wetlands will tend to retract as water levels become less and less available. Wetlands store water and contribute to the groundwater recharge and

can therefore release water during dry periods, making it economically valuable in that sense. Wetlands can control water movement during periods of floods and can also remove dangerous pollutants from the greater area. One of the most important functions of wetlands is water purification as well as that they are rich in biodiversity and provide habitats for fauna and flora.

The global knowledge of wetlands has grown immensely over time, and our understanding of wetland characteristics as of now can still be greatly improved (Kotze *et al* 1996).

1.2 Carbon in wetlands

Although wetlands only cover a small portion of the Earth’s land surface, they contain a substantial amount of the carbon present on the planet (Amthor *et al* 1998). Of all the Earth’s terrestrial ecosystems, wetlands have the highest carbon density (Scholz 2011). The accumulation or turnover of carbon in wetlands can be explained by the carbon cycle (Fig 1.1).

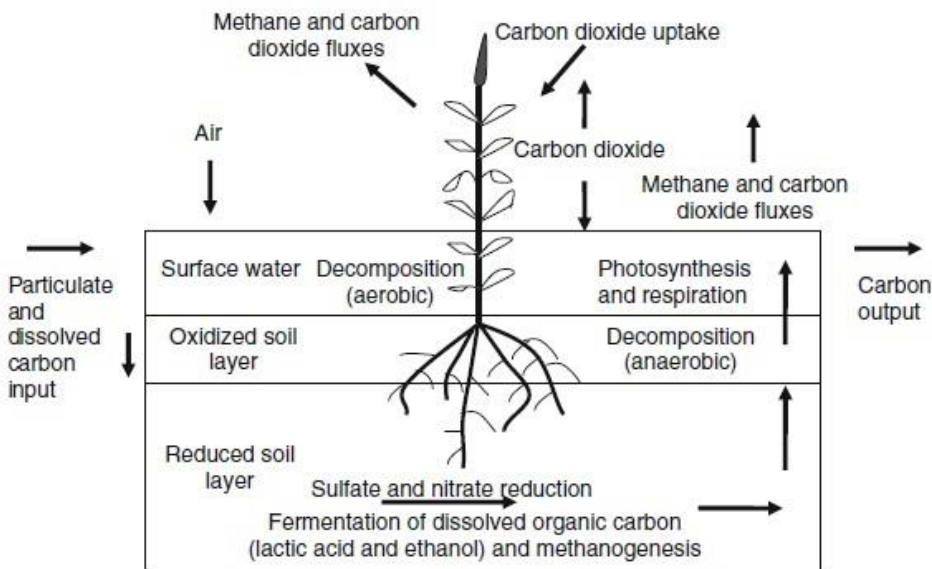


Figure 1.1: Carbon cycle (Kayranli *et al* 2010)

There are numerous reactions within wetlands that involve carbon, such as redox and non-redox (organic compounds) reactions. Some important processes are listed (Kayranli *et al* 2010):

- Respiration in the aerobic zone
- Fermentation
- Methanogenesis
- Ferric iron, sulphate and nitrate reduction in the anaerobic zone

Microbial activity is encouraged by the presence of organic matter (Zweifel 1999). Wetlands typically have between 45 and 50% organic matter content within the soil profile (Bano *et al* 1997). The oxidation of the dissolved organic carbon through bacterial means is known as mineralisation, and this process involves organic matter being converted to inorganic substances (Hensel *et al* 1999). Respiration on the other hand, is the transformation of carbohydrates to carbon dioxide. In wetlands, the organic carbon is transformed to carbon dioxide and methane, as well as being stored in the detritus matter or microorganisms. The five main carbon reservoirs in wetlands are: plant biomass carbon, dissolved organic carbon, particulate organic carbon, microbial biomass carbon and gaseous carbon (methane and carbon dioxide). The active carbon biomass consists of the wetland plants and the microorganisms which are attached to inundated surfaces. The particulate organic carbon comprises of decaying plant matter. The soil microbial biomass is considered to be a significant carbon sink (Kayranli *et al* 2010).

Aerobic and anaerobic processes are responsible for the complexity of wetland decomposition. Under anaerobic conditions, the decomposition of organic matter is incomplete. The amount of oxygen (or lack thereof) is a primary factor which determines decomposition of organic matter, and thus detritus turnover (Collins and Kuehl 2001). Preservation of detritus can be observed in the majority of global wetlands (Mitsch and Gosselink 2007). The accumulation of organic matter however, is a function of the organic matter that is produced *in situ* and the organic matter that is produced *ex situ* of

the wetland (Scholz 2011). The relationship between input and output for organic matter in wetlands is important when assessing carbon accumulation. Factors such as high levels of precipitation, soil disturbance, nature of the organic material and rates of decay under waterlogged conditions all play a part in the organic matter accumulation in wetlands (Gorham *et al* 1998).

Organic matter accumulates in wetlands when the production is faster than the decomposition. This results in a net accretion of organic matter in the system (Mitsch and Gosselink 2007). Wetland components (water, soil, organic matter) are subjected to both aerobic and anaerobic conditions. Gaseous products are formed as a result of these conditions. When anaerobic conditions dominate, methane and carbon dioxide are formed through the process of decomposition of the organic matter. When aerobic, only carbon dioxide forms (Scholz 2011). Anaerobic soils are soils that are free of any oxygen. The depletion of oxygen in anaerobic soils by soil biota surpasses the diffusion of oxygen into the soil environment (Inglet *et al* 2005). This process results in a net oxygen free environment within the soil. Due to the fact that wetlands are mostly waterlogged throughout significant periods of the year, wetland soils are generally anaerobic in various degrees. When wetland soils become saturated with water, the amount of oxygen present becomes significantly less. This can be due to the oxygen in the pore spaces becoming displaced (Inglet *et al* 2005). Oxygen can still be supplied to respiring organisms through diffusion from the nearest aerobic region. This process is very slow however, as the diffusion of oxygen in water is 10 000 times slower than through air (van der Valk 2012).

1.3 Redox potential

Soil redox potential measures the intensity of the anaerobic conditions within the soil, which is linked to the degree of water saturation (Reddy *et al* 2000). Similar to pH (the measure of the hydrogen activity), the redox potential (Eh) measures the activity (e^-) of the electrons within the soil. The dynamics of water and its redox potential have large influences on the genesis of wetland soils (Fiedler and Sommer 2004). A relationship

occurs between the redox potential (Eh) and the oxidation-reduction reactions in terms of thermodynamics. This relationship can be explained by the Nernst equation.

$$E_h = E^\circ - \frac{RT}{nF} \ln\left(\frac{[Reductant]^c}{[Oxidant]^a [H^+]^b}\right)$$

Figure 1.2: Nernst equation (Reddy *et al* 2000)

In the Nernst equation, the listed symbols are explained (adapted from Reddy *et al* 2000):

- Eh is the redox potential.
- E° is the standard electrode potential.
- R is the gas constant.
- T is the absolute temperature in Kelvin.
- F is the Faradays constant.
- n is the number of electrons that have been transferred.
- [] is the activity of the chemical species

It is worth noting that the Nernst equation applies when predicting the activity of reduced and oxidised species only when the system is at equilibrium, which is hardly ever the case in soils, which makes it difficult to interpret redox data of natural systems. The chemical reactions in the soil can be slow due to the heterogeneity of soils. Redox potential values measured in the field can still be an important guide of the general redox status of the soil. For example, the redox potential (Eh) is positive in oxidising systems, whereas the Eh is negative in reducing systems (Sparks 2003). In flooded soils, the Eh is expected to be either slightly positive or slightly negative due to the reducing conditions. The rate of the Eh decrease upon introduction of reducing conditions (flooded soils) is dependent on the soil organic matter, nature of the e⁻ acceptors, temperature and the inundation time (Sparks 2003).

Reliant on the characteristics of the wetland soil, Eh generally decreases with time and approaches a fixed value after saturation, most likely due to the system reaching a steady state. The negative value of Eh represents anaerobic conditions and high

electron activity, which are typical of waterlogged conditions such as wetlands. The positive values of Eh represent moderately anaerobic to aerobic conditions and low electron activity, typical of the transitional zone of a wetland. As a general rule, soils exhibiting Eh values greater than +300 mV are considered to be aerobic and upland soils (Inglet *et al* 2005). Soils exhibiting Eh values less than +100 mV are considered redoxic and wetland soils. Iron oxides are stable within the suboxic range of +100 to +400 mV. When the redox potential drops below +100 mV to the redoxic range, aqueous ferric iron starts to become reduced to ferrous iron.

Oxygen provides an oxidant (electron acceptor) for microbial oxidation of reduced carbon compounds, also known as respiration. Oxygen is the preferred oxidant by thermodynamic ruling for microorganisms (Inglet *et al* 2005). Once all the oxygen is depleted in the soil, the bacteria and microorganisms have to respire anaerobically. The order of electron acceptors under anaerobic conditions is as follows: NO_3^- followed by Mn^{4+} followed by Fe^{3+} followed by SO_4^{2-} and finally CO_2 . Table 1.1 shows the electron acceptors, decomposition end products and microbial groups for each redox potential class (aerobic or anaerobic).

Table 1.1: Microbial groups involved in wetland soils redox reactions (adapted from Inglet *et al* 2005).

Redox potential (mV)	Electron acceptor	Decomposition end products	Microbial groups
Aerobic >300	O ₂	CO ₂ , H ₂ O	Aerobic fungi and bacteria
Fermenting -100 to +300	Organics	Organic acids, CO ₂ , H ₂ O, alcohols, amino acids	Fermenting bacteria
Facultative anaerobic +100 to +300	NO ₃ ⁻ Mn ⁴⁺ Fe ³⁺	N ₂ O, N ₂ , CO ₂ , H ₂ O Mn ²⁺ , CO ₂ , H ₂ O Fe ²⁺ , CO ₂ , H ₂ O	Denitrifying bacteria Mn(IV) reducers Fe(III) reducers
Obligate anaerobic <-100	SO ₄ ²⁻ CO ₂ and acetate Organic acids	HS ⁻ , CO ₂ , H ₂ O CH ₄ , CO ₂ , H ₂ O Acetate, CO ₂ , H ₂	Sulphate reducers Methanogens H ₂ -producing bacteria

1.4 Wetland methane production

Natural wetlands produce 20%-39% of the total worldwide methane emissions on average (Denman *et al* 2007). Methane is a known greenhouse gas, having a 25 time higher global warming potential value than carbon dioxide (Olson *et al* 2015). Wetlands typically have high levels of organic material, in which soils with organic carbon higher than 20% is considered peat in South Africa. When peat is drained of water, or when the water table of the wetland is lowered, it decomposes rapidly and could lead to massive acidification (Andriessse 1998). When the drained peat is rejuvenated with water (water table in wetland rises), oxygen is consumed very quickly. Global wetland methane flux rates are estimated to be about 10⁻⁶ kg.m⁻².d⁻¹. These methane flux rates quantify the net effects of microbial production and consumption (Whalen 2005). Wetland methane fluxes differ from region to region depending on various climatic

conditions and it is not possible to assign a certain methane flux rate to any given wetland.

Methane production in wetlands is an anaerobic process, which occurs mostly in anoxic soil layers (Jerman *et al* 2009). The oxidation of methane in freshwater wetlands depends on the abundance of oxygen. The oxidation of methane may regulate the flux of methane, thus reducing emissions. The process of methane production, called methanogenesis, depends on a certain order of microbial processes. These processes are:

- Hydrolysis of polymers to fatty acids and alcohols
- Primary and secondary fermentation where the fatty acids and alcohols are converted to acetate and H₂
- Methanogenic conversion of acetate and H₂ and CO₂ (Conrad and Frenzel 2002)

Acetate and H₂ are typical products of fermentation, and these products provide substrates for terminal oxidation chemical processes (Jerman *et al* 2009). The oxygen availability and transport, is limited by the depth of the water table. The water table can therefore be an important factor in the production of wetland gasses such as methane (Aerts and Ludwig 1997).

Temperature, along with availability of oxygen, is another important factor in methanogenesis. One of the most widely accepted facts about temperature and methane production is that methanogenesis is more likely to dominate at low temperatures (Metje and Frenzel 2005). One of the debates surrounding wetlands is whether they act as carbon sources or sinks. For example, when the water table is low (drier conditions), methane oxidation causes wetlands to act as a methane sink, contributing to the removal of atmospheric methane. However, when the water table is high (saturated conditions), the wetland becomes a source of methane (Kayranli *et al* 2009). Redox potential is also an important factor in methane production. The availability of oxidants in the soil (such as oxygen and carbon dioxide) used as acceptors of electrons for organic matter, contributes greatly to the microbiological

processes within the soil (Hou *et al* 2000). It was found that methane emissions were linked to changes in redox potential, where significant emissions of methane occurred solely at redox potentials lower than -100 mV (Hou *et al* 2000).

Methanogenic bacteria produce methane by decomposing (breaking down) organic material anaerobically (absence of oxygen), this releases CO₂ and CH₄ according to the reaction below:

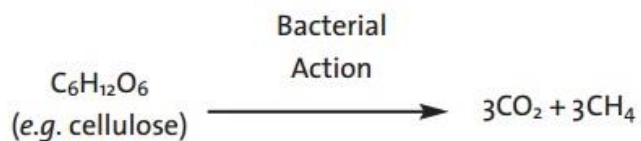


Figure 1.3: Methanogenic bacteria products (Jardine *et al* 2002)

Methanotrophic bacteria, as opposed to methanogenic bacteria, oxidise methane to form carbon dioxide.

1.5 Wetland carbon dioxide production

In the aerobic zone of a wetland, photosynthesis by microbes and most importantly plants uses atmospheric carbon and light to create organic matter, which reduces carbon (C⁴⁺) from the 4+ state in CO₂. The produced organic matter, in turn, is decomposed through respiration (figure 4), joining the oxidation of C to the reduction of O₂ in the aerobic zone, or the less favourable electron acceptors such as Fe³⁺, Mn⁴⁺, sulphate and carbon dioxide within the anaerobic zone (Vepraskas 2016). The oxidation of methane transforms methane into carbon dioxide, with concurrent reduction (electron acceptor) of sulphate and/or nitrate.

Carbon dioxide emissions increase with increasing temperature, and increases with a lower water table (Waddington *et al* 2001). Thus, under drained (drier) conditions, carbon dioxide production is theoretically higher, and lower under saturated conditions.

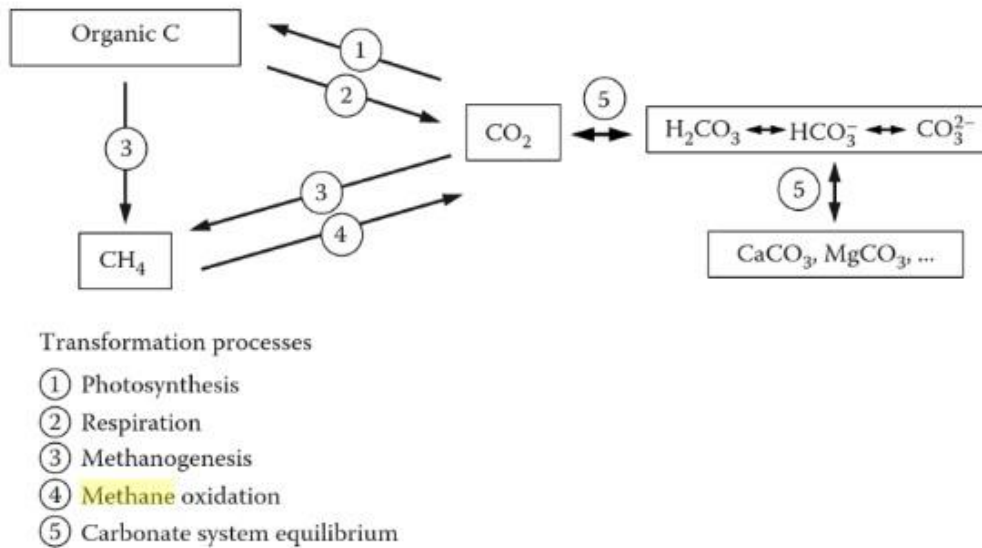


Figure 1.4: Major transformations of the carbon cycle (Vepraskas 2016)

The following terms as illustrated in figure 1.4 are explained below:

Photosynthesis: This is the process by which bacteria and plants use energy from the sun to produce glucose from CO₂ and H₂O. Photosynthesis has the following general equation (Chemistry for biologists 2016):

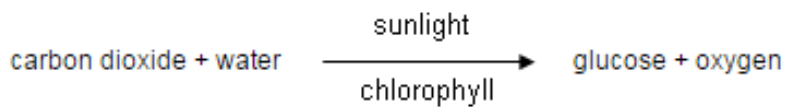


Figure 1.5: Photosynthesis reaction

Chlorophyll is responsible for the conversion of sunlight into usable plant energy.

Respiration: Soil respiration is when carbon dioxide is released from the soil. The source of the CO₂ comes from aerobic microbial decomposition of SOM (soil organic matter). The respiration from microbes and autotrophic respiration is necessary for

growth and functioning. When SOM is being decomposed, organic nutrients within the organic matter such as P, N and S, are transformed to inorganic forms, which are then made obtainable for plant uptake (Soil Quality 2011). This is also known as carbon mineralisation.

Methanogenesis: Methanogenesis follows the following transformation sequence: hydrolysis of polymers to fatty acids and alcohols, followed by primary and secondary fermentation where the fatty acids and alcohols are converted to acetate and H₂, And finally the methanogenic conversion of acetate, H₂ and CO₂ to CH₄ (Conrad and Frenzel 2002).

Methane oxidation: Methane oxidation requires oxygen to be present, and happens when methane is oxidised to form carbon dioxide, coupling with electron acceptors such as nitrates and sulphates.

Carbon system equilibrium: Aqueous carbon in solution is in equilibrium with the carbon in the atmosphere (Aqion 2016).

Organic matter becomes decomposed and gets transformed to CO₂ under aerobic conditions. Under anaerobic conditions, however, CO₂ and CH₄ emissions can provide a measurement of the total soil respiration (Bridgman and Richardson 1992).

1.6 Measurement of carbon dioxide emissions

The most common and widely used method of measuring carbon dioxide is using non-dispersive infrared (NDIR) technology. The principle of NDIR technology is based on the ability of gas molecules to absorb infrared light. Adsorption of different gases occurs at different wavelengths of light (Seitz and Tong 2013). Carbon dioxide has high absorbance abilities at a wavelength of 4.26 μm. A band-pass filter is fitted on the light bulb, which only allows the specific wavelength to be emitted through to the thermophile, as illustrated in figure 1.6. The gas molecules therefore absorb radiant energy and the change measured at the thermopile side gives a reading of carbon dioxide levels. This principle follows the Lambert-Beer law: $I = I_0 \cdot e^{-k \cdot c \cdot l}$. I is the transmitted energy picked up on the thermopile detector side, I_0 is the initial intensity transmitted by

the bulb and e^{kcl} is the gas specific absorption coefficient of the target gas (Seitz and Tong 2013), the gas concentration, and the length of the absorption path.

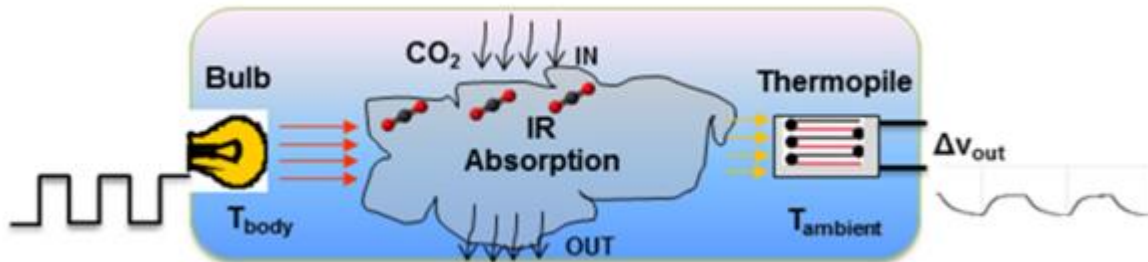


Figure 1.6: NDIR principle (Seitz and Tong 2013)

Another method of measuring carbon dioxide and methane emissions involves the use of static gas chambers and gas chromatography. Static gas chambers are closed chambers without air flow-through. Gas emissions from the soils are trapped within the chamber, and the rates of flux are measured by determining the change in gas concentration over time inside the headspace of the chamber (Collier *et al* 2014). The static chamber method has been widely used and is considered a reliable method of measuring soil flux for small experiments. Important factors to consider when using the static chamber method are: chamber design, calibration, experimental design, field sampling techniques, sample analysis and data analysis (Collier *et al* 2014). For chamber design, it is important to use a non-reactive material such as PVC or stainless steel.

A simplified explanation of the gas chamber method is as follows:

- Setup sealed chamber with soil medium inside
- Attach a septum to the top of the sealed chamber, which connects to a syringe
- The pipe between the chamber and the syringe has a stopcock valve for prevention of gas leakage
- Over several time intervals, the syringe will be drawn and gas will be transferred to vials.

The vials will contain gas samples at different time intervals, which will be then subjected to gas chromatography in order to determine gas concentrations.



Figure 1.7: Gas chamber in the field (Sattazahn 2012)

For gas chromatography, detection of CO₂ must be done with an infrared gas analyser, and a flame ionisation detector for CH₄ (Collier *et al* 2014). After gas chromatography, conversion of trace gas concentration from volumetric to mass is done using the Ideal Gas Law: PV = nRT, where P = pressure, V = volume, n = moles of gas, R = gas law constant and T=temperature. Therefore the following Ideal gas Law equation is applicable:

$$\frac{V \text{ trace gas } \text{L} \cdot 1 \text{ L}^{-1} \cdot P \text{ atm}}{(0.08206 \text{ L atm mol}^{-1} \text{ }^{\circ}\text{K}^{-1}) \cdot (273 + T \text{ }^{\circ}\text{C})^{\circ}\text{K}} = \text{Mol trace gas } \text{L}^{-1}$$

Figure 1.8: Ideal Gas Law for conversion of volumetric to mass (Collier *et al* 2014)

The results can be plotted on a graph of concentration versus time. The slope of the regression line is used to calculate the flux. Flux can be calculated by the following

formula: $F = S.V.A^{-1}$, where F = flux, S = slope of regression line, V = chamber volume in litres, and A = area of chamber in m^2 (Collier *et al* 2014). Below is an illustration of the general procedure.

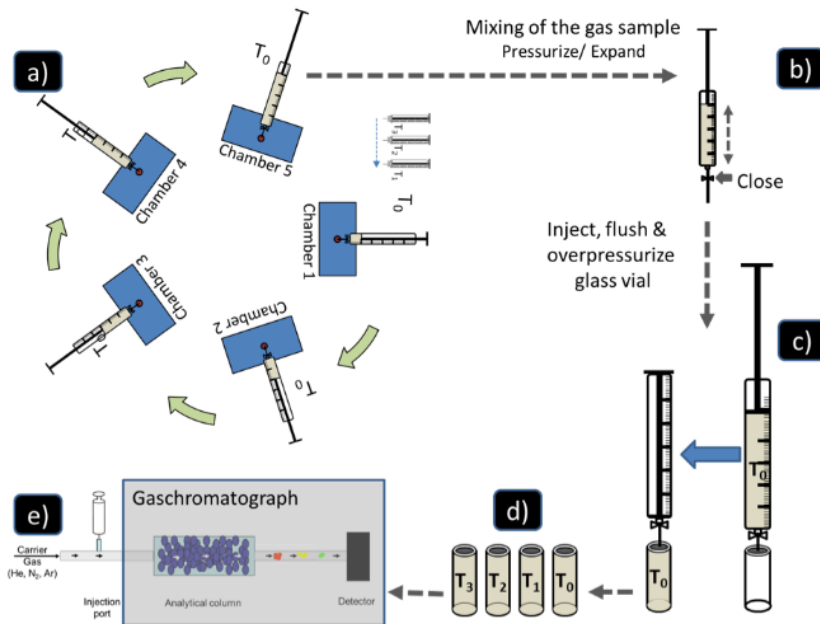


Figure 1.9: General procedure: a) static gas chambers, b) gas extraction by syringe, c) transfer of gas from syringe to collection vial, d) labeling of vials, e) gas chromatography (adapted from Arias-Navarro *et al* 2013)

1.7. Acid mine drainage from Mpumalanga Highveld coal mines

1.7.1 Coal producing regions

The economic development of South Africa is closely linked to the progression of coal mining. Large scale commercial coal mining originated in Molteno, Eastern Cape, in 1864. Coal mining eventually started in Witbank, which is on the Mpumalanga Highveld. The impact of the coal mining in and around Witbank has had large impacts on the greater Olifants river catchment (McCarthy and Pretorius 2009). South Africa's deposits of coal occur in the Karoo Supergroup, which is a sequence of sedimentary rocks which were deposited and formed some 300 to 180 million years ago. More specifically, the coal seams occur in a subgroup known as the Ecca subgroup

(McCarthy and Pretorius 2009). The coal seams come from large organic deposits from deltas entering the prehistoric Karoo Sea. Figure 1.10 shows the location of these coal producing regions in eastern South Africa (shown by the red lines).



Figure 1.10: Location of the coal producing regions of eastern South Africa (McCarthy and Pretorius 2009)

1.7.2 Acid mine drainage

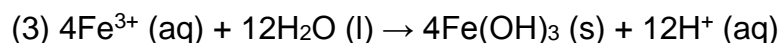
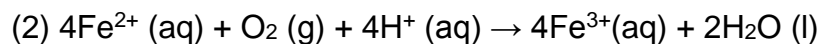
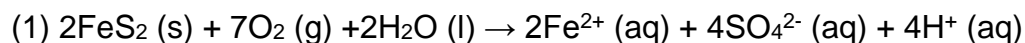
Acid mine drainage (referred to as AMD) is one of the biggest environmental problems facing the mining industry (Domville *et al* 1994). AMD can have the following negative effects on the environment (Vermeulen *et al* 2008):

- Devastation of fish and aquatic habitat
- Decrease of aquatic system pH to highly acidic
- Effectively impossible to reverse effects with existing technology
- Extremely expensive and complex to treat AMD

For mines, it is very important to know the capacity/characteristics of the waste rock, pit falls, pit floor, tailings and overburdens to predict if AMD will occur or not (Vermeulen *et al* 2008).

The development of AMD is the chemical reaction between pyrite (FeS₂), which is present in the host rock as well as in the coal, and percolated rain water (oxygen-bearing water). The natural production of AMD is very slow because the rocks of the Karoo Supergroup have low permeability and the acid is neutralised by equally slow reactions (McCarthy and Pretorius 2009). In the mining environment, however, the rocks are broken up and the surface area of the coal and pyrite becomes significantly increased, together with the increase in pathways for water movement, the chemical processes that drive AMD production is significantly accelerated (McCarthy and Pretorius 2009). Some rocks contain minerals which can help neutralise AMD (such as calcium carbonate and dolomite: calcium magnesium carbonate), however many of the rocks that are associated with coal have limiting amounts of calcium carbonate.

There are several stages in the development of AMD. The availability of oxygen acts as a limiting factor for oxidation under natural conditions. The natural source of water recharge into mine, rainwater, contains oxygen (Vermeulen *et al* 2008). This oxygen is available for chemical reactions with the constituents in the soil, such as organic material, pyrite (FeS₂), pyrrhotite (FeS) and chalcopyrite (FeS.CuS). This process is an oxidation process, and produces sulphates. This process produces sulphates. The production of these sulphates occur via the following generalised chemical reactions:



AMD can be severe, where the pH drops below 3. This involves inorganic and organic processes and chemical reactions. In order for significant oxidation to occur, the

sulphide minerals should produce an optimal situation in which rapid oxidation occurs within the system (Vermeulen *et al* 2008). The amount of alkaline material within a rock determines the potential of the sulphide-bearing rock to generate acid. When the sulphides, such as pyrite, are exposed to water and oxygen, oxidation and the generation of acid begins. Calcium carbonates will immediately try to neutralise the acidity. As the neutralising agent becomes depleted, acidity is generated, and the pH decreases. This decrease in pH creates optimal conditions for further acid generation (Vermeulen *et al* 2008). This process continues, and at each specific pH, a different neutralising agent becomes available. If this process depletes all neutralising agents, the pH is expected to drop below 3, and extremely severe AMD will be generated.

1.7.3 Lime-treated acid mine drainage for agricultural use

Measures to inhibit acid mine drainage from polluting the environment has been a large topic of research. Acid water is neutralised with hydrated lime ($\text{Ca}(\text{OH})_2$) or limestone (CaCO_3). One of the commonly used liming agents in the Mpumalanga Highveld region is hydrated lime, or $\text{Ca}(\text{OH})_2$. Treatment of AMD with hydrated lime produces gypsum ($\text{CaSO}_4 \cdot 2\text{H}_2\text{O}$). This produces a saline effluent (gypsiferous water) with a typical electrical conductivity (EC) of 130 to 290 $\text{mS} \cdot \text{m}^{-1}$ (Jovanovic *et al* 1998). The safe disposal of mine water has long been an issue in South Africa.

The Mpumalanga Highveld coal fields have one of the highest agricultural potential land areas in South Africa (Annandale *et al* 2001). The significance of this is that South Africa has a very low arable land percentage. Therefore, the use of gypsiferous mine water is an obvious solution to supplying arable land, in an arid country, with treated acid mine water.

The use of lime-treated acid mine water (saline mine water) for irrigation does pose many problems. Elevated levels of magnesium (Mg) in the water can result in an increasing EC. The lime-treated water can cause salinisation of rivers, dams, soils and catchment areas if used for agriculture (Annandale *et al* 2001). The short-term effects of the saline mine water have proven to have no significant deterioration of groundwater

as yet (Annandale *et al* 2001), but the long-term effects on the salinity, groundwater quality and effect on the catchment are not yet fully understood.

CHAPTER TWO: Carbon dioxide emissions in mine affected environments

2. Introduction

Chapter two aims to develop a field method of measuring carbon dioxide emissions from wetlands in the field. The Rietvlei study wetland acted as a monitoring site (effectively a trial run), where three wetlands (Wetland A, B and C) from the Mpumalanga Highveld acted as the basis of this chapter. Between 35% and 50% of all wetlands in South Africa have been degraded or destroyed completely (Dini 2004). Different wetlands were studied in order to compare wetlands that are directly affected by the industrial activity (Wetland A), wetlands that have been rehabilitated (Wetland B), and wetlands that have not been directly affected by industrial activity (Wetland C). An organic wetland will be included in this chapter in order to distinguish any differences between carbon dioxide emissions from mineral wetlands versus organic wetlands (high organic carbon wetlands). Organic wetlands contain the highest amount of carbon percentage per mass of soil, typically containing more than 10 percent organic carbon. Laboratory analysis was done on the organic and mineral wetlands, followed in chapter three, in order to study what response an organic O horizon as well as a mineral horizon has when subjected to synthetic acid mine drainage.

Chapter two will focus on three wetland study sites, in which field measurements were taken for pH, Electrical Conductivity (EC), redox potential and CO₂. For each study site, soil classification was done to delineate the different wetland zones. This was followed by representing the data spatially in the form of interpolated maps. Finally, statistical analyses were done to compare and correlate the data obtained in the field. The statistical analyses are shown at the end of the chapter.

The hypothesis for the study is that the permanent zone of a wetland will have the highest levels of carbon dioxide release than the surrounding seasonal and terrestrial zones.

2.1 Field method of measuring carbon dioxide emissions

The field method for measuring carbon dioxide emissions took place within the Rietvlei Nature reserve, Gauteng. The study area was located on a small portion within the Rietvlei Nature Reserve. The Rietvlei Nature Reserve was established in 1948 and acts as an ecological hub, aiming to conserve 3 800 hectares of the grassland and undulating hills that the reserve is located on (City of Tshwane 2015). The Rietvlei Nature Reserve consists of the large Rietvlei dam located in the western portion of the nature reserve. The dam is part of the Rietvleirivier watercourse, which flows south to north, before forming the Rietvlei dam.

The study area is located within the Pretoria Group of the Transvaal Supergroup. More specifically, the study area is located within the Daspoort formation of the Pretoria Group. The Pretoria Group rocks in this region consist of andesitic lava and conglomerates. To the west and east, is the Malmani Group, which consists of dolomite and chert. The dolomite influence gives rise to red loamy soils high in manganese. The influence of the Malmani dolomites on the hydrology of the area will be significant, as the Malmani Group contains one of South Africa's largest aquifers (Kafri and Foster 1989).

A field study was conducted from the 28th of November 2016 to the 2nd of December 2016. The aim of this field study was to delineate the wetland according to soil wetness indicators, followed by monitoring the carbon dioxide emissions emitted from each sample point within each wetland zone. The wetland delineation process also involved the classification of the soil forms which were encountered within the different wetland zones. A grid study was designed over the study area, consisting of 40 sample points, covering 4.34 hectares. The same sampling grid was used for the carbon dioxide measurements. The wetland delineation process was as follows:

- Terrain unit and topographical maps to determine where wetlands are most likely to occur using GIS software
- Identification of hydromorphic (wetland) soils

- Soil form and wetness indicators to establish permanent, seasonal, and temporary wetland zones. Assessed with the use of an auger, GPS, soil classification manual, Munsell soil colour chart and any other information available about the area (yellow arrows indicate wetland/terrestrial interface).
- Identification of hydrophytes (wetland plants)
- Historic and current satellite imagery (e.g. Google Earth) (Fig 2.1).

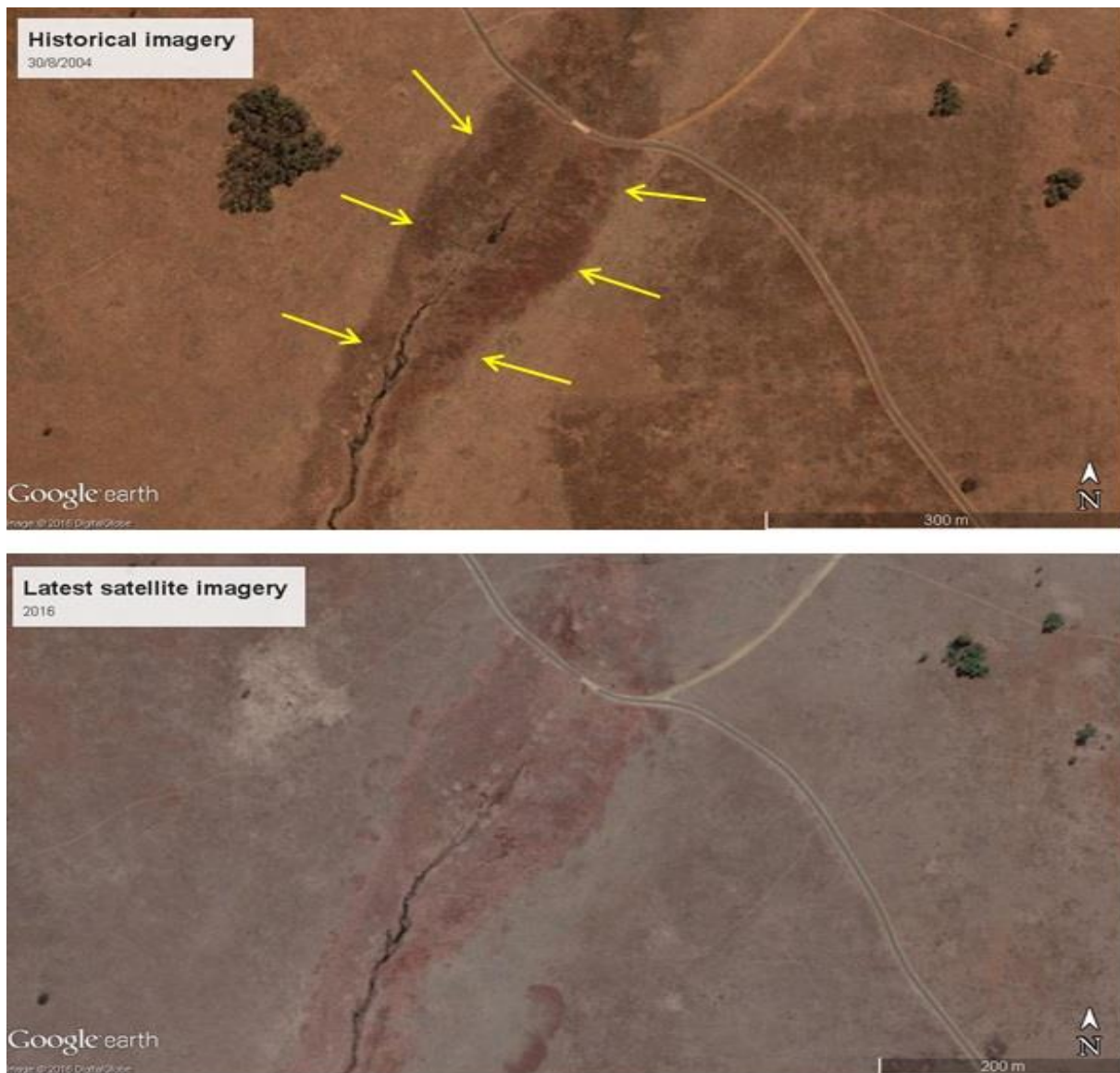


Figure 2.1 Satellite imagery from 2004 and the latest satellite imagery from 2016

The identification of the soil zones within and around the wetland area is illustrated in figure 2.2.

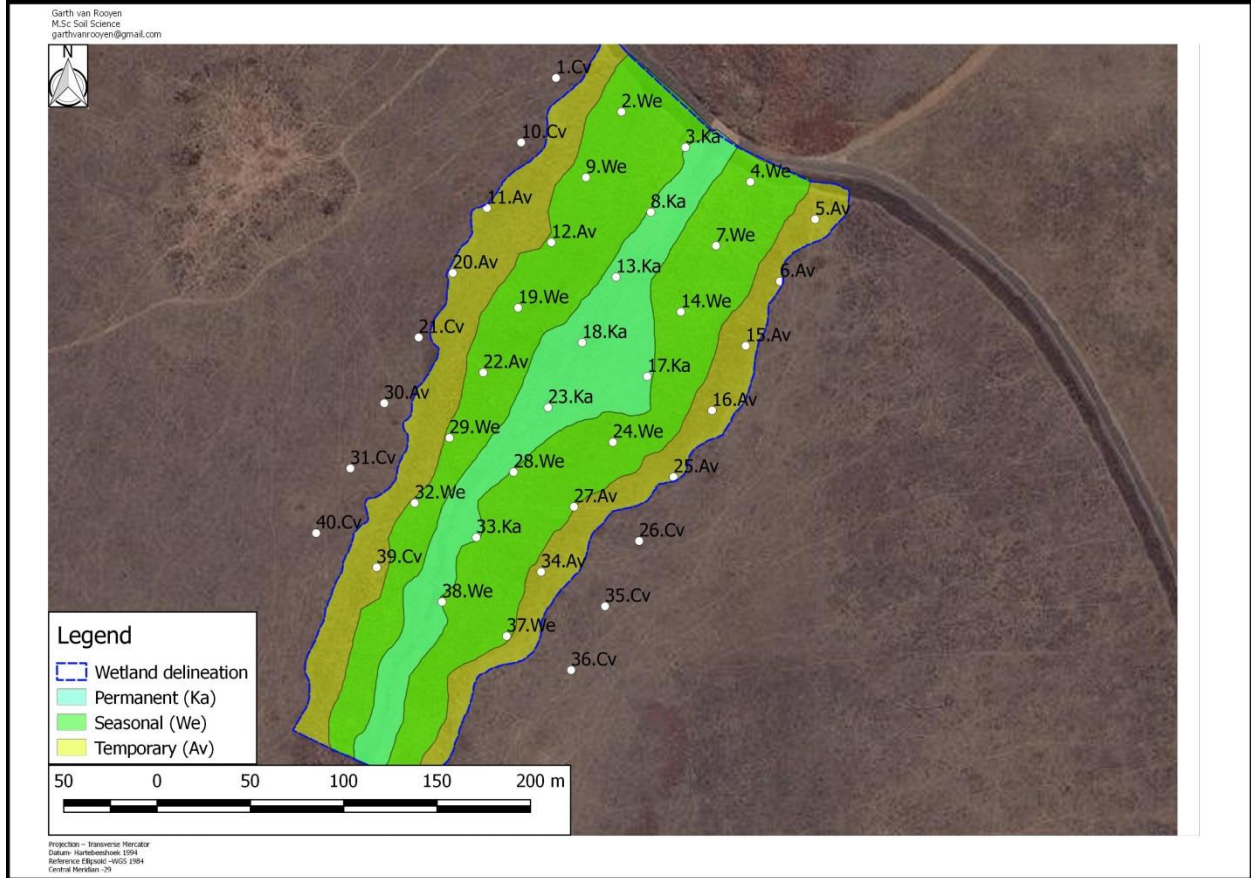


Figure 2.2 Soil forms and wetland zones

According to the field study, the wetland proved to have three distinctive wetland zones which all correlated to certain soil properties. The terrestrial zone consisted of the Clovelly (Cv) soil form as you approach the wetland down the landscape. The Clovelly soil forms encountered showed no signs of wetness, such as redoximorphic features (mottles). The temporary zone consisted of the Avalon (Av) soil form. The diagnostic characteristic of this zone were signs of wetness deep in the profile (600-1000 mm). The Avalon soil form consisted of a soft plinthic horizons underlying a yellow brown apedal B horizon. Figure A1 in the Appendix illustrates the Avalon soil profile. The

profile depicted in figure A1 is heavily disturbed as a dutch and a bucket auger was used to extract the soil, which was then recreated on the surface indicating the profile and depths. As one moves downhill towards the permanent zone, the soft plinthic horizon gets closer and closer to the surface, which means the water table becomes closer to the surface. The yellow brown apedal B horizon as a result, becomes more mottled until a point where the mottling becomes greater than 10 percent. In the seasonal zone of the wetland, the Westleigh (We) soil form was encountered. This mottling is illustrated in Figure A2 of the Appendix. The permanent zone of the wetland consisted of the Katspruit (Ka) soil form, which is an orthic A horizon overlying a G horizon. Wetland vegetation that was observed included *Typha capensis*, *Schoenoplectus* sp. and *Cyperus* sp. The permanent zone of the wetland was dominated by *Typha Capensis*. A photograph of the permanent zone of the wetland exhibiting these plant species can be seen in appendix A, figure A3.

2.2 Carbon dioxide emissions from the Rietvlei wetland

A grid study of 40 sample points measuring the amount of carbon dioxide released was done on the now delineated wetland. A non-dispersive infrared (NDIR) carbon dioxide meter was used to measure the amount of carbon dioxide in parts per million. NDIR sensors work using spectroscopy. When a sample of gas is pumped into the gas sample chamber, certain gases such as carbon dioxide act as a filter, absorbing a specific wavelength of energy within the infrared spectrum (Seitz and Tong 2013). As more carbon dioxide is introduced within the sample chamber, less light reaches the detector, and thus a lower carbon dioxide level is read on the meter. The NDIR sensor is illustrated in Figure 2.3.

The NDIR sensor was calibrated using the following method:

- Prepare sealed chamber with N₂ gas (equivalent to 0 parts per million carbon dioxide)
- Insert meter into chamber
- Hold in “SET” + “PWR” on device to enter calibration mode, choose “0 ppm Nitrogen mode”

- Leave for 10-12 minutes to complete calibration



Figure 2.3 NDIR carbon dioxide sensor field experiment setup

The following methodology was used in measuring the carbon dioxide emissions from the wetland:

- Insert the PVC column into the soil to a depth of 10cm, leaving a 5cm headspace
- Turn on the NDIR sensor and wait for equilibrium steady state to be reached for the carbon dioxide readings
- Note the carbon dioxide readings in ppm, the temperature in degrees Celsius and the pressure in hPa. These values are important when calculating mass of carbon dioxide according to the ideal gas law

All the carbon dioxide field measurements were inserted into a database. The database was in the form of the attribute table of a shapefile (.shp) which can be used in GIS software. The carbon dioxide measurements were then interpolated using Inverse Distance Weighted (IDW) interpolation to create a visual map showing areas of equal

carbon dioxide emissions. The two main interpolation methods are the Inverse Distance Weighted (IDW) interpolation and the Triangulated Irregular Network (TIN) interpolation. IDW interpolation uses an interpolation method that estimates cell values by averaging the values of sample data points. The data points that are averaged are in the neighborhood of each processing cell. The closer a point is to the center of the cell being estimated, the more weighted it becomes on the averaging process. TIN interpolation methods are commonly called Delaunay interpolation. TIN interpolation creates triangles formed by its nearest neighbours points (Sutton *et al* 2009). A disadvantage of the TIN interpolation is that the surfaces created are not smooth and it is not suitable for extrapolation beyond the study area, a factor that is important when interpolating wetland carbon dioxide emissions. A disadvantages of the IDW method is that the interpolated quality decreases if the dataset is located unevenly to one another. The data used for the wetland studies were obtained on a fixed grid, which allows maximum accuracy upon interpolation. This was the main reason the IDW method was used. Figure 2.4 illustrates the interpolated map.

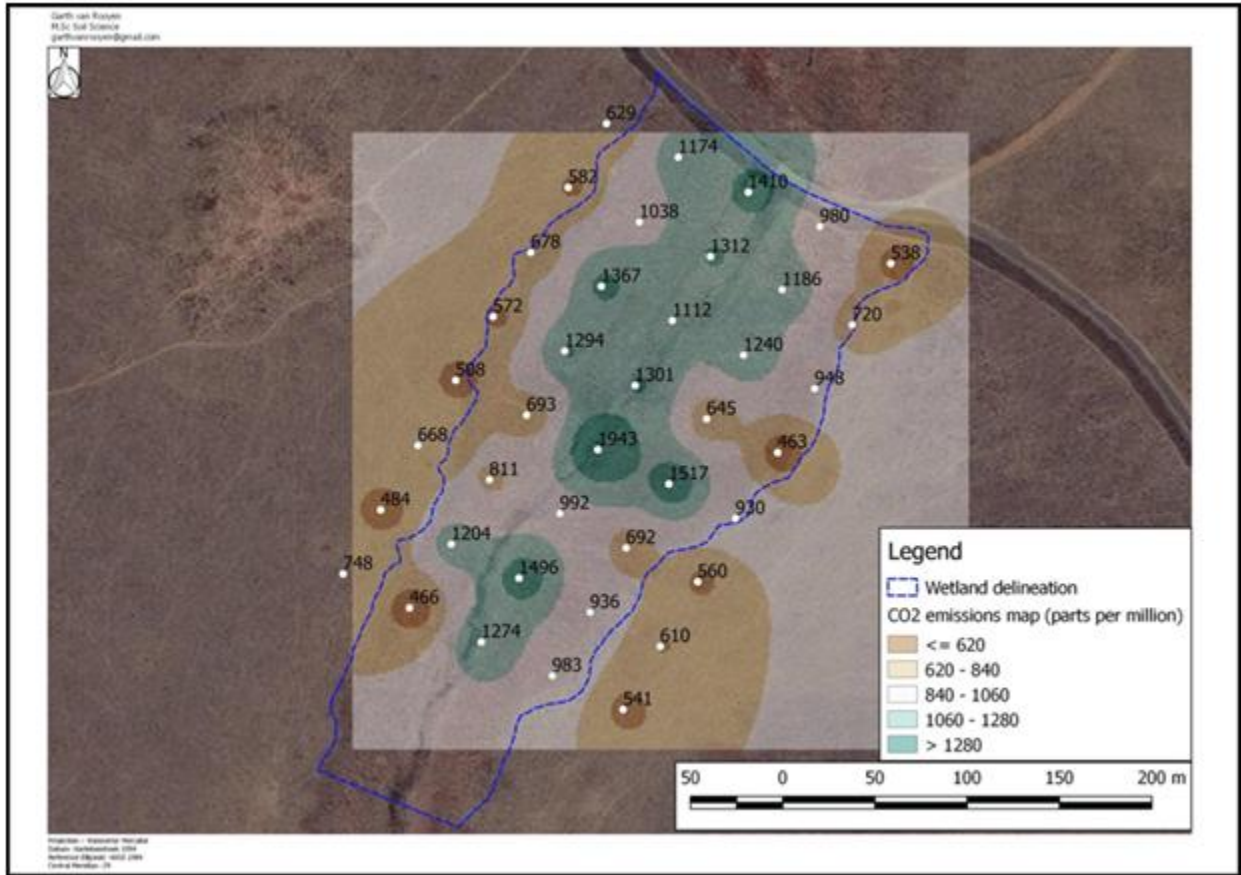


Figure 2.4 Interpolated carbon dioxide emissions for the Rietvlei wetland

Figure 2.4 illustrates how the carbon dioxide emissions from the wetland were highest within the permanent zone of the wetland. The carbon dioxide emissions decreased as one moves out of the permanent wetland zone towards the terrestrial zone. These results indicate a brief, but insightful view on carbon dioxide emissions from the different wetland zones. Although microbial activity and respiration from wetlands is a complex process (factors affecting respiration include pH, carbon in the soil, C:N:S:P ratio and nutritional status), this chapter focused on the effect that acid mine drainage (AMD) has on the release of carbon dioxide from wetlands, in addition to investigating basic relationships between carbon dioxide release, electrical conductivity, pH, redox potential and disturbance. Three additional sites from the Mpumalanga Highveld region were investigated using the same procedure followed for the Rietvlei wetland. The Rietvlei

wetland acted as a monitoring site where the experimental procedure (NDIR monitoring) was refined and perfected in order to investigate the mine affected wetlands of the Mpumalanga Highveld.

2.3 Mpumalanga Highveld wetlands: study area and location

The study area is located approximately 20 kilometers west of Emalahleni, Mpumalanga, and approximately two kilometers south of the N4 motorway. The site is accessible via the R104 road which can bring you within close distance of the three study wetlands. The study area is located in the quaternary catchment B20G of the Upper Olifants catchment, which is located in the quarter degree square 2529CC. The study area is located within close proximity to Evraz Highveld Steel and Vanadium Limited. The Upper Olifants catchment region has been impacted by mining activities and the resultant loss of ecological function of watercourses within this region have prompted research and rehabilitation in order to mitigate these effects. Figure 2.5 illustrates the locality of the study area.

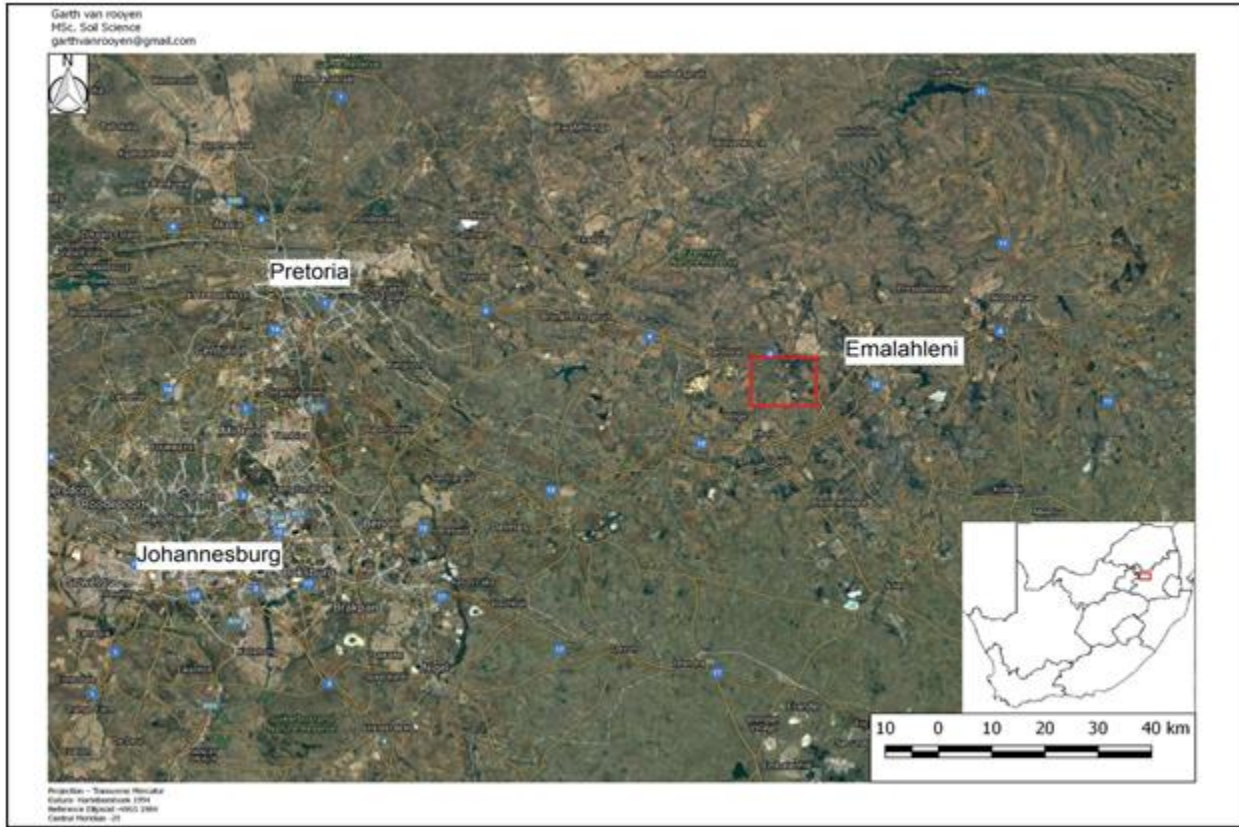


Figure 2.5 Locality map

The red square box illustrated in figure 2.5 contains three study wetlands, namely Wetland A, Wetland B and Wetland C. Figure 2.6 illustrates the position of these three wetlands relative to each other on a zoomed-in locality map. In figure 2.6 it is evident that the northern section is impacted by industrial activity, whereas the southern section is to a lesser extent impacted by agriculture. Wetland A was chosen as the wetland which has been impacted by mining related industries, with highly alkaline slag being discharged into the wetland. “Mine soils” are soils that have been formed in areas affected by mining activities (Han *et al* 2016). In the Mpumalanga Highveld in the Emalahleni area, most soils can be considered disturbed “mine soils”. Once soil becomes disturbed, the labile carbon fraction is transformed and released as carbon dioxide, leaving behind the recalcitrant carbon in the soil. The SOC content of mine soils are more inert to microbial degradation compared to soils without mining influence, and

as such, tend to be more resistant to chemical and thermal oxidation (Rumpel *et al* 2000).

Wetland A is primarily fed by culverts originating from alkaline slag effluent via a steel and vanadium plant. Wetland B was chosen as the rehabilitated wetland, which will indicate successful rehabilitation measures when compared to the upstream Wetland B. For the purposes for this study, wetland C is seen as a reference wetland as it has not been directly impacted by mining effluent, although agricultural affected runoff will impact the quality and salinity of the water. Wetland C is located 2.20 kilometers north from its source, which is a seepage wetland located 2.20 kilometers downstream. This is seen as being relatively close to its source, suggesting that the impacts of its water quality will be minimal as opposed to a location being far from its source, Increasing its probability to changes in water quality through anthropogenic means. Section 2.5 will provide elaborated information on each wetland.

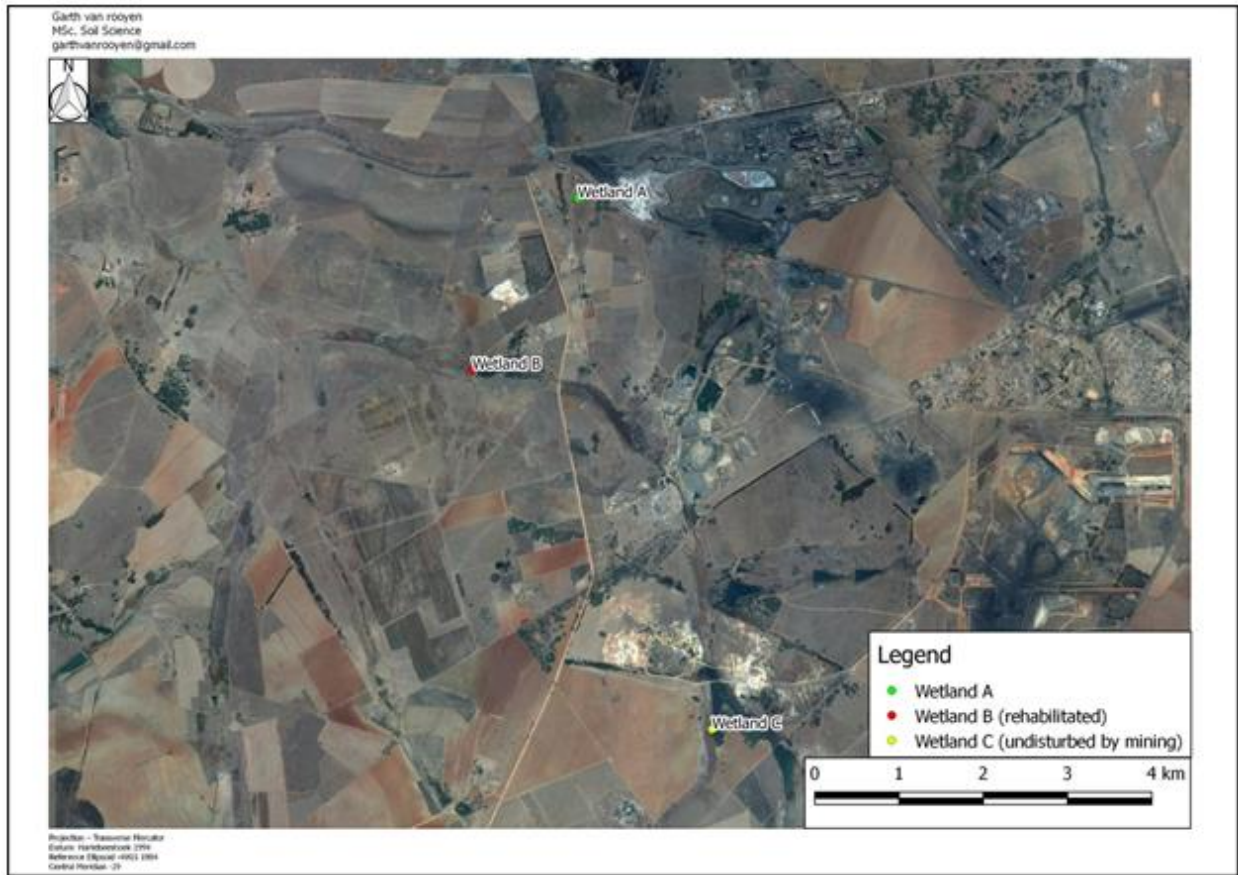


Figure 2.6 Detailed locality map

From figure 2.6, it is evident that the landscapes in which the three study wetlands are situated have been impacted by agriculture and/or industrial activities such as mining. A detailed description of each study wetland will be discussed later in this chapter.

2.3.1 Geology

The geological setting of each of the three study wetlands is important to understand as the wetlands fall within different geological units within close proximity to one another. Figure 2.7 shows the location of the three study wetlands within each geological setting.

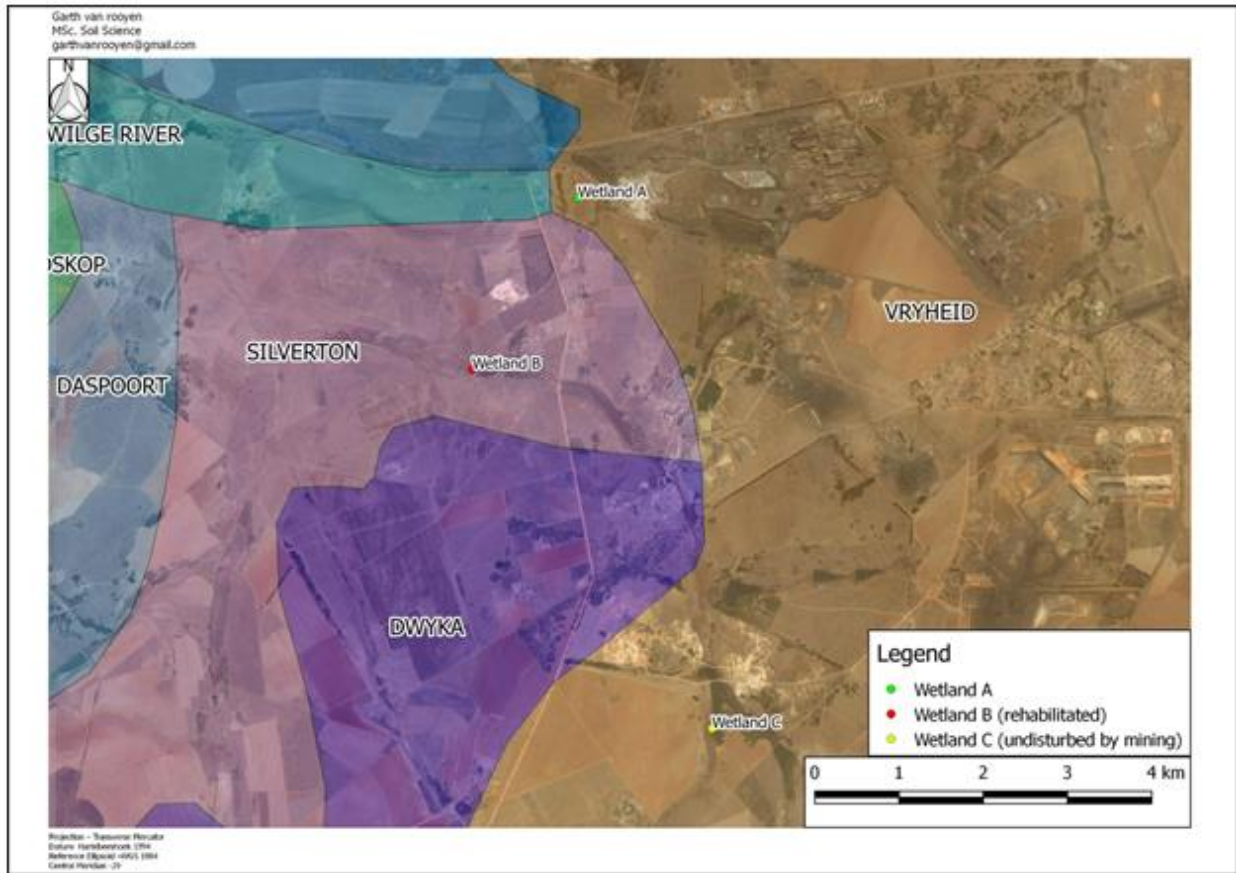


Figure 2.7 Geology map (Council for Geoscience 2017)

Wetland A and Wetland C are situated on the Vryheid formation. The Vryheid formation belongs to the Ecca Group of the Karoo Supergroup consisting of fine to coarse grained sandstone, along with shale and coal seams. Wetland B is situated on the Silverton Formation of the Pretoria Group, although also within the larger Karoo Supergroup. The Silverton Formation consists of shale, small amounts of limestone and dolomite, as well as tuff and basalt. The Dwyka Formation lies approximately one kilometer south of Wetland B and approximately two kilometres north west of Wetland C. The Dwyka Formation also belongs to the larger Karoo Supergroup consisting of diamictite, which are polymictic clasts set in a fine-grained, poorly sorted matrix (Geoscience 2017). The Dwyka Formation also consists of mudstone, varied shale and fluvio-glacial gravel. The Wilge River formation lies approximately 500 meters to the immediate west of Wetland

A. The Wilge River formation forms part of the Waterberg group (or Waterberg Supergroup) and consists of medium to coarse grained sandstone (reddish-brown to purple in colour), minor shale and subordinate conglomerate (Council for Geoscience 2017). Although the larger study area consists of a variety of geological formations, the area is still dominated by sedimentary rocks, particular shale and sandstone. Upon site investigation, it was observed that the study area consisted of large amounts of sedimentary rocks with the occasional coal seams being exploited by mining.

Figure 2.8 illustrates the hydrology flow direction and elevation of the study area. If one compares the geological map of Figure 2.7 to Figure 2.8, it can be seen how closely the geology influences the flow of water in a landscape, with the more eroded areas (watercourse systems) belonging to the less weathering resistant Silverton formation.

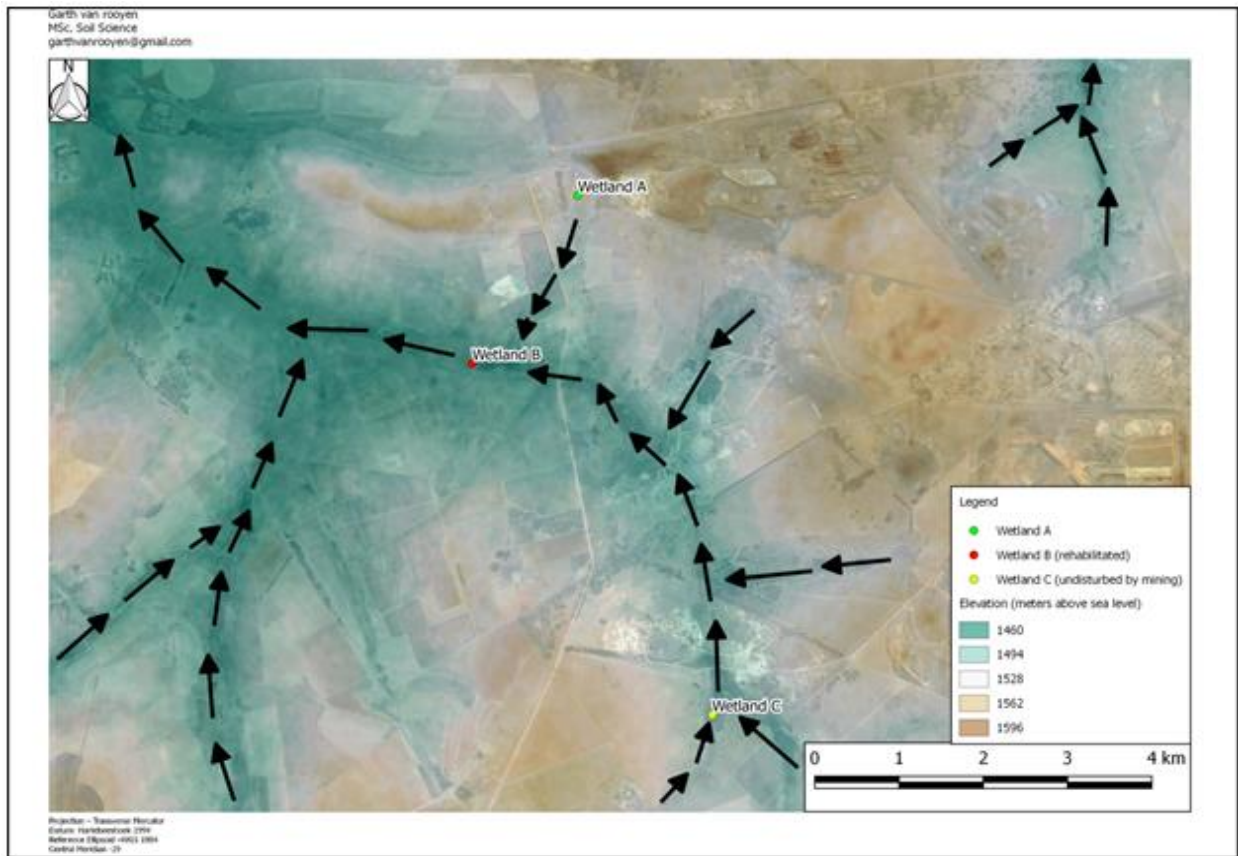


Figure 2.8 Hydrology of study area

2.4 Field study

A field study was conducted in the summer months consisting of periodic site visits between November 2016 and April 2017. During this period, the nearest weather station (Emalahleni) recorded an average 480 millimeters of rain (Meowweather 2017). The average annual rainfall for Emalahleni is 636 millimeters of rain, which means during the period of November 2016 to March 2017, 75 percent of the average annual rainfall occurs. It is worth noting that the 2015/2016 drought period could have skewed any rainfall averages mentioned. The period of site investigation occurred within the summer months, where rainfall is at its highest within a calendar year.

The study of the organic wetland was an important component to understand carbon dioxide emissions from wetlands as the wetland contains an organic soil horizon, which is a soil horizon which contains more than 10% organic carbon. Soils that contain more than 20% organic carbon are now classified as peat soils. The diagnostic criteria for classifying peat, per the new soil classification book (green book) for South Africa, stipulates that peat contains more than 20% organic carbon; associated with water inundation for extended periods. Wetland C consisted of organic soils, very close to peat (in terms of organic carbon %). In the South African classification system, 3 types of peat are listed according to their stage of decomposition. Fibric peat is the least decomposed peat, has a low bulk density and high saturated water content. Hemic peat has an intermediate degree of decomposition. Sapric peat is highly decomposed with the smallest amount of plant fibres and a high bulk density (Soil Classification Working Group 2018).

Peat also falls within a macro classification: “coal rank”. Coals of lower ranks are more susceptible to decomposition by microorganisms, with peat being of the very lowest rank (Han *et al* 2016). The term “coal rank” refers to the degree of coal metamorphism. Chemical and physical parameters are used to measure rank differences at higher or lower ranks. For example, equilibrium moisture is an important parameter at lower ranks (such as peat), but intermediate ranks are classed on volatile matter. Vitrinite reflectance is another important parameter for higher ranks, eliminating chemical

reflectance bias (Mastalerz *et al* 2011). The differences in rate of decomposition between coal (highest rank) and peat (lowest rank) are due to differences in hydrophobicity and aromaticity. The contents of volatile matter are as follows: in the order of anthracite < bituminous coal < sub-bituminous coal < lignite < peat. In addition to low aromaticity, the volatile matter and amount of oxygen contribute to the amount of decomposition of SOC in peat. The volatile organics present in peat have been shown to be used as food by microorganisms (Guillén and Manzanos 2002).

From the previous baseline study at Rietvlei, the wetland was a mineral wetland, and the permanent zone had the highest carbon percentage as well as the highest carbon dioxide release when compared to adjacent seasonal, temporary and terrestrial zones.

Samples of the organic wetland, with high percentages of carbon present in the soil, was taken back to a soil laboratory and introduced to synthetic acid mine drainage in order to observe changes that occurs between the carbon in the soil and the acid mine drainage. The response of this wetland to acid mine drainage and wetland soils will be discussed in chapter three.

2.5 Wetland A field study

Wetland A was selected as a study wetland because of its direct influence by mining and industry. Wetland A is in close proximity to a steel and Vanadium plant, with a slag effluent being discharged directly into the wetland (see Appendix, figure A7 and A8). The water source of the wetland appears to be entirely dependent on the effluent discharge into the system. Large ash dumps are located adjacent to the upstream section of the wetland, which may increase the amount of effluent entering into the wetland.

The sample points of Wetland A are illustrated below in figure 2.9. The wetland delineation as well as the permanent zone is also shown on the map, with the conclusion of the delineation and permanent zone to be discussed.

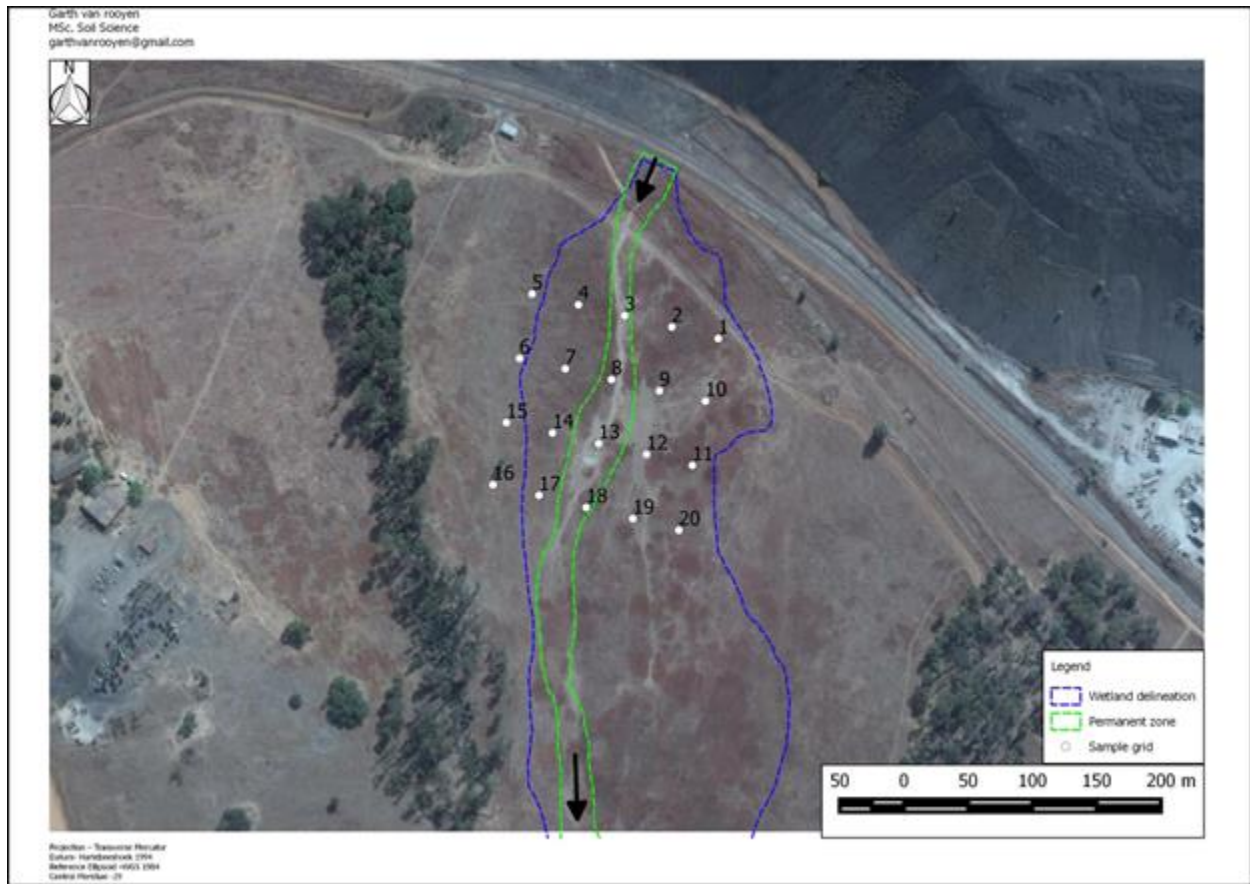


Figure 2.9 Wetland A sample points

2.5.1 Soil classification

The wetland delineation process and soil classification procedure follow the same guidelines as outlined previously. As shown in figure 2.9, Wetland A consists of 20 sample points. Each sample point was augered and the soils were classified according to the taxonomic system for soil classification in South Africa. Hydromorphic and terrestrial soils were identified, if present, for each sample point. Figure 2.10 illustrates the soil map.

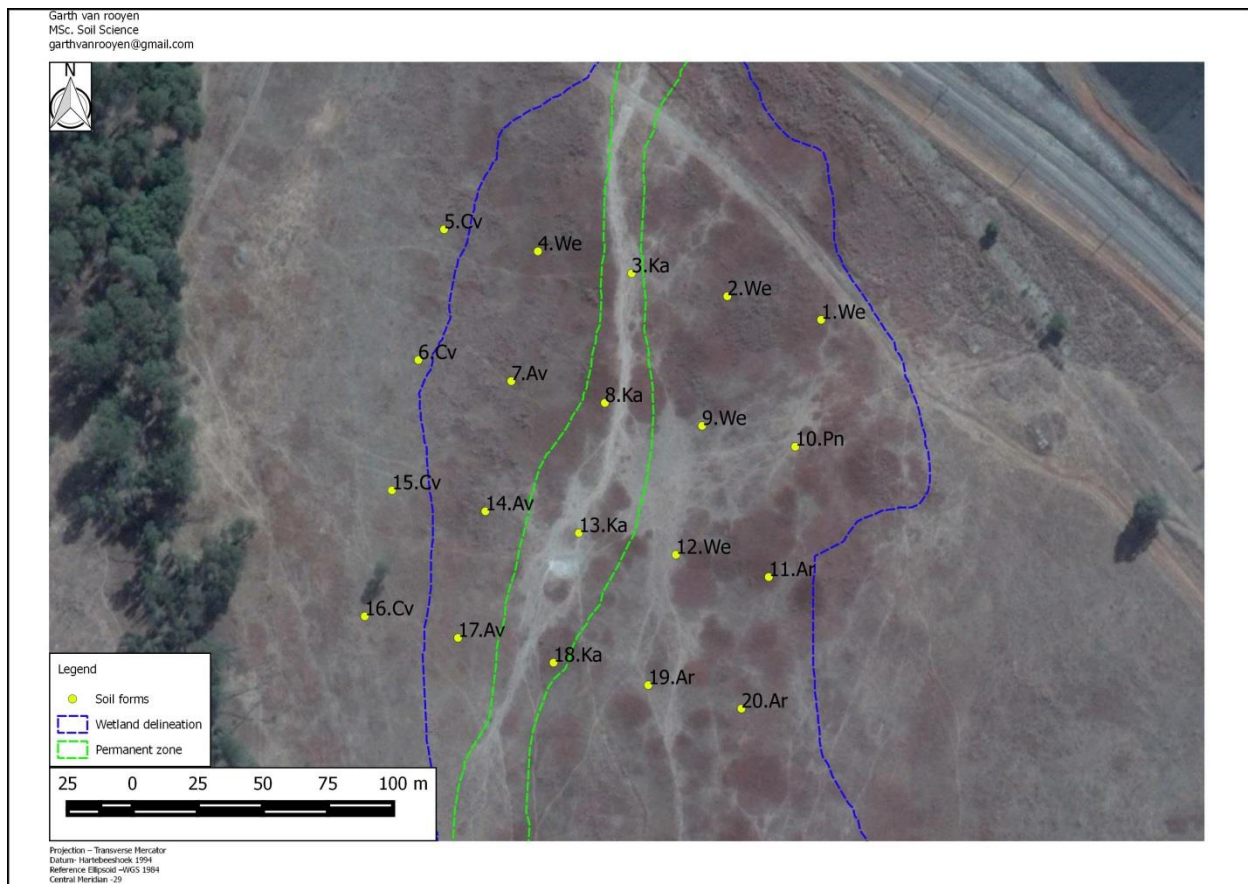


Figure 2.10: Delineation and Soil map for Wetland A

Wetland A proved to be a mineral wetland with the soils identified being mineral soils (<10% organic carbon in the topsoil), meaning no organic O horizons were identified. Soil forms that have been identified at Wetland A are the Pinedene (Pn), Clovelly (Cv), Avalon (Av), Arcadia (Ar), Katspruit (Ka) and Westleigh (We) soil forms. The Katspruit, Westleigh and Avalon soil forms were identified previously at the Rietvlei wetland. The Pinedene and Clovelly soil forms consist of both Orthic A horizons overlying yellow-brown apedal B horizons. The difference between the two soil forms is that the Pinedene has a horizon under the B horizon that is unspecified showing signs of wetness. The Clovelly soil form has the same underlying unspecified horizon, but there are no signs of wetness within 1 500 mm of the soil profile. The Clovelly soil form, in this case, was identified in the terrestrial zone outside of the delineated wetland. The

Pinedene soil form was thus included in the outer regions of the wetland (temporary zone) due to its signs of wetness present in the soil. The notable soil identified in the wetland was the Arcadia soil form, identified at sample points 11, 19 and 20. The Arcadia soil form consists of a vertic A horizon. A vertic horizon according to the Taxonomic System for South Africa (the blue book), is defined as having strongly developed structure with visible slickensides (Soil Classification Working Group 1991). A vertic horizon is dominated by 2:1 smectitic clay minerals. Smectite is a 2:1 clay mineral with a slight negative charge due to ionic substitutions in the octahedral and tetrahedral layers. One of the diagnostic characteristics of smectitic clays, and thus vertic horizons, is that they have the ability to shrink and swell in response to moisture. Water is a polar molecule which can enter the unit layers of smectite and cause the clay to swell. Smectite can therefore also shrink when the water molecules are removed from the unit layers. Vertic horizons can, when dry, exhibit visible cracks on the soil surface. Large cracks were identified in the region surrounding sample points 11, 19 and 20. Amongst various other factors, Vertic horizons can be due to a basaltic igneous bed rock beneath the soil horizon (Soil Classification Working Group 1991). Wetland A is in very close proximity to the Silverton formation which contains basalt, and the geology could be the reason for the presence of a vertic horizon. The visible surface cracks can be seen in the appendix, Figure A5. The regularly occurring slickensides can also be seen in the appendix, Figure A6.

2.5.2 Carbon dioxide emissions for Wetland A

A grid study of 20 sample points measuring the amount of carbon dioxide released was done on the delineated wetland using the same non-dispersive infrared radiation (NDIR) carbon dioxide meter used previously, as well as the same IDW interpolation in GIS software. Figure 2.10 illustrates the interpolated map.

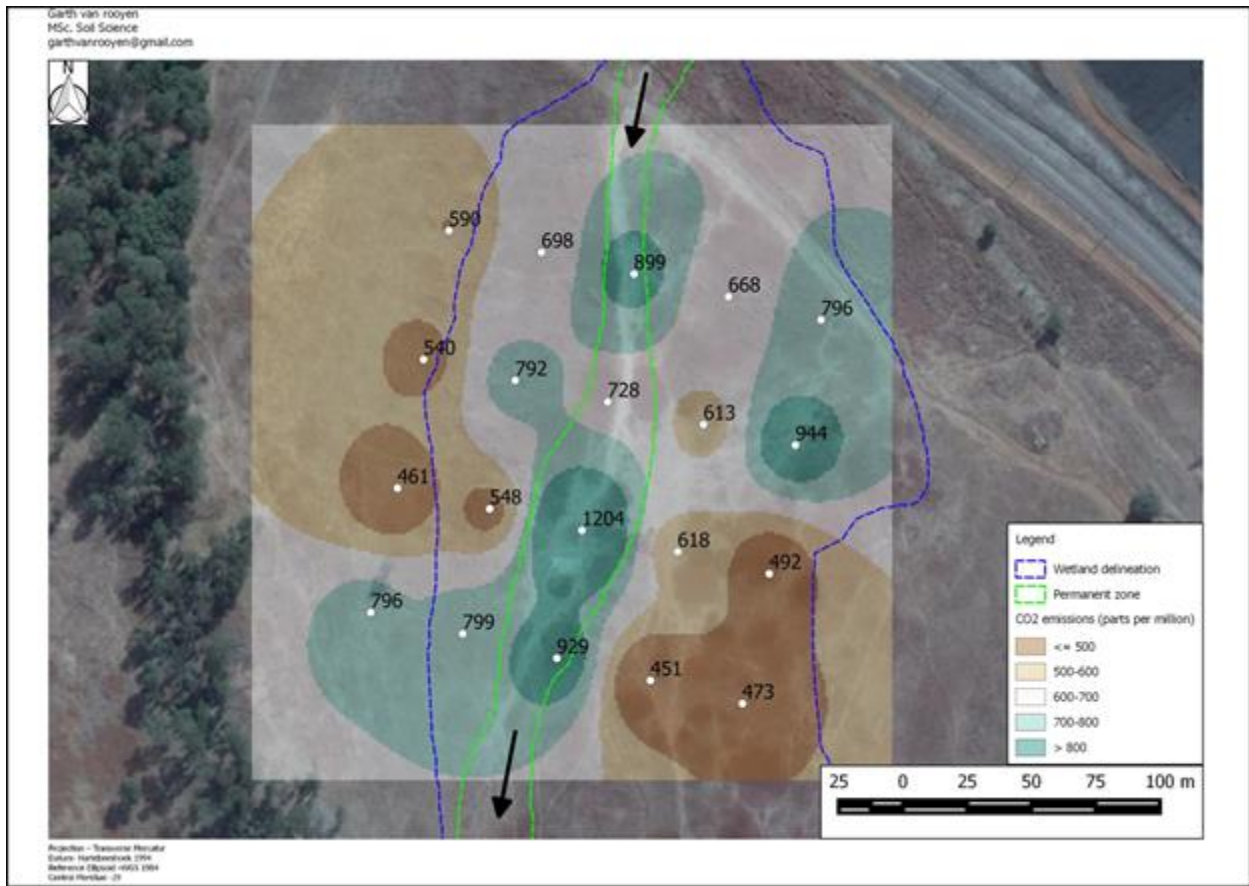


Figure 2.11 Carbon dioxide emissions for Wetland A

From figure 2.11, it can be concluded that the permanent zone of the wetland releases the highest amount of carbon dioxide emissions, as measured in the field. A pattern similar to the study wetland at Rietvlei can be seen in Wetland A, with the amount of carbon dioxide released increasing towards the permanent zone.

To put the measured values into perspective, literature reports soil surface CO₂ readings of 410 ppm for forest peatlands (Astiani *et al* 2015), as well as values ranging from 400-700 ppm for tropical peatlands (Iriana *et al* 2016). The amount of literature quantifying the amount of CO₂ emissions is minimal, especially literature on CO₂ emissions for soil types of Southern Africa. However, from the results, it can be

assumed that values greater than 500 ppm represent highly elevated levels of carbon dioxide emissions. The measured atmospheric CO₂ emissions on site was 380 ppm.

The effluent being fed directly into the permanent zone of Wetland A may be a contributing factor to the high levels of carbon dioxide emissions seen. Sample points 11, 19 and 20 (bottom right section in figure 2.10) were measured as having lower carbon dioxide measurements than the terrestrial zone sample points of 5, 6 and 15 (top left section of figure 3.10). It was not expected that some sections of the wetland were to have lower carbon dioxide measurements than the surrounding terrestrial zone. Sample points 11, 19 and 20 were the vertic soils, and also the soils with the lowest carbon dioxide measurements. The vertic soils had a similar degree of wetness to the surrounding soils, and thus it can be assumed that the cracks in the vertic soils create preferential pathways for carbon dioxide release. This means that when the vertic soils are cracked and exposed to the air, carbon dioxide is assumed to be released almost instantaneously, as opposed to the slow and constant release of orthic mineral soils, and therefore the carbon dioxide measurements will be low and close to atmospheric levels (in this case the atmospheric carbon dioxide measurement was 392 parts per million). In contrast, a moist vertic soil that has been swollen shut might release less carbon dioxide than the same vertic soil that exhibits cracking. Structure in a dry vertic soil is generally moderate to strong angular blocky. Vertic soils are dominated by 2:1 clay morphology, with the Carbon (C) of macroaggregates being 1.65 times higher than that of microaggregates. SOM is expected to be the primary binding agent in 2:1 clay-dominated soils. This can be explained by the organic matter complexes (polyvalent) bridging in between the negatively charged clay surfaces (Six *et al* 2000). This higher level of SOM in 2:1 dominant clays, and the fact that SOM is intimately associated with the clay, thus stabilizing it, could partially explain the lower levels of CO₂ measured in the dry cracked vertic soils. Literature concurs that textural differences in soils tend to exhibit different CO₂ emission patterns, with high clay soils that swell upon the introduction of moisture, having lower CO₂ emissions than sandier soils. Soils that exhibit swelling properties when moist, have difficulty releasing CO₂ into the atmosphere, which in turn limit emission production (Carbonell-Bojollo *et al* 2012).

2.5.3 Spatial pH, EC and redox potential distribution for Wetland A

Field measurements of pH, Electrical Conductivity (EC) and redox potential were also taken (on the same sampling grid). pH and EC readings were taken using the Mettler Toledo portable meter, using the accompanying pH and EC probes. The redox potential measurements were taken using a Sentix Oxidation-Reduction probe (ORP). The interpolated CO₂ map spatially illustrates the distribution of CO₂ release within the wetland.

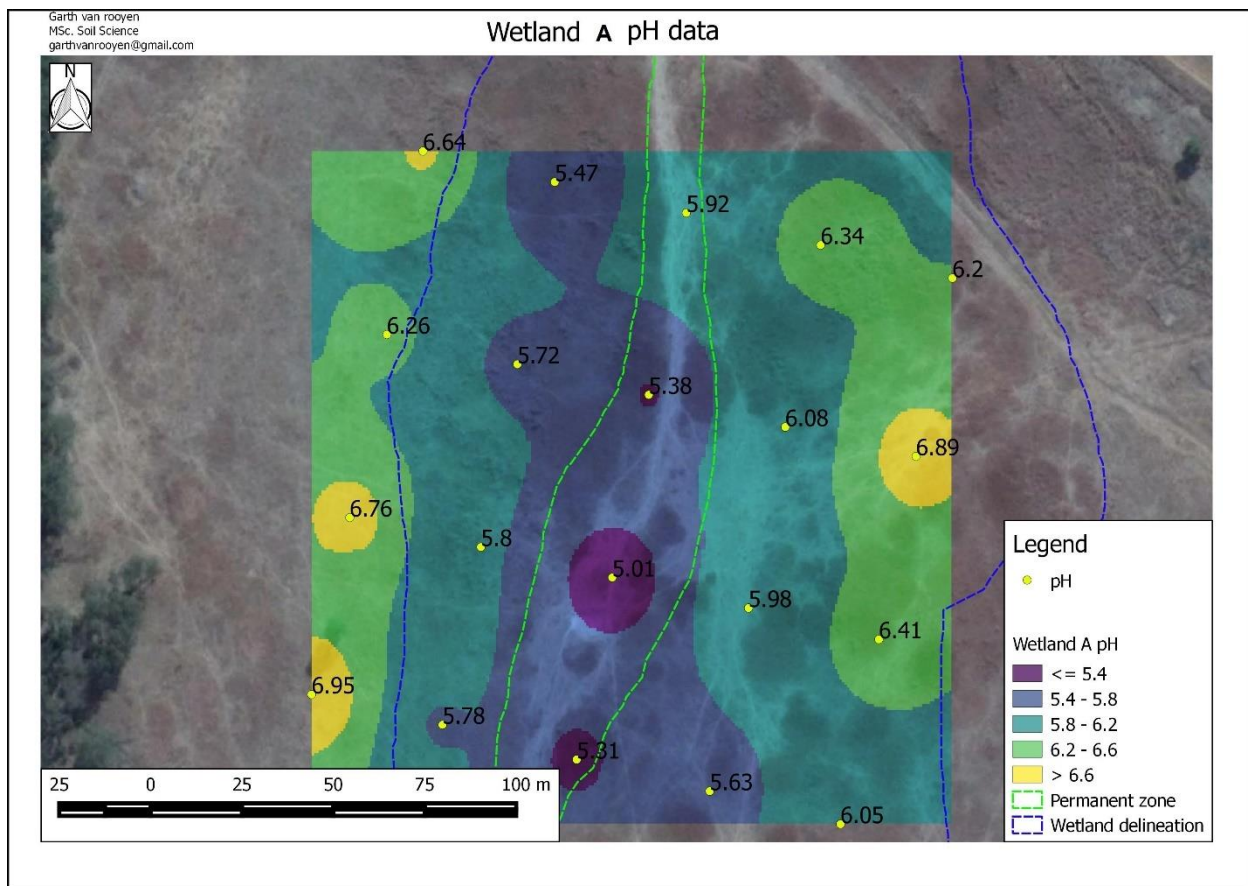


Figure 2.12: Wetland A spatial pH distribution

It is visually apparent that the permanent zone of Wetland A had the lowest pH measurements, with the pH generally increasing the further you move away from the permanent zone.

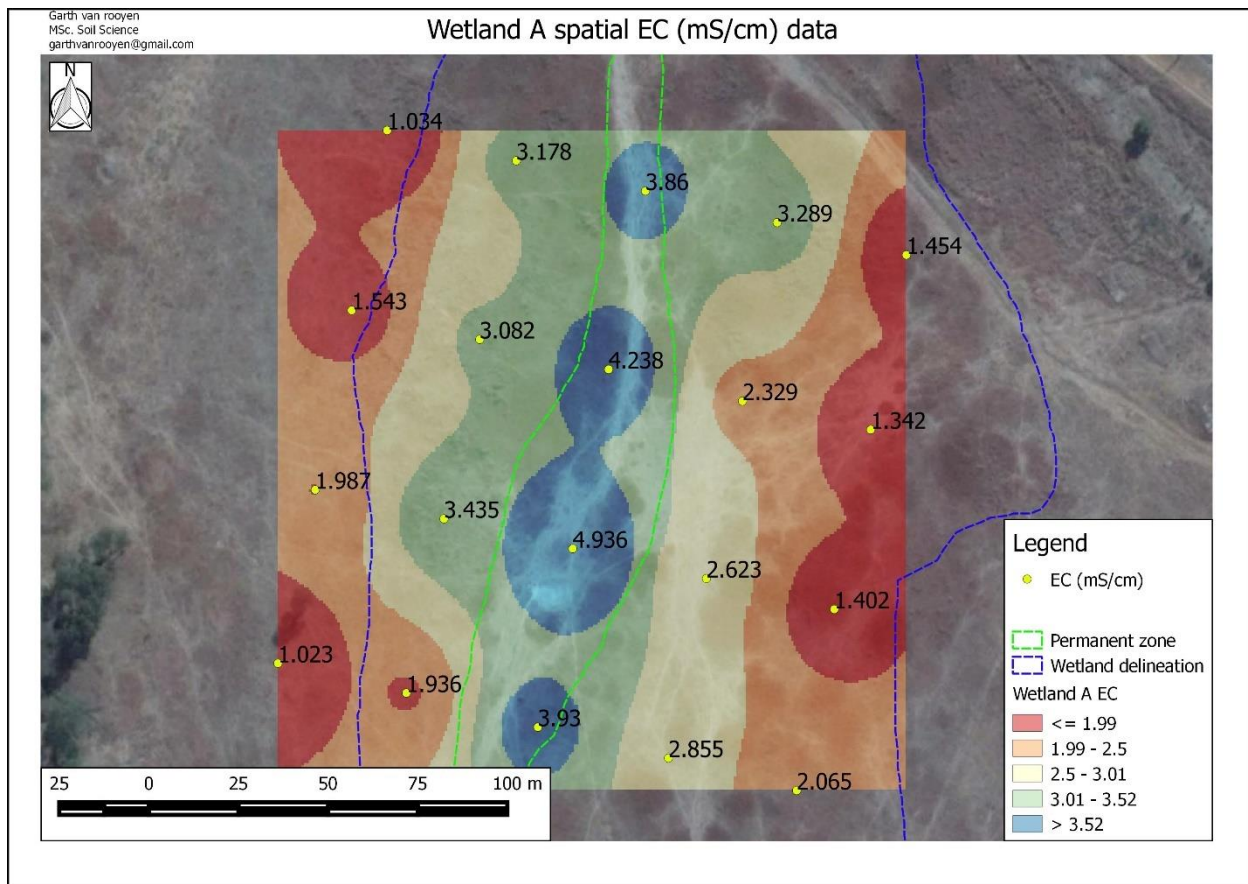


Figure 2.13 Wetland A spatial EC distribution

The permanent zone of wetland A contains the highest EC measurements, ranging from 3.86 mS/cm to 4.936 mS/cm. The salinity of the permanent zone will result in organisms and plants experiencing salt stress, such as rates of metabolism and nutrient cycling (DWAFF 1996). The high salinity can be a result of the effluent discharge, as well as the acid-base chemistry where the neutralization of an acid generates salts. The further you move away from the permanent zone of the wetland, the lower the EC becomes. The reason for the higher EC measurements in the permanent zone is because of salt accumulation, especially due to the surrounding industrial activity. The permanent zone acts as the ‘zone of accumulation’ in the landscape, thus causing soluble salts (such as sulfates) to accumulate in this zone.

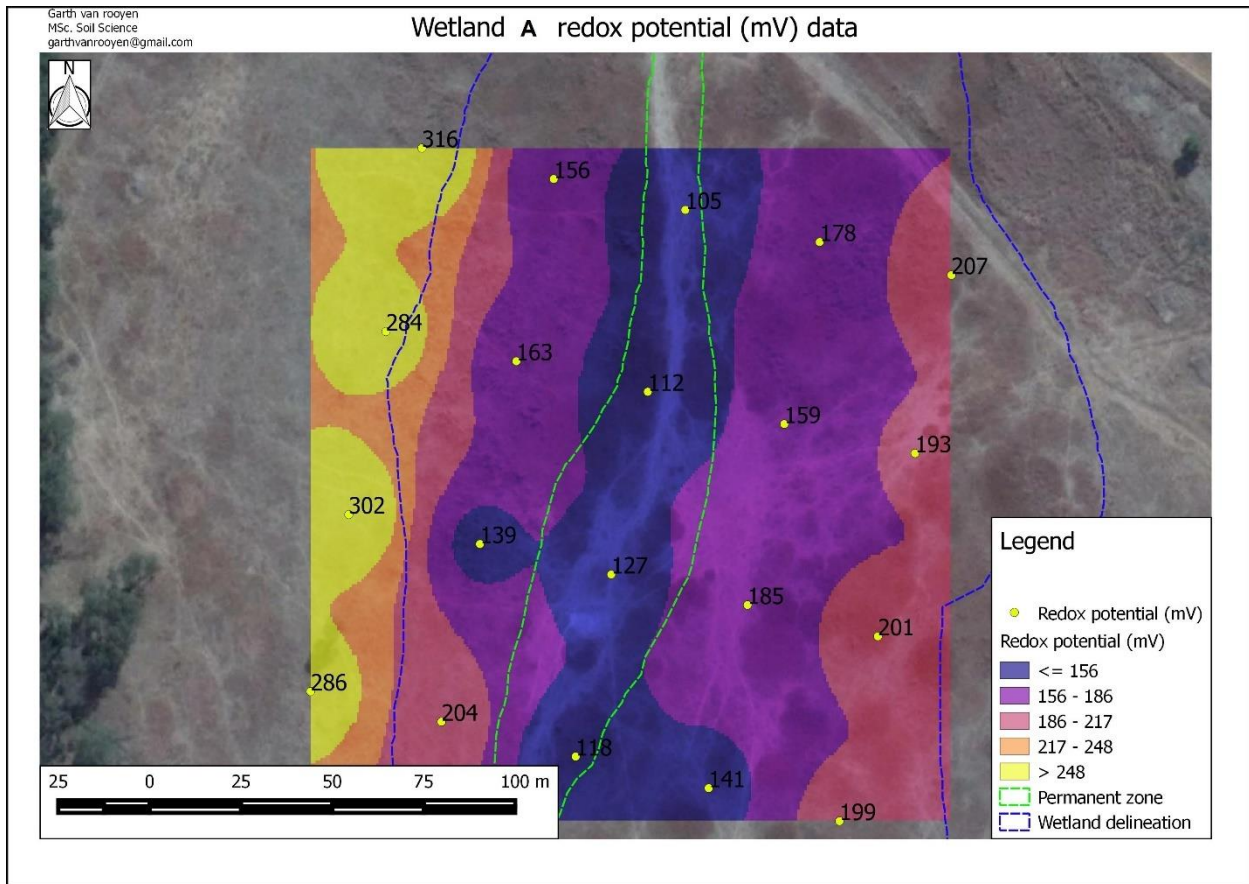


Figure 2.14 Wetland A spatial redox potential distribution

The spatial distribution of redox potential data shows a good correlation with wetland zones. The permanent zone having the lowest redox potential readings (although still high per water quality guidelines) and the outer terrestrial zone having the highest redox potential measurements. An increase in soil saturation can normally lead to a decrease in reduction-oxidation potential. Physical processes such as the limitation of atmospheric gas diffusion can result in finite amounts of oxygen in soil pore spaces. The available oxygen is partially depleted by soil reductants and microorganisms. The chemical changes that occur during prolonged soil saturation can include denitrification and the reduction of iron and manganese (Pezeshki and DeLaune 2012). These physical and chemical processes associated with prolonged saturation causes lower redox potentials in saturated soils.

2.6 Wetland B

Wetland B was chosen as the rehabilitated wetland study site. Wetland B is commonly known as the Zaalklapspruit wetland, which forms part of the Grootspuit and Zaalklap watercourses, and was rehabilitated in 2013 through a South African National Biodiversity Institute (SANBI) initiative together with Working for Wetlands (SANBI 2014). The rehabilitation of the Zaalklapspruit wetland was a success and the following positive changes were acknowledged post rehabilitation (de Klerk *et al* 2015):

- Increased gravitational drainage
- Increased soil contact, increasing the filtration and pollutant removal mechanisms of the wetland
- pH restored from 3.5 to levels in the natural freshwater range (5.5-7)
- Alkalinity increased to natural freshwater level range
- Sulphates decreased by 65 percent (concentration)
- Total Dissolved Solids (TDS) concentration decreased by half
- Chlorophyll α concentration increased
- Overall ecological function improved

The soil classification map is illustrated in figure 2.15. The wetland delineation process and soil classification procedure follow the same guidelines as outlined previously. Wetland B has erratic soil distribution and the design of the sample grid was done in such a way as to try and cover a section of the wetland that contains all three wetland zones. White patches surrounding the Zaalklapspruit wetland permanent zone can also be seen in figure 2.11 (near sample point 4 and 2). The white areas are sulphate precipitates from the upstream industrial activities (visible in Fig 2.15), including Highveld Steel and Elandsfontein Colliery. Acid mine drainage is often limed before leaving a mine in an effort to increase the pH of the effluent. The gypsum precipitation could also have been created where the alkaline Highveld Steel effluent met and neutralised the AMD from the coalmines, leaving gypsum as a signature of the neutralisation that occurred. The gypsum was visible on the surface of the shallower signs of wetness soils, such as the Westleigh soils.

A photograph of the white precipitate (gypsum) can be seen in the appendix. Upon site investigation, it was evident that successful rehabilitation had been done on the wetland. The Zaalklapspruit wetland is extremely modified, with gabions and concrete structures present at several intervals along the permanent zone of the wetland (see appendix).

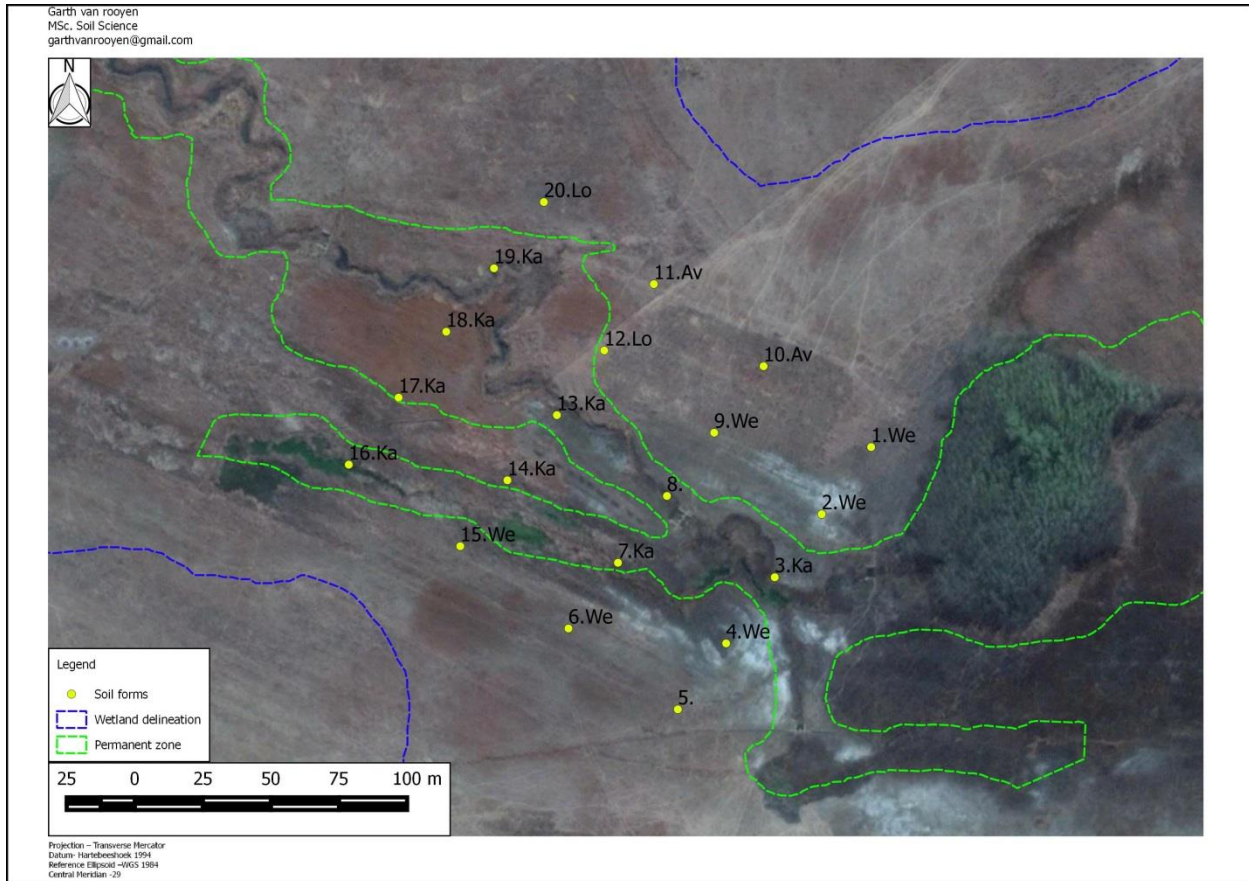


Figure 2.15 Wetland B soil forms

Sample point 5 contained heavily disturbed soils and thus does not have a soil form assigned to it. Sample point 8 does not have a soil form assigned to it either as this sample point contains flowing water (stream). The soil forms identified within the study area consisted of the Avalon soil form in the temporary zone, Westleigh and Longlands soil form in the seasonal zone, and the Katspruit soil form in the permanent zone. All

soil forms have been identified at either the Rietvlei wetland or Wetland A, with the exception of the Longlands soil form. The Longlands soil form is characterised by an Orthic A horizon overlying an E horizon which is overlying a soft plinthic B horizon. An E horizon is generally a bleached horizon often lighter in colour than the overlying horizon (Soil classification working group 1991). An E horizon has gone marked *in situ* removal of iron oxides (such as ferric iron reduction removal), organic matter and silicate clay (colloidal matter), and is therefore not seen as a gleyed horizon. An E horizon can also be distinguished using a Munsell soil colour, where the colour of an E horizon changes values and chroma upon drying. The location of the E horizon within wetland A was found at sample points 12 and 20. Since the sample grid only covered a small portion of the wetland, it is expected that a significant area of the seasonal/temporary of the larger wetland area may contain E horizons, which could indicate sub surface lateral water flow into the lowest point of the landscape.

The E horizon for both sample points 12 and 20 had a moist Munsell soil colour value of 5YR 4/1. After drying, the Munsell soil colour value changed to 5YR 6/1. According to the taxonomic system for South Africa, it states that an E horizon, if hue is 5YR, then values of 5 or more and chromas of 2 or less should be seen in the dry state. The E horizon felt sandy and gritty to the touch with a notable absence of clay.

2.6.1 Carbon dioxide emissions for Wetland B

The same method was used to measure the carbon dioxide emissions using an NDIR carbon dioxide meter and IDW interpolation. Figure 2.12 illustrates the interpolated map.

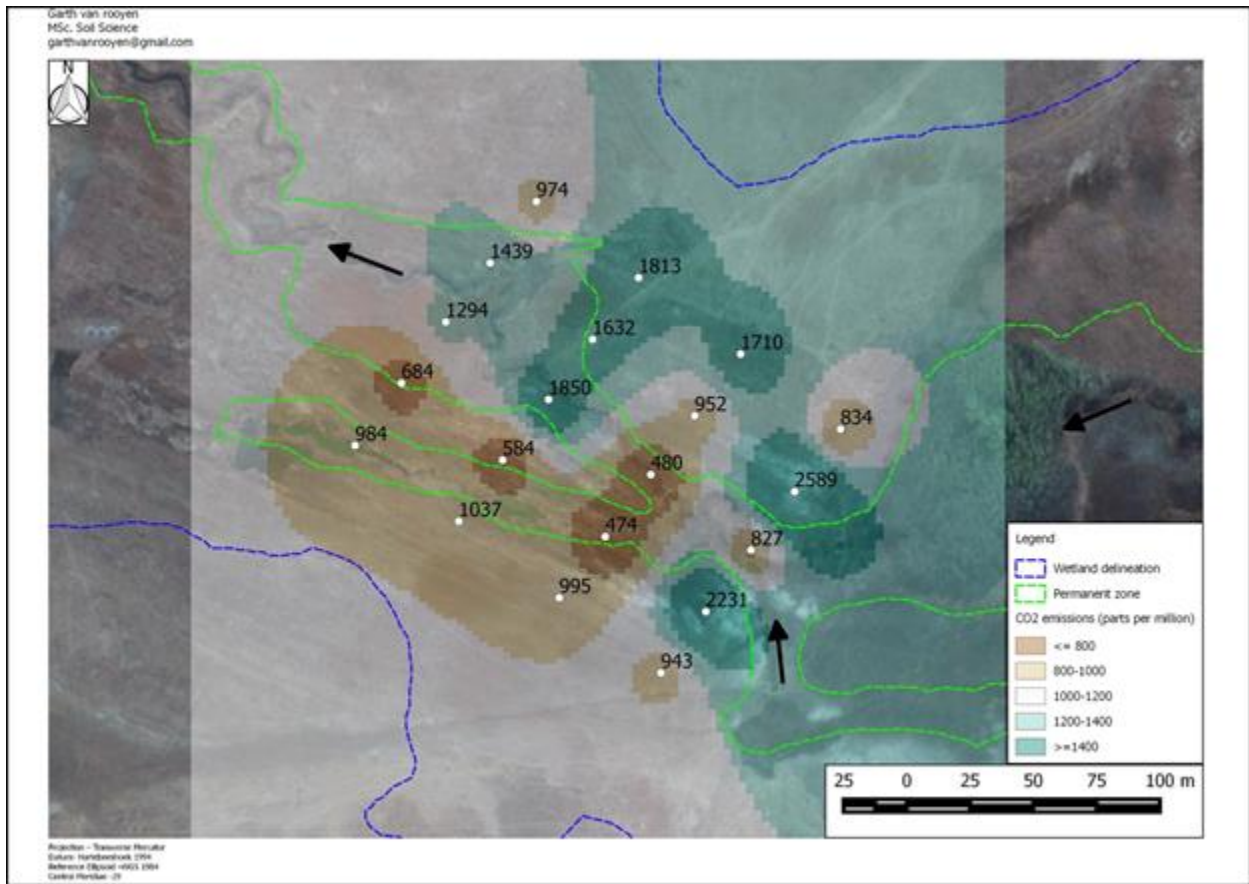


Figure 2.16 Carbon dioxide emissions for Wetland B

The distribution of carbon dioxide readings had a large range, ranging from the lowest value of 474 ppm to the highest value of 2589 ppm.

The delineation of the wetland was extensive, as shown by the blue dashed line. Wetland B is again a mineral wetland, containing no peat (%C>20%). No clear carbon dioxide emission trends can be drawn from these results, which in itself is a result because this confirms the level of disturbance and the spatial heterogeneity of the wetland. The permanent zone does not necessarily have the highest emissions, as seen at the previous study wetlands, nor do the sample points in the temporary zone have the lowest carbon dioxide emissions. Some of the highest carbon dioxide measurements were in fact in the temporary and seasonal zone, with sample points 11

and 10 (temporary zone) having carbon dioxide readings of 1710 parts per million and 1813 parts per million respectively. Sample point 7, which is in the permanent zone, had the lowest carbon dioxide reading of 474 parts per million. Because the EC of the soils have high ranges, the lowest EC recorded being 0.863 mS/cm and the highest EC recorded being 2.386 mS/cm, the soils have a similar erratic CO₂ emission pattern. A possible explanation for the spatial EC variability could be that the E horizons (lateral flow) is responsible for lower EC measurements (filtering effect), where the higher EC measurements are a result of overland flow. Variations in salinity as well as variations in wet-dry cycles, will lead to changes in CO₂ emissions (Liu *et al* 2017). The dissolved organic carbon (DOC) is also expected to have high levels of spatial variability. The increase in salinity will ultimately lead to a decrease in plant activity within the wetland. This means that carbon input into the wetland will be slower when salinity is increased. This ultimately leads to a lower level of microbial activity and slower DOC decomposition rates (Setia *et al* 2013).

Because the Zaalklap wetland has been extremely modified and rehabilitated, the wetland does not quite function as a 'healthy' wetland. The permanent zone is irregular and the transition from seasonal to the temporary zone is not easily identifiable. The carbon dioxide, pH, EC and redox measurements (see Table A4 in the Appendix) taken from the Zaalklap wetland (Wetland B) align with the hypothesis that a recently rehabilitated wetland will not act and behave as an older wetland that is in a state of equilibrium. The study on the Zaalklap wetland was done four years after rehabilitation, and although some wetland parameters such as pH and alkalinity levels have stabilised to healthy levels, the carbon and microorganism function of the wetland has clearly not been restored. Moreno-Mateos *et al* 2012, researched 612 wetlands from across the world that were studied for several years in order to assess the effect that restoration (rehabilitation) has on wetlands in comparison to reference wetlands. The storage of carbon was well documented throughout the studies. The storage of carbon and nitrogen was drastically reduced immediately after rehabilitation took place. After rehabilitation, responses appeared variable. Carbon storage increased initially but then

flattened out below reference levels (see Fig 2.17). Reasons for this being that degradation, or disturbance, to wetlands causes oxidation of stored accumulated organic carbon and releases CO₂ into the atmosphere, where microbial activity under aerobic conditions accelerates the process. As time goes on and as hydrological regimes are restored, anaerobic conditions allow the organic carbon to accumulate again in the soil. After 20 years, soil carbon storage in rehabilitated wetlands were still 50% lower than reference wetlands, where organic matter slowly accumulated to 62% of the original reference wetlands (Moreno-Mateos *et al* 2012). In certain study wetlands after 50 years, organic matter accumulation only reached a maximum of 74% of the original reference wetland values.

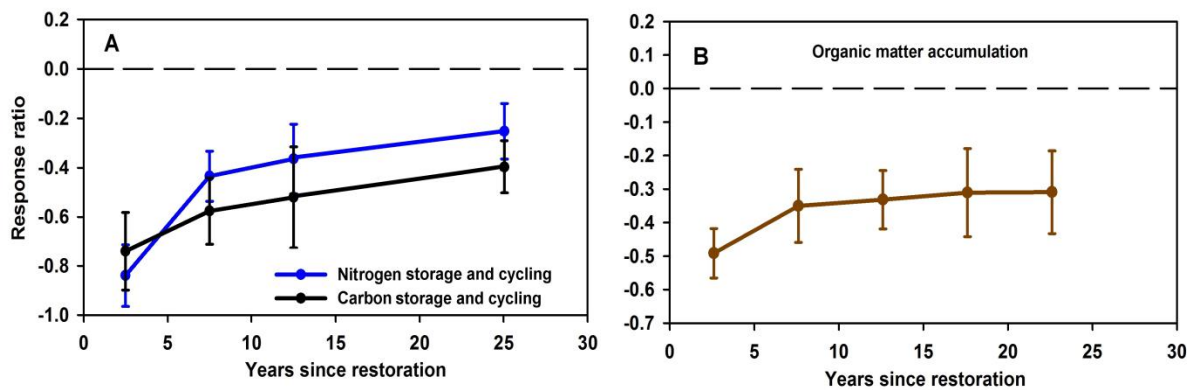


Figure 2.17 Carbon storage and organic matter accumulation after wetland restoration (Moreno-Mateos *et al* 2012) The ‘zero value’ dashed line represents reference wetlands.

The carbon content of the wetland and the microorganisms play a major role in the release of carbon dioxide and methane gas into the atmosphere, as well as sequestration of carbon. Once the soil becomes disturbed, carbon function is disturbed and the equilibrium between microbial activity, soil organic accumulation rates and carbon fluxes become seriously altered. Concrete structures in the Zaalklap wetland cause changes to inundation patterns, which have caused localised flooding or pooling

of water. CO₂ release is a result of oxidation, and since CO₂ gas cannot escape as efficiently through water than it can through atmospheric air, lower CO₂ readings were recorded in inundated regions. In one area on the Zaalklap wetland, carbon dioxide was not being released through a pool of water, and once the soil was disturbed with an auger, large quantities of carbon dioxide was released (see figure A10 in the appendix for a photograph of gasses bubbling out the water once disturbed). The rate of carbon accumulation together with the carbon storage and cycling rates have not reached reference levels. It is still uncertain what the case may be in the long term, but certainly in the short term, the Zaalklap wetland a long way to go before it acts as a healthy wetland. The real issue is that restored wetlands equilibrate its hydrological regime to that of its environment, and the environment of the Zaalklap is one of large-scale environmental degradation due to mining.

2.6.2 Spatial distribution of pH, EC and redox potential for Wetland B

The field measurements were again interpolated using IDW interpolation to spatially illustrate the pH, EC and redox potential measurements.

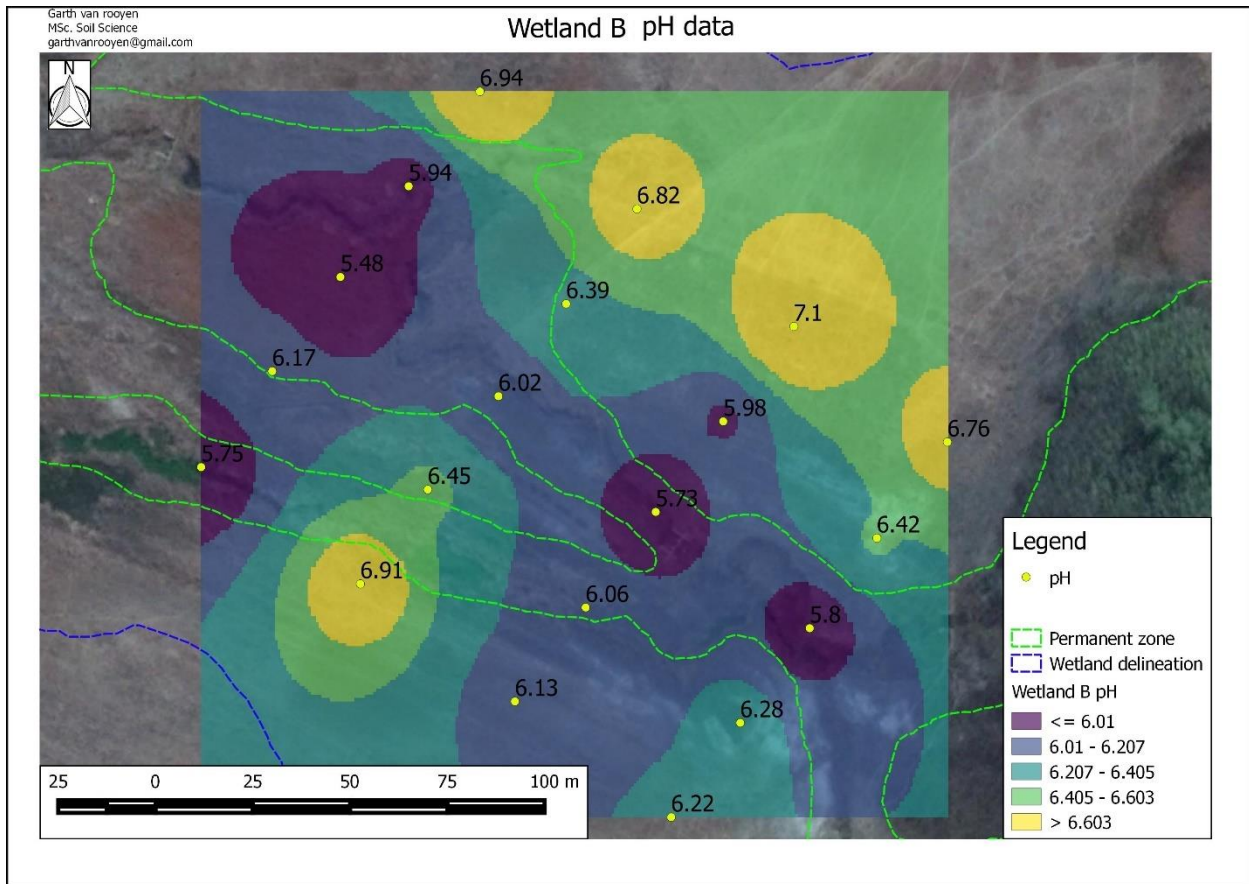


Figure 2.18 Wetland B spatial distribution of pH data

The pH distribution does not follow a definitive correlation with the wetland zones, however the permanent zone tends to exhibit lower pH values than the surrounding seasonal zone.

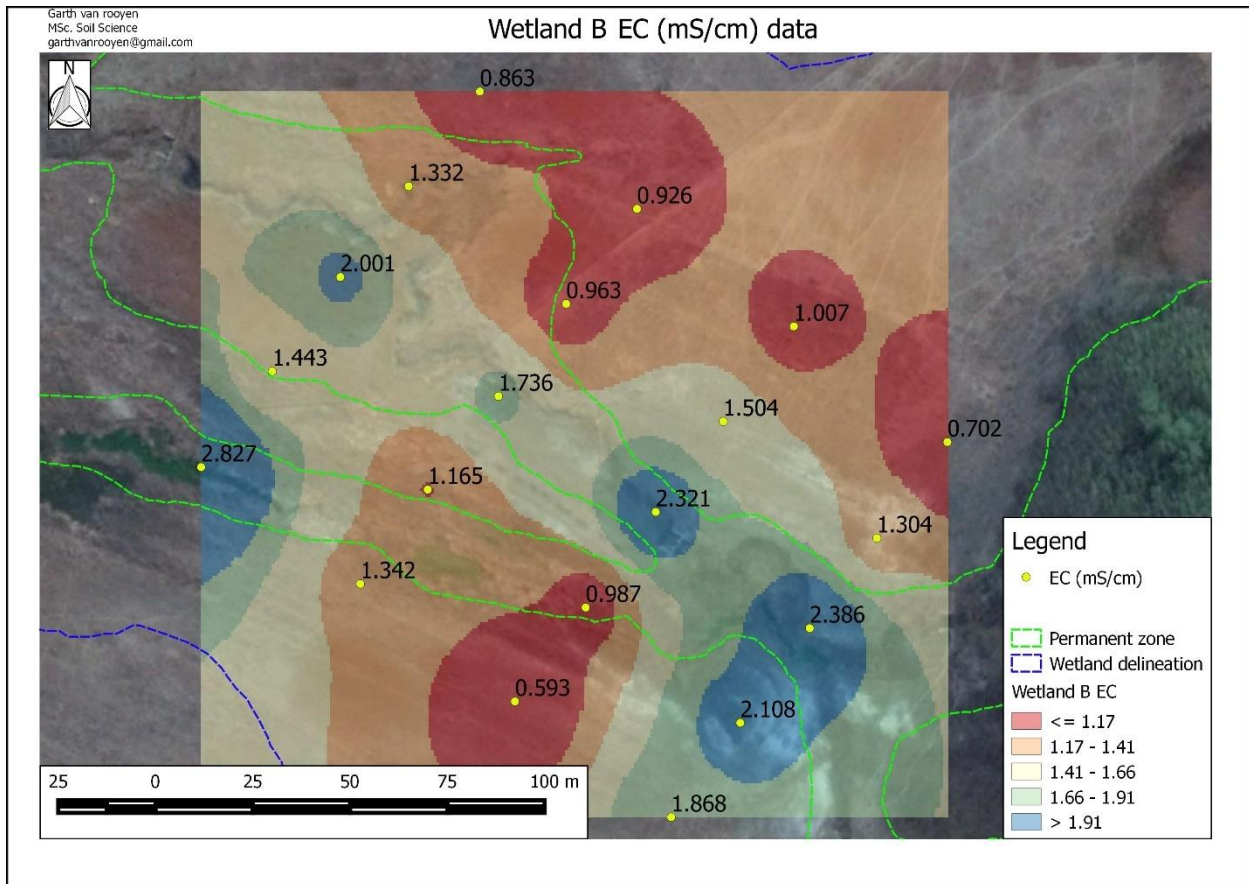


Figure 2.19 Wetland B spatial distribution of EC data

The measured Electrical Conductivity for Wetland B shows a moderate correlation with the permanent zone. The south-eastern section of the study site (EC readings of 2.386 mS/cm and 2.108 mS/cm) showed some of the highest EC readings, with visible white sulfate precipitation on the soil surface (see Appendix Figure A9).

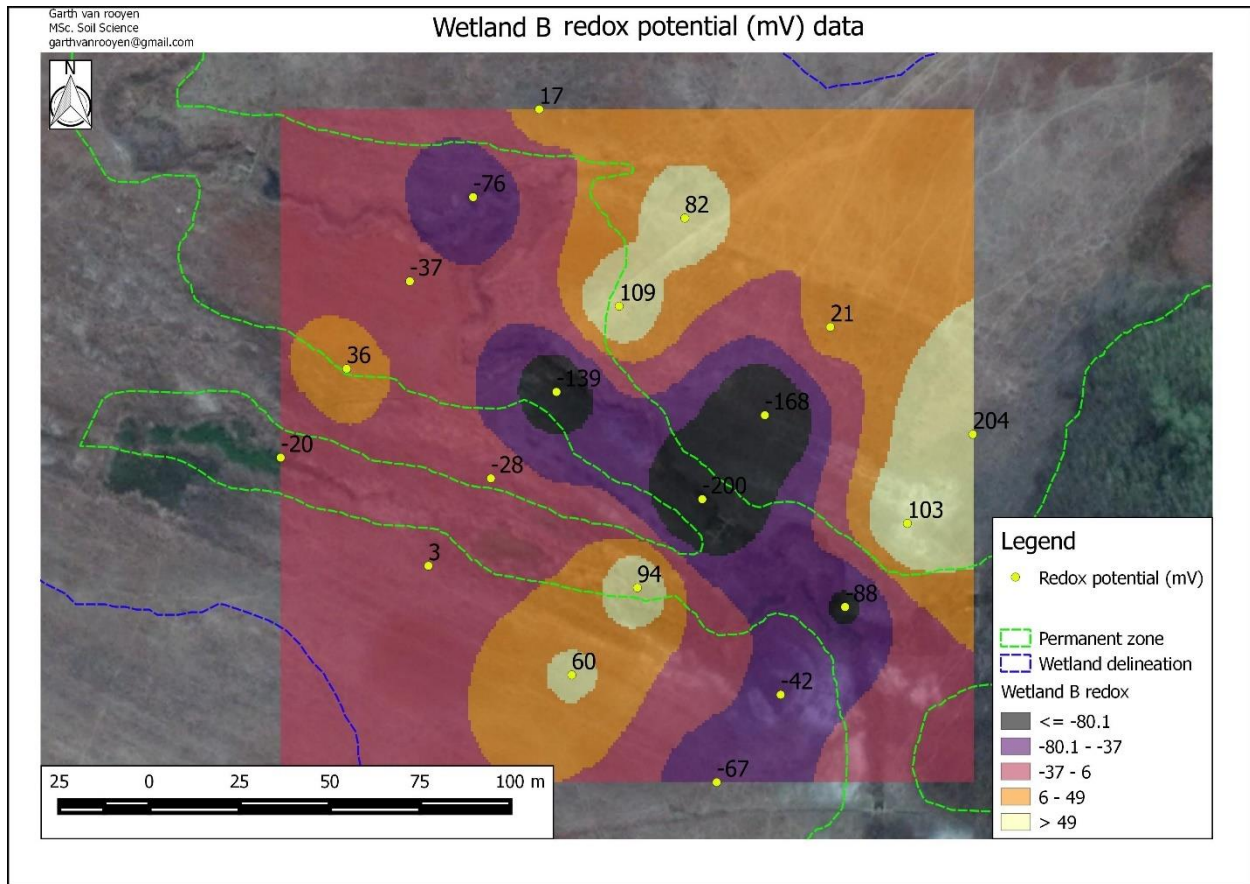


Figure 2.20 Wetland B spatial distribution of redox potential data

The redox potential measurements show no correlation with the wetland zones. The redox potential shows a mix between reduced and oxidised conditions scattered throughout the system. This is typical of a disturbed wetland system.

2.7 Wetland C

Wetland C was chosen as the reference wetland that has not been directly impacted by mining activities, with no effluent being directly discharged into the wetland. Wetland C is also an organic wetland, which is comprised of an organic O horizon in the permanent zone. The organic carbon percentage of the O horizon is 19.7%. Note that this is very close to a diagnostic peat horizon. This wetland was used as a reference in a previous study by de Klerk *et al* (2015). The reason this wetland is ideal is the negligible

disturbance it experienced, especially from mining. According to the article by de Klerk *et al*, the sulfate concentrations, alkalinity, total dissolved solids and pH remained the same throughout their sampling period, which included periodic site visits between 2013 and 2014, with emphasis being placed on sampling during the same hydrological regime and seasons. This supports that no effluent is being discharged into the wetland, as mine affected wetlands would exhibit fluctuating values with each effluent discharge. Wetland C was saturated and the wetland delineation process and soil classification procedure follows the same guidelines as outlined previously. The permanent zone of Wetland C was quite extensive and made up more than half of the delineated wetland (for the study section). Figure 2.21 illustrates the soil forms.

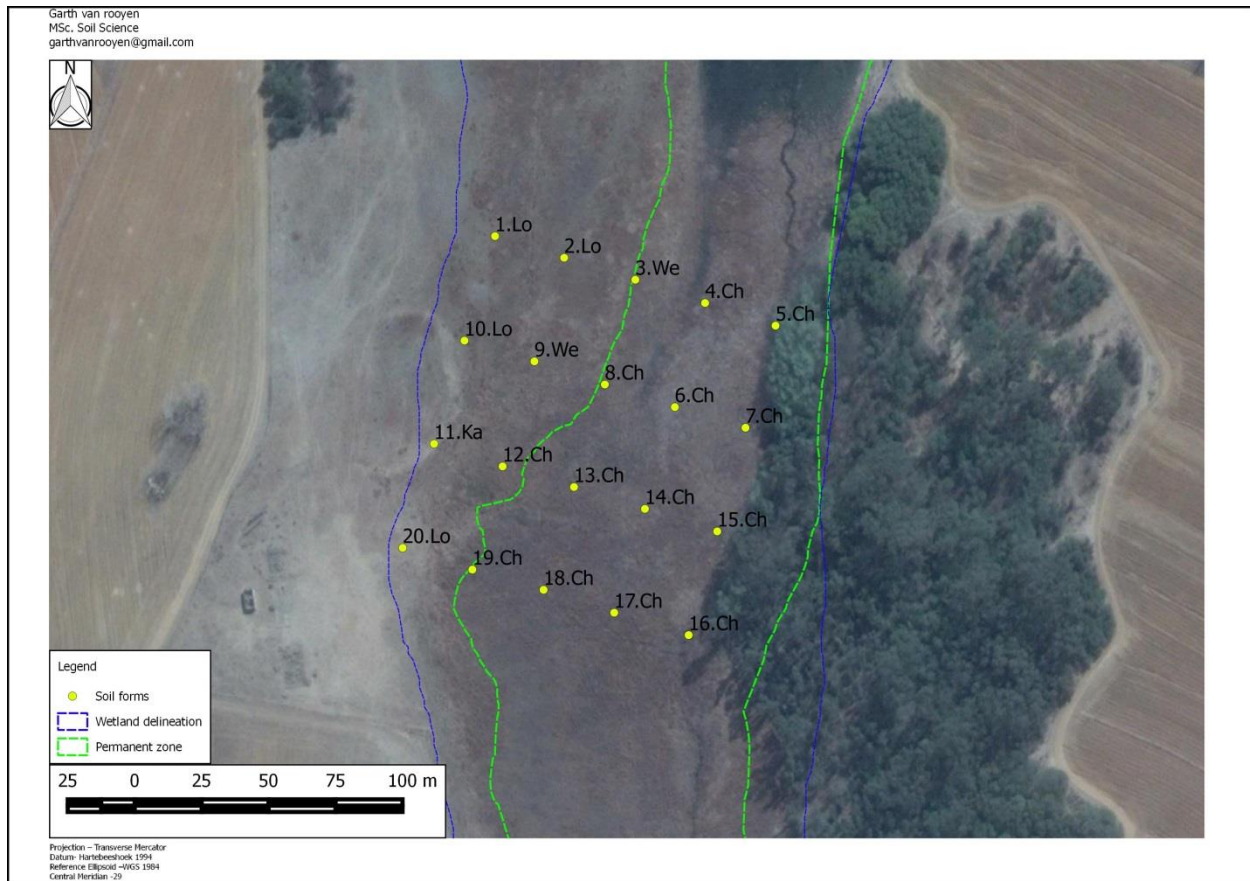


Figure 2.21 Wetland C identified soil forms

The soil forms that were identified within the study area of Wetland C included the Longlands soil form, Westleigh soil form, Katspruit soil form and the Champagne soil form.

The Champagne soil form consists of an organic O horizon. The O horizon, according to the South African taxonomic system is an organic horizon formed at the surface through the accumulation of plant material under anaerobic or non-anaerobic conditions. The organic material can vary from debris to loose leaves, to decomposed organic material (Soil Classification Working Group 1991). All samples were augered to a maximum possible depth, which was 2100 millimeters. No bedrock or saprolite was encountered and fibrous plant material was visible in all organic O samples. The soil form is therefore Champagne 1200 soil form, with the soil family being the Manhica family (fibrous plant material dominant and underlying material not consolidated). Due to the heterogeneous nature of the O horizon, the Munsell soil values varied across each sample, although an 'average' soil colour that was experienced was 10R 1/1 (black), with the ever so slight reddish hue coming from the hydrous ferric oxide precipitates at the suboxic-redoxic interface (see appendix, Figure A12).



Figure 2.22 O horizon sample at 400 mm depth

2.7.1 Carbon dioxide emissions for Wetland C

The same method as outlined previously was used to measure the carbon dioxide emissions using an NDIR carbon dioxide meter and interpolated using IDW interpolation in GIS software. Figure 2.23 illustrates the interpolated map.

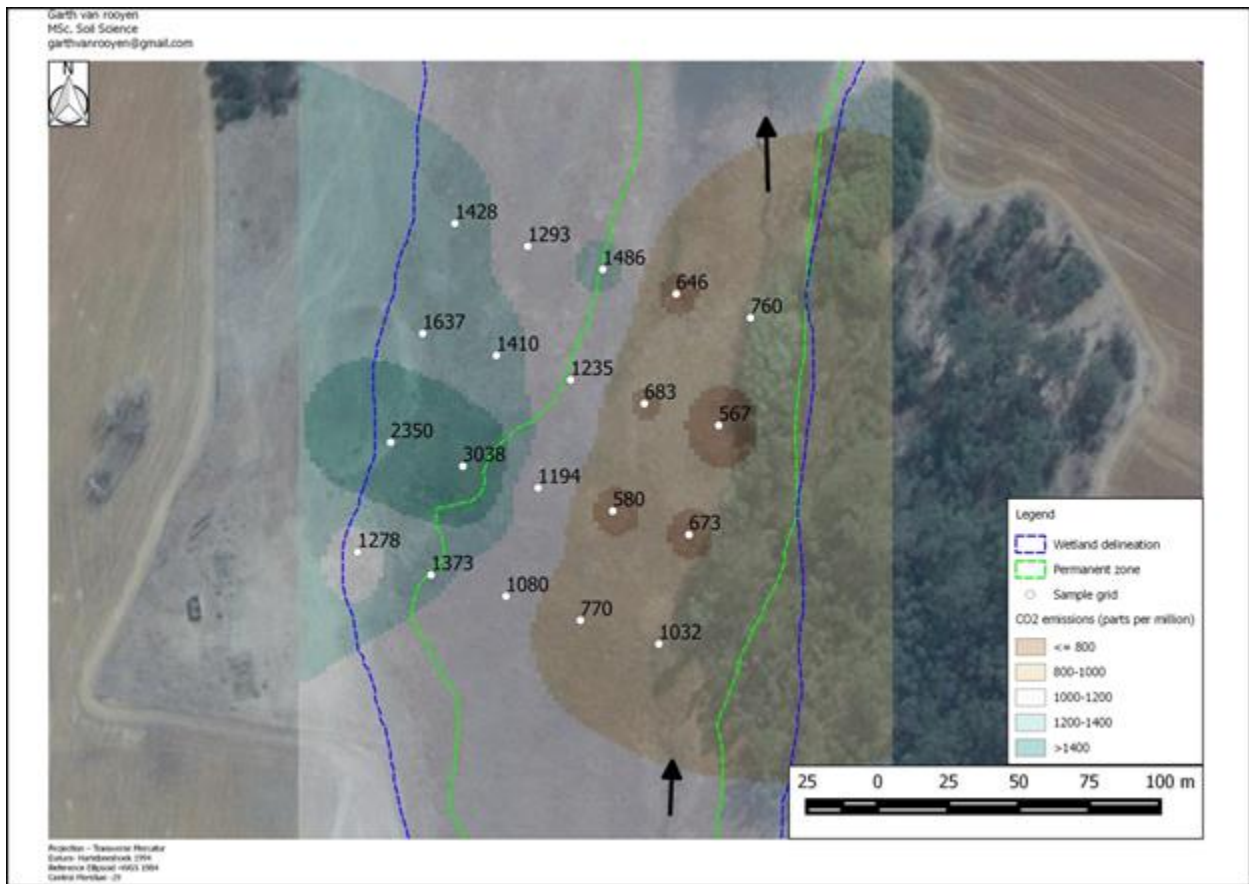


Figure 2.23 Carbon dioxide emissions for Wetland C

In the organic Wetland C, the permanent zone has lower carbon dioxide readings than the adjacent seasonal and temporary zones to the west. This trend seen here in an organic wetland is opposite to the trends seen in the mineral wetlands, where the carbon dioxide emissions increase upon increasing wetness, and increases towards the permanent zone of the wetland. This trend stayed true for all four west to east transects. The lowest carbon dioxide reading was 567 parts per million, which was the closest to

the atmospheric level reading of 392 parts per million. The highest carbon dioxide reading was measured at sample point 12, measuring 3038 parts per million of carbon dioxide, followed by the next highest reading of 2350 parts per million at sample point 11. Point 12 is an unsaturated soil in the temporary zone. The high organic content shows that it is periodically saturated. At this sample point, there is more of the important electron acceptor oxygen here, which then oxidises carbon from C(0) to C(+4) during aerobic microbial respiration. The highest measurement at sample point 12 comprised of a dry O horizon. This is significant as the lowest carbon dioxide measurement was 567 parts per million at sample point 14, which comprised of a wet, saturated O horizon. When the water table drops within an organic wetland (typically a peatland), the organic horizon changes from a source to a sink of methane due to higher levels of methane oxidation. Since some carbon dioxide is formed through methane oxidation, this would ultimately lead to higher levels of carbon dioxide release in peatlands with lower than usual water tables (Freeman *et al* 2004). This tells us that saturated organic soil is at equilibrium with its environment under anaerobic conditions, and does not release significant carbon dioxide emissions when saturated, possibly due to the dissolved oxygen levels being low. However, when the organic soil dries out completely, higher levels of carbon dioxide are released when the environment is aerobic. The low carbon dioxide release could be why these soils are so high in organic material as they are not releasing their carbon, but rather storing it. This is a very important factor when considering the effect that mining related effluent will have on organic wetlands (as well as mineral wetlands) which will immediately change the chemistry of these soils. The introduction of acid mine drainage into wetlands could potentially enhance the release of carbon dioxide from these wetlands, Because of increase in dissolved oxygen levels or dissolved ferric iron. Oxidation reactions (biological or non-biological) are less favourable at low pH.

2.7.2 Spatial distribution of pH, EC and redox potential data

The interpolated data is illustrated below.

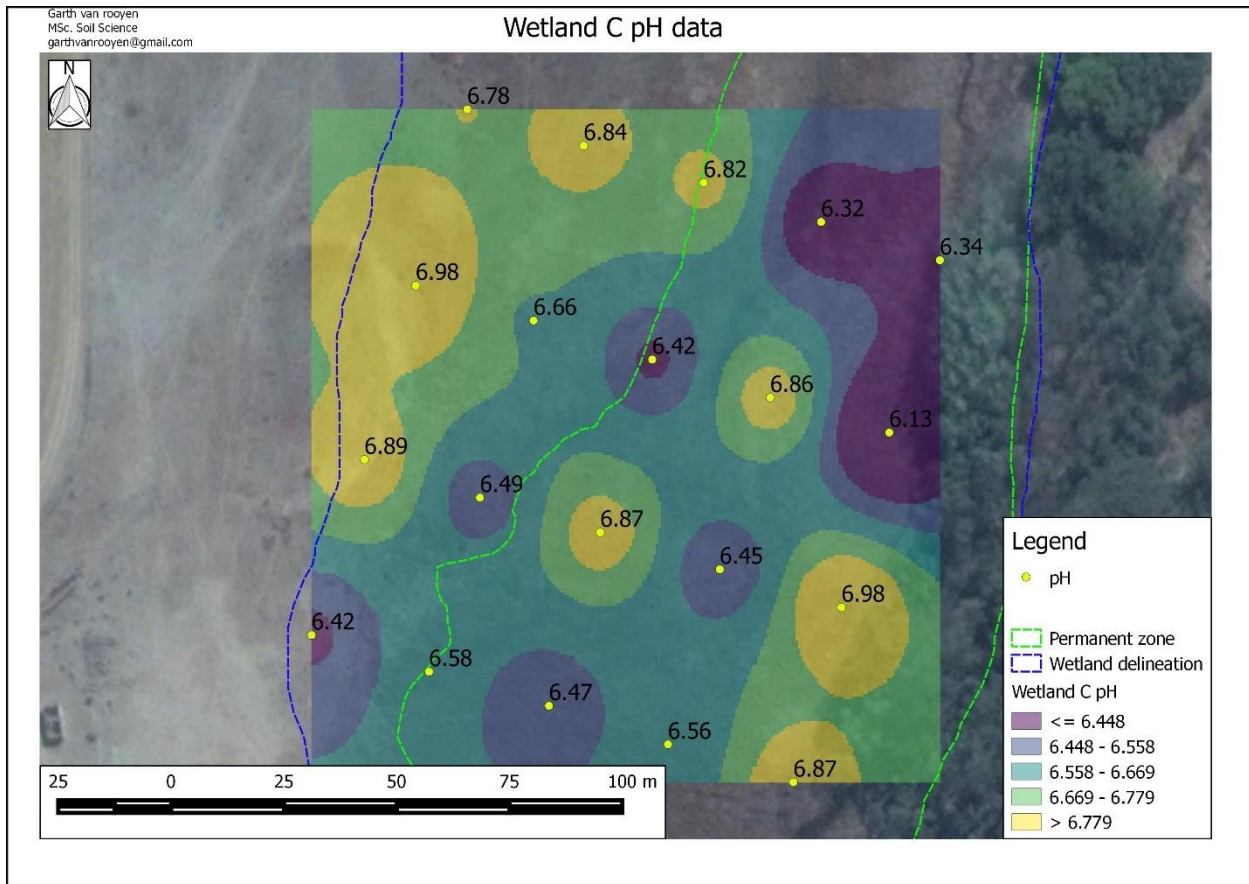


Figure 2.24 Wetland C spatial distribution of pH data

Wetland C showed no correlation with the wetland zones. The range of pH values were rather small, with 6.13 being the lowest measured pH and 6.98 being the highest measured pH value.

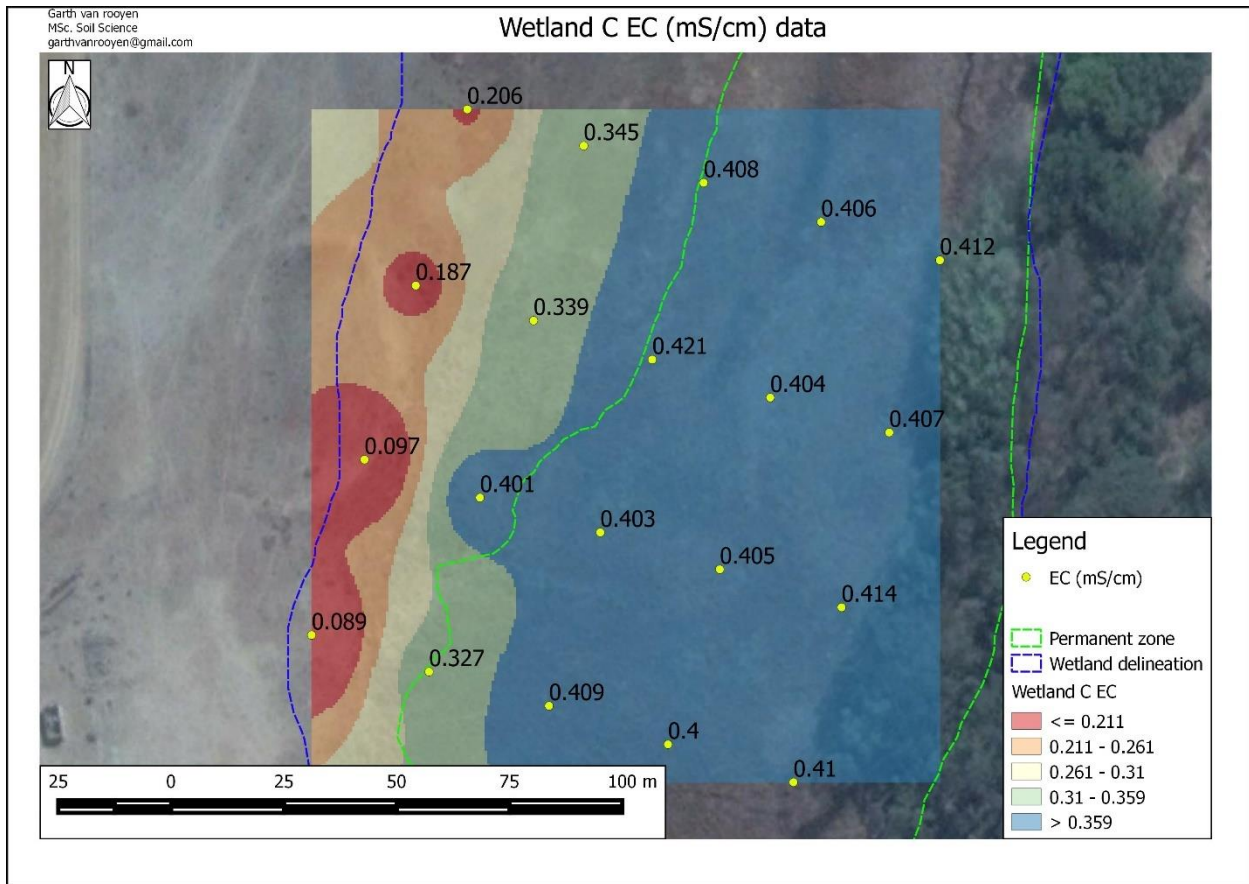


Figure 2.25 Wetland C spatial distribution of EC data

Wetland C showed a visible EC distribution pattern with the wetland delineation. The EC in the permanent zone contained the highest measured EC category, all showing values of >0.359 mS/cm (although still very low compared to the other wetlands). The transition from permanent zone to seasonal zone and out towards the terrestrial zone, exhibited a decrease in measured EC. This correlation is typical of salt accumulation in the permanent zone. Salt accumulation is preferential in areas of lower geomorphic positions (Herrero *et al* 2015).

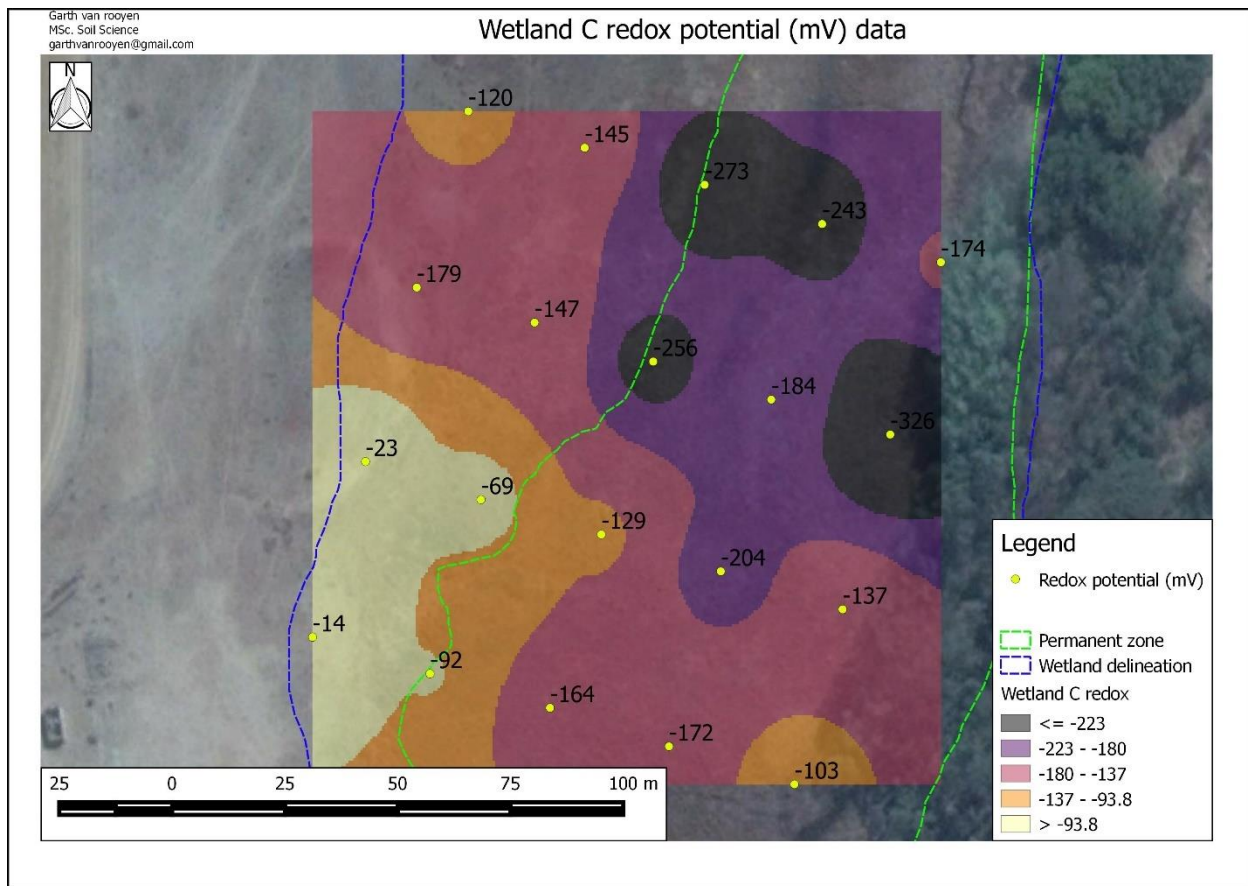


Figure 2.26 Wetland C spatial distribution of redox potential data

The redox potential measurements suggest that it is a highly reduced system. Wetland C is an organic wetland, which corresponds with a system you expect to be very effective in accumulating organic carbon. The redox conditions inhibit C(0) from oxidation and volatilisation to C(+4), thus resulting in a higher organic carbon content.

2.8 Statistical analysis

The results obtained from the field measurements of the three wetlands included the following:

- Carbon dioxide measurements
- pH
- Redox potential
- Electrical Conductivity (EC)

Statistical analysis was done on these results, specifically Pearson correlation tests, to determine correlation strengths between the parameters. The Pearson correlation test is a measure of the linear correlation between two variables X and Y. For each correlation test, the permanent zone is correlated separately to the seasonal zone (seasonal zone contains sample points located within the temporary and seasonal zones). The separation of the two zones is classified according to annual saturation periods, with the permanent zone being saturated all year round, and the temporary and seasonal zones being saturated on a 'seasonal' basis. The blue line (and blue diamonds) represent the seasonal soil forms, and the orange line (and orange squares) represent the permanent soil forms.

2.8.1 Redox potential vs. pH

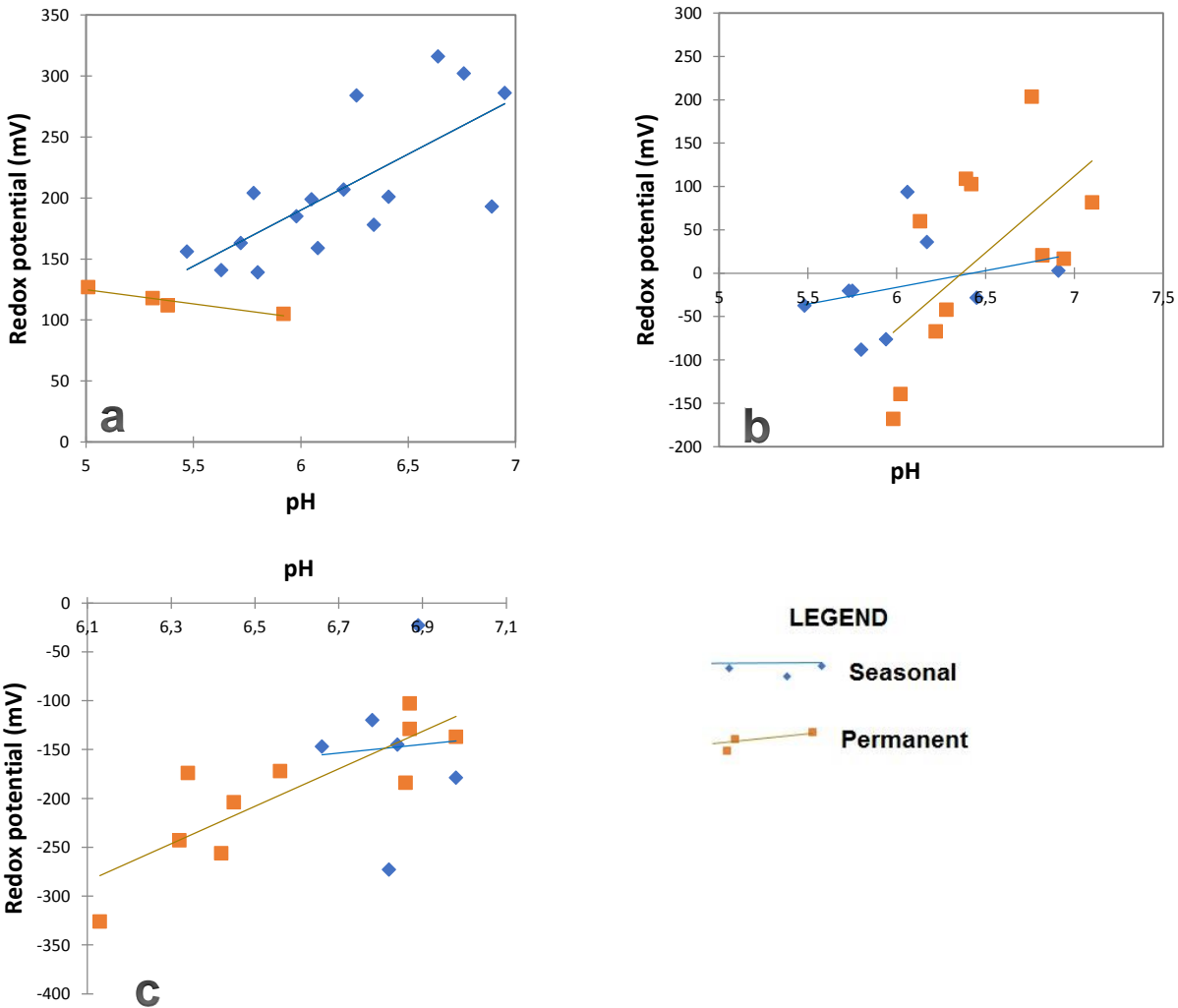


Figure 2.27 a) Redox potential vs pH for Wetland A, b) Redox potential vs pH for Wetland B, c) Redox potential vs pH for Wetland C

According to the Nernst equation, any change in pH will affect the redox potential (Reddy *et al* 2000). As seen in figure 2.27a, the increase in pH led to an increase in redox potential for the seasonal wetland zone (blue line). The permanent zone of wetland A showed a strong correlation where an increase in pH led to a decrease in redox potential. Wetland A and B showed the same correlation for both zones, where increase in pH leads to an increase in redox potential in the soil. This is significant as an

increase in acidic (or alkaline) effluent that is discharged into a wetland, will alter the pH of the system and thus cause a change in the redox potential of the system.

2.8.2 Measured CO₂ vs Electrical Conductivity

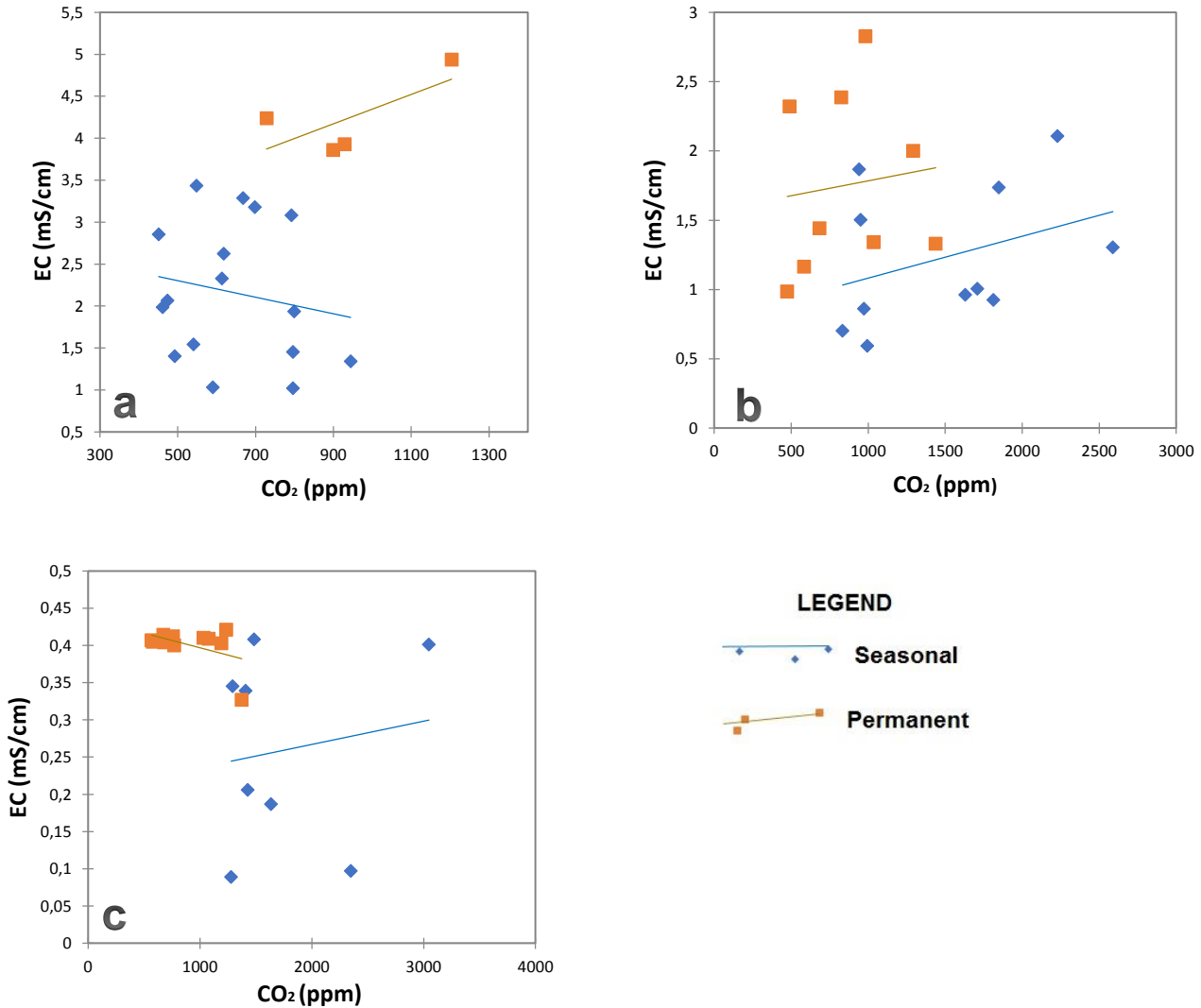


Figure 2.28 a) CO₂ vs Electrical Conductivity for Wetland A, b) CO₂ vs Electrical Conductivity for Wetland B, c) CO₂ vs Electrical Conductivity for Wetland C

The permanent zone for wetland A shows somewhat that an increase in EC led to an increase in CO₂. Since increased salinity can decrease the solubility of gases in

solution, the salinity could be a driving factor for CO₂ emission (explored in chapter three). Wetland B is the rehabilitated Zaaklap wetland, and the random distribution of data shows that no clear correlations are present which suggests that the wetland is not yet functioning in equilibrium with its environment. Wetland C also exhibited a random distribution of data, however the high EC values and low CO₂ measurements characterize the permanent zone of the wetland (organic soils). It is also worth noting the amount of carbon dioxide measured. Wetland A had a maximum reading of 1204 ppm (permanent zone) where Wetland C had a maximum reading of 3038 (permanent-seasonal zone transition).

2.8.3 Measured CO₂ vs redox potential

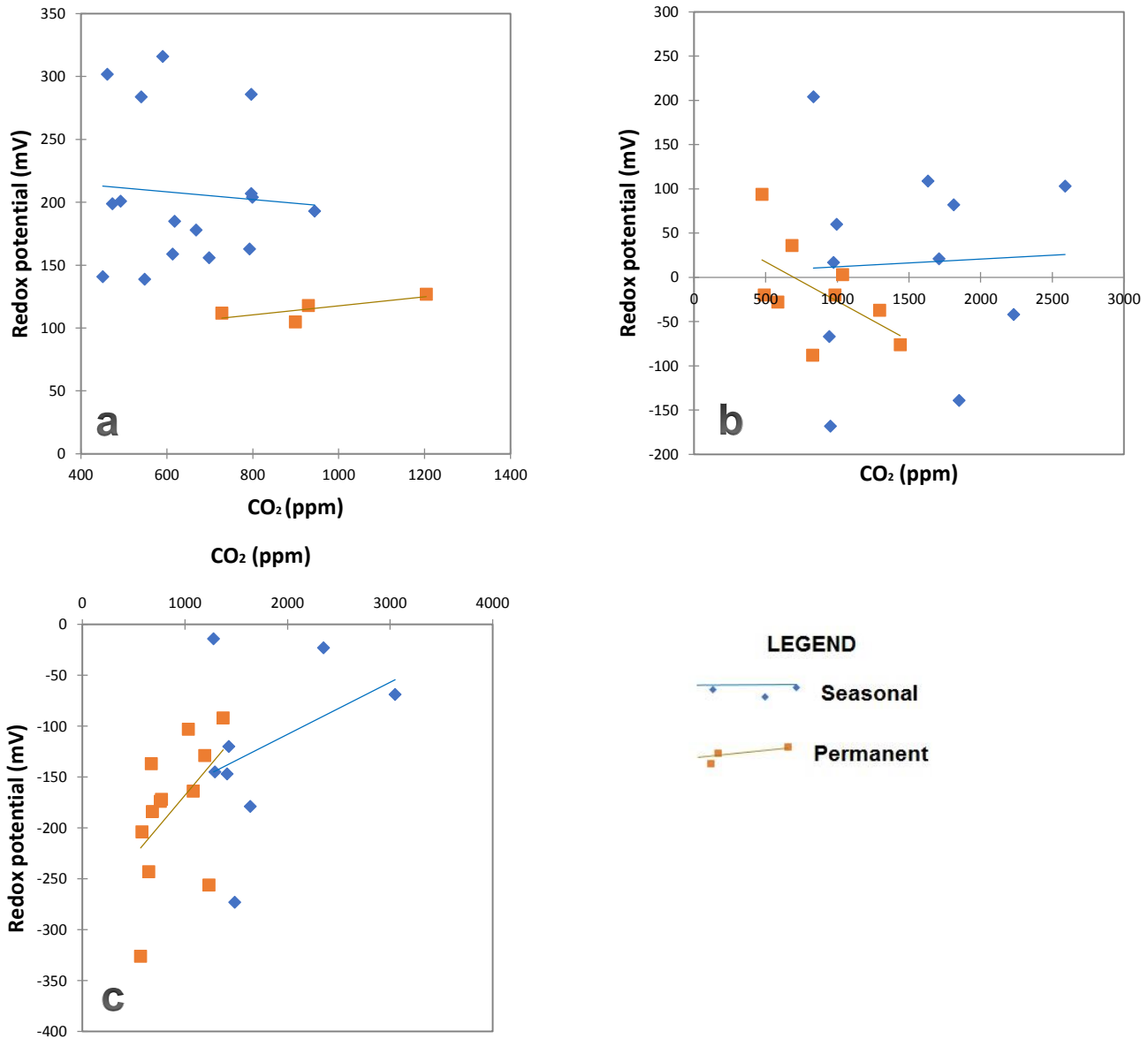


Figure 2.29 a) CO₂ vs Redox potential for Wetland A, b) CO₂ vs Redox potential for Wetland B, c) CO₂ vs Redox potential for Wetland C

Wetland A showed a random distribution of data for the seasonal zone, where the permanent zone showed a stronger correlation with a higher redox potential (mV) reading resulting in a higher CO₂ measurement. Wetland B again shows no real

correlation, while Wetland C shows that highly reduced conditions exhibit lower levels of CO₂ emissions in the permanent zone. In general, the populations of the permanent and seasonal zones for all three wetlands are separated.

2.8.4 Measured CO₂ vs pH

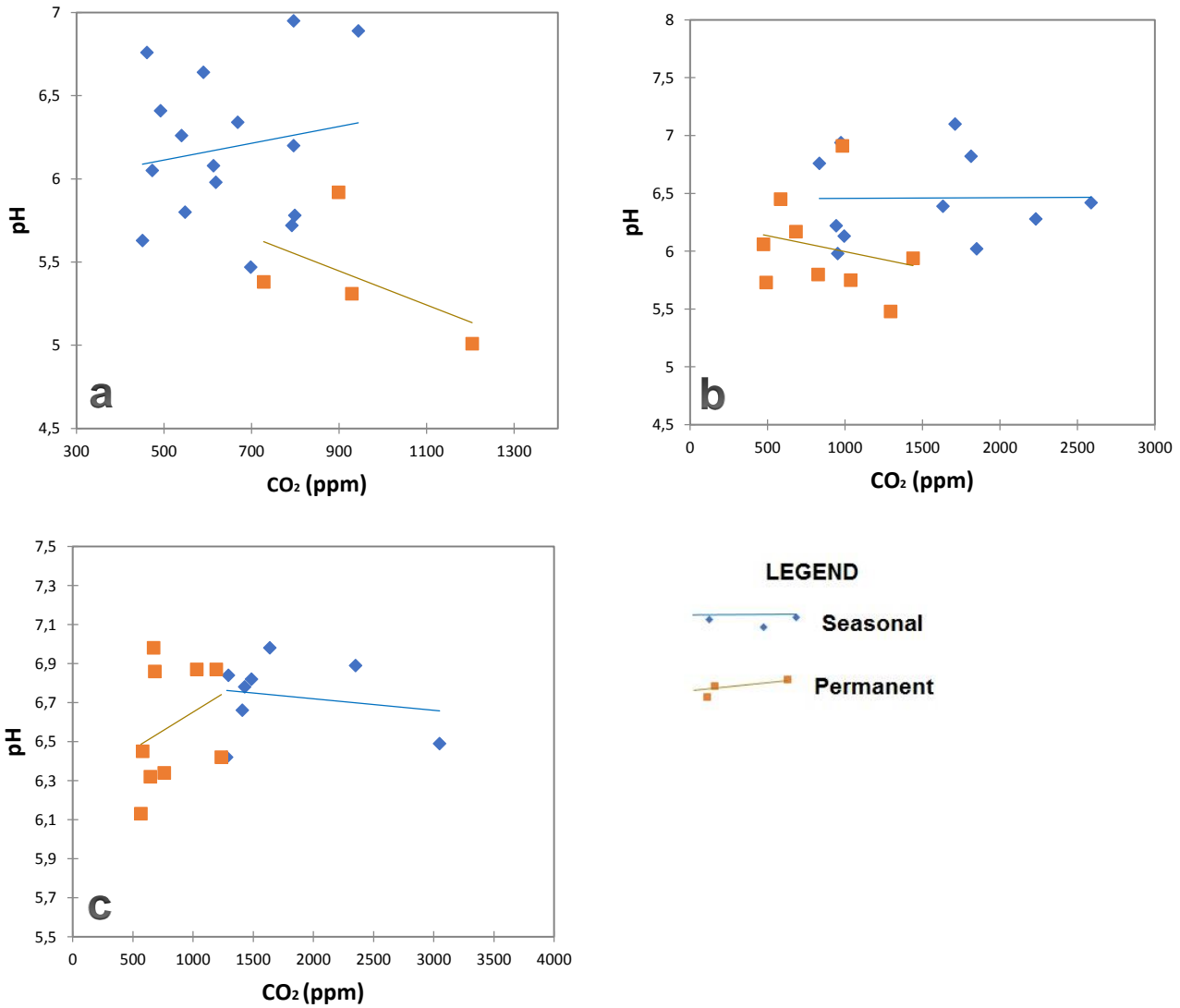


Figure 2.30 a) CO₂ vs pH for Wetland A, b) CO₂ vs pH for Wetland B, c) CO₂ vs pH for Wetland C

Weak correlations exist between measured CO₂ and pH for all three wetlands. The seasonal and permanent zones of the wetlands showed a random distribution of data, showing that pH does not affect the amount of CO₂ released. For Wetland A it seems the seasonal and permanent zone populations are generally well separated, suggesting they are effectively different systems. For Wetland B, in general, the seasonal and permanent populations represent a continuum rather than separate populations.

Table 2.1 Correlation coefficients

Site	Coefficient of determination (R ² values)			
	Redox vs pH	CO ₂ vs EC	CO ₂ vs redox	CO ₂ vs pH
Wetland A				
<i>Permanent</i>	0.907	0.489	0.575	0.283
<i>Seasonal</i>	0.520	0.031	0.006	0.027
Wetland B				
<i>Permanent</i>	0.370	0.013	0.309	0.005
<i>Seasonal</i>	0.091	0.128	0.002	0.00007
Wetland C				
<i>Permanent</i>	0.705	0.212	0.251	0.104
<i>Seasonal</i>	0.003	0.023	0.141	0.036

The most statistically significant linear correlations in the permanent zones exist between pH and redox potential. In terms of CO₂ release, statistically, the redox potential appears to be the driving force behind the amount of CO₂ released in the permanent zone of a wetland.

Wetland A showed higher salinity levels, higher reduction-oxidation potential (more oxic wetland) and elevated CO₂ emissions in the permanent zone. Good correlations were found between the variables in Wetland A, with the pH affecting the redox potential (and vice versa), which in turn caused elevated levels of CO₂ release. Wetland B exhibited typical signs of disturbance from a chemical and physical point of view, with no

statistically significant relationships being found between pH, EC, redox potential and CO₂ release. High salinity levels were found in certain areas of Wetland B with sulfate precipitates visible on the soil surface.

In the case of Wetland C there is a characteristic suppression of CO₂ emissions in the saturated zone, possibly forming deeply reduced pockets, the other characteristic is the low salinity. The low levels of measured CO₂ were found to be a result of the highly reduced conditions. The depletion of oxygen due to prolonged saturation and stagnation results in low oxygen levels which are not enough to sustain oxidation breakdown (respiration) of organic matter, possibly consuming CO₂ simultaneously. Wetland C is in essence storing its carbon rather than releasing (respiring) its carbon, thus resulting in an organic wetland.

From a soil form perspective, the main three soil forms encountered with the highest levels of CO₂ emissions are Longlands, Avalon and Westleigh. These three soils all contain soft plinthic horizons. Soft plinthic horizons can act as a supply of water for the soil profile, thus resulting in a soil profile which is wet for longer periods, enhancing the period for microbial respiration. Redox potential was shown to have a large influence on the release of CO₂, and a soft plinthic horizon is evident of periodically saturated conditions. The amount of oxidative breakdown and respiration in a soft plinthic horizon may be the reason for elevated levels of CO₂ release measured in these soils.

Table 2.2 Mean CO₂ release by soil form (descending order)

Soil forms	CO₂ (ppm)
Longlands	1373
Avalon	1215
Westleigh	1148
Katspruit	1029
Pinedene	944.0
Champagne	882.8
Clovelly	596.8
Arcadia	472.0

Chapter three will investigate the chemistry of these soils and the effect of acid mine drainage (AMD) on the release of carbon dioxide. AMD being released into wetland soils with the highest carbon content (organic soils) will be compared to AMD being released into a mineral terrestrial soil with very low carbon content. The comparisons between the two wetland soil types will be in the form of carbon dioxide emissions.

CHAPTER THREE: Initial response of organic and mineral soils to acid mine drainage (AMD)

3.1 Introduction

Chapter three aims to investigate the effect that acid mine drainage will have on the initial carbon dioxide release in organic and mineral soils. The initial carbon release is emphasized due to a soil phenomenon known as the “Birch Effect”. The Birch Effect states that rewetting of a soil causes the soil to release an initial pulse of CO₂ emissions. The Birch Effect is ultimately a rapid increase in CO₂ respiration in response to a change in moisture conditions (Waring and Powers 2016). The Birch Effect is still not fully understood (Jarvis *et al* 2007), however literature suggests that a rapid (initial) pulse of CO₂ release is caused by dead microbial mass mineralization, an impulsive increase in microbial and fungal biomass in response to increased water availability (Unger *et al* 2010). The hypotheses for this chapter follows on that hydrological and chemical disturbance with AMD will result in a large initial release of CO₂ from soils, with the organic soil releasing a larger quantity of CO₂ than a mineral soil.

Soil samples from Wetland C were collected and placed into one-litre transparent PVC columns which were sealed to limit and prevent further oxidation of organic material. Three organic soil samples from Wetland C were collected and three mineral terrestrial soils from the University of Pretoria experimental farm were also collected. The reason for selecting these soils was that an organic soil is representative of a high carbon soil, and a terrestrial mineral soil is representative of a low carbon soil.

Each soil column had a carbon dioxide NDIR sensor (MIC thermo-hygro CO₂ meter) placed inside of it to measure the carbon dioxide emissions in real time. Synthetic acid mine drainage was then introduced into the system, and any changes in carbon dioxide emissions were then recorded using the MIC thermo-hygro CO₂ DataLog V2.3w1 software. The column experiment was done in a constant temperature room (25 degrees Celsius), with the pH, electrical conductivity, redox potential, percentage

carbon and carbon dioxide emissions noted before and after the introduction of acid mine drainage.

3.2 Synthetic acid mine drainage

Acid mine drainage (AMD) was synthesized in the Soil Science laboratory of the University of Pretoria. It is acknowledged that the spatial variability surrounding the concentration of certain elements within AMD is very high. The reason for using synthetic AMD rather than “real” mine water is because a field sample collected represents a specific point in time, and the sample time and seasonal bias can possibly result in inaccurate water quality measurements. It was decided that it is scientifically sounder to subject long-term mine water data to statistical inference and based on this prepare synthetic AMD. By preparing and synthesizing AMD, more control is therefore achieved with respect to water quality.

The synthetic AMD was based upon a nearby undisclosed colliery water quality measurements (Appendix, Table A3). It is assumed that standard acceptable water sampling and analysis protocols were followed. Measurements of mine water from the colliery, dating from 05-12-2008 till the most recent available measurement in 07-03-2016, were recorded. From all these measurements, the median was calculated for the purpose of selecting a median value from which to base the synthetic acid mine drainage. The reason for using the median rather than the mean is because the dataset from colliery contains outliers which will skew the mean, whereas the median values do not get skewed by outliers. It is chemically incorrect to select median concentration of individual ions from various water analyses and attempt to prepare a “median” solution based on this. The reason is a solution overall should be chemically consistent and charge-balanced. The correct approach is to select a single complete water analysis, that is: 1) Charge balanced and therefore an accurate analysis and 2) Overall concentration of the solutes are close to median concentration of its constituents.

Table 3.1 Synthetic AMD ion concentrations

pH	EC (mS/cm)	Fe ²⁺	Mn	Al	K	Ca	Mg	Na	Charge balance
		(mg/l)							
3.03	4.063	283	98.5	175	5.15	203	125	17.5	-4.35

The anion was sulphate and the small charge balance error is within acceptable limit of 5%.

3.3 Column experiments

The column experiments aim to understand the soils response to initial exposure to acid mine drainage. The outcome is to quantify the amount of carbon dioxide released when acid mine drainage is introduced to the soil system, whilst observing possible chemical changes. The soils that were used were a high organic content (percentage carbon) soil and a low organic content soil.

Table 3.2 Soil physical properties

Properties	Organic soil	Mineral soil
Soil horizon	Organic O	Orthic A
Percentage carbon (%)	19.7	0.786
Bulk density (g/cm ³)	0.43	1.45
Gravimetric water content (θ_g)	1.08	0.31

Table 3.3 Variables for experiment

Independent variables	Dependent variables	Controlled variables
<ul style="list-style-type: none"> • Soil type 	<ul style="list-style-type: none"> • Measured carbon dioxide emissions • Redox potential of the soil • pH of the soil • Electrical conductivity (EC) of the soil • Percentage carbon (Walkley-Black method) 	<ul style="list-style-type: none"> • Temperature of columns (set at 25 degrees Celsius) • Bulk density • Amount of synthetic AMD introduced into the soil column • Distance of NDIR carbon dioxide sensor from the soil • Closed seal of the soil column (no air exchange)

3.3.1 Methods and materials

Three soil columns were collected from Wetland C, in the permanent zone of the wetland, these represented the high organic content soil (peat). It is acknowledged that collecting undisturbed soil samples is virtually impossible, and care was taken to limit the amount of disturbance. The soil columns consisted of one-liter volume, 7.5 centimeter diameter transparent PVC column with permanently sealed bottom and removable air tight seal lid with carbon dioxide sensor inlets and outlets. The soil samples were collected by inserting the column into the peat, twisting the column slightly to loosen any fibrous material and then slowly extracting it. This method created suction in the column, and when the column was pulled out, a core sample of the peat remained firmly placed within the column.

Three orthic A low organic content terrestrial soils were also collected. The collection of the soil samples was done slightly different than the peat. The bulk density of the mineral soil was first measured and then repacked into the soil column according to its

bulk density, as to replicate field conditions in the laboratory. The soil columns were sealed and brought back to the University of Pretoria soil laboratories on the same day and stored in a dark room at 4 degrees Celsius in order to limit microbial activity that may or may not be altered from field conditions. The column experiments commenced within a constant temperature room (25 degrees Celsius) the following day, first allowing the columns to equilibrate to 25 degrees Celsius.

The amount of synthetic AMD that needs to be added into the soil column was calculated according to the area of potentially affected wetlands surrounding the coal fields. According to literature, 360Mℓ of AMD can be generated each day in the Mpumalanga coalfields. The sampling site (Wetland C) is located in the Olifants catchment, where 170Mℓ/day of AMD generation is suggested (Grobbelaar *et al* 2004). Using GIS software and the National Freshwater Ecosystem Priority Areas (NFEPA) data (Driver *et al* 2011), wetland areas were calculated within the coalfield surrounding eMalahleni (Figure 3.1). The total area is approximately 11 743 hectares of wetlands that are at direct risk of AMD contamination. The amount of AMD potentially at risk of entering these wetlands are calculated as follows:

$$\frac{170\,000\,000\text{ litres}}{11\,743\text{ hectares}} = 14\,476\text{ l/ha}$$

The area of the column opening was then calculated:

$$A = \pi(3.75)^2 = 44.18\text{ cubic cm} = 0.0000004418\text{ ha}$$

$$\frac{14\,476\text{ l}}{1\text{ha}} = \frac{x\text{ l}}{0.0000004418\text{ ha}}$$

Therefore $x = 0.064\text{ℓ} \approx 0.01\text{ℓ} = 10\text{ mℓ}$

The amount needed to add to the surface of the soil within the column is 10 mℓ, which is representative of 170Mℓ/day AMD generation which can potentially end-up in 11 743 hectares of nearby rivers and wetlands. This amount represents absolute worst-case scenario. 10 mℓ of AMD inserted onto to the top of the soil would represent direct AMD

discharge into a wetland from the top (overland flow), rather than indirect contamination (seepage flow). It is also acknowledged that the amount of AMD generated and fed into wetlands will vary greatly, and thus the volume added during the experiment is kept constant for all soils in order to observe initial soil responses to a fixed volume of AMD.

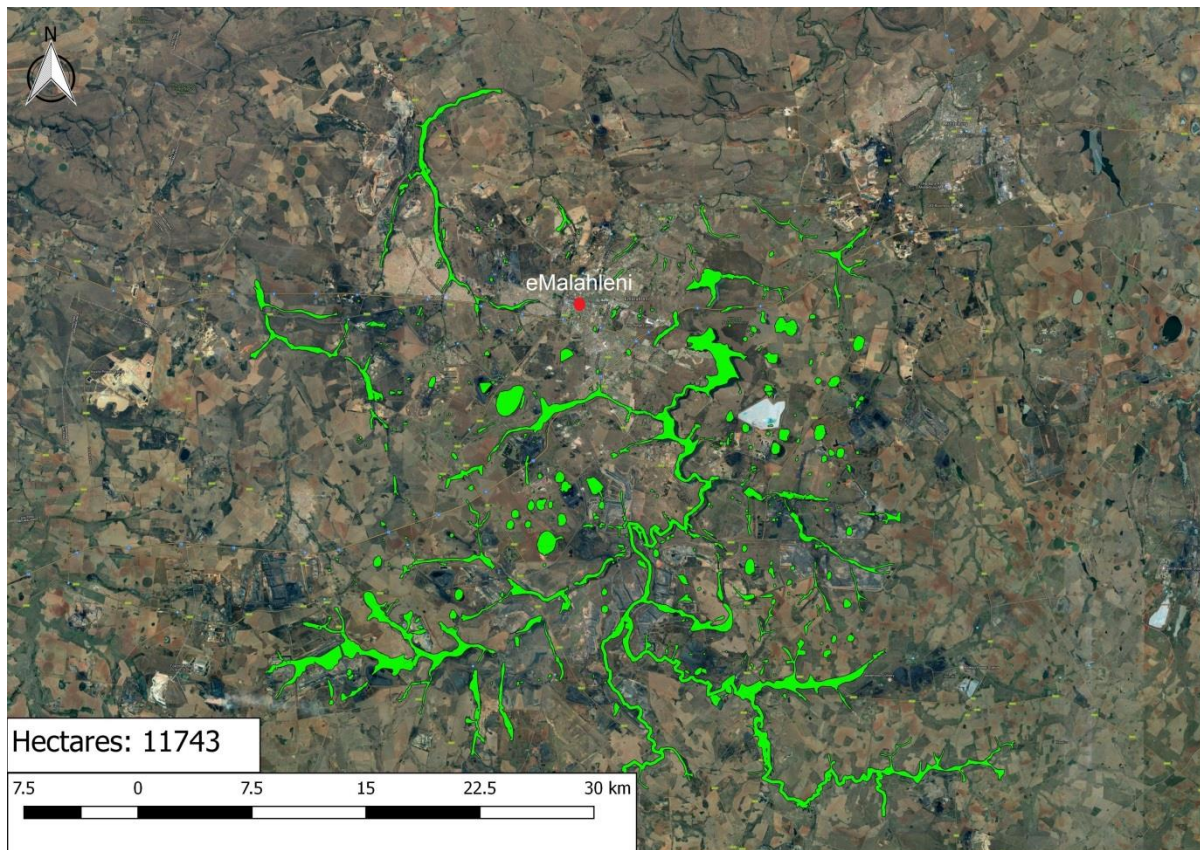


Figure 3.1 Directly affected watercourses (NFEPA)

The approach for the soil column experiment was as follows:

- The NDIR carbon dioxide sensor was placed on the top of the sealed soil column, five centimetres from the soil-air interface
- The NDIR carbon dioxide sensor is turned on and allowed to reach equilibrium with the carbon dioxide emissions being released from the soil

- Once equilibrium was reached (where NDIR carbon dioxide sensor reading does not change), 10 milliliters of synthetic AMD was injected via a nozzle into the soil column from the top.
- The carbon dioxide readings were logged using the datalogger software provided (initial response of the soil to the AMD).
- laboratory analysis of the soil is done in order to compare the pH, EC, and redox potential of the soil post-experiment to that of the soil pre-experiment.
- Experiment was repeated for each soil repetition (3) and different soil.

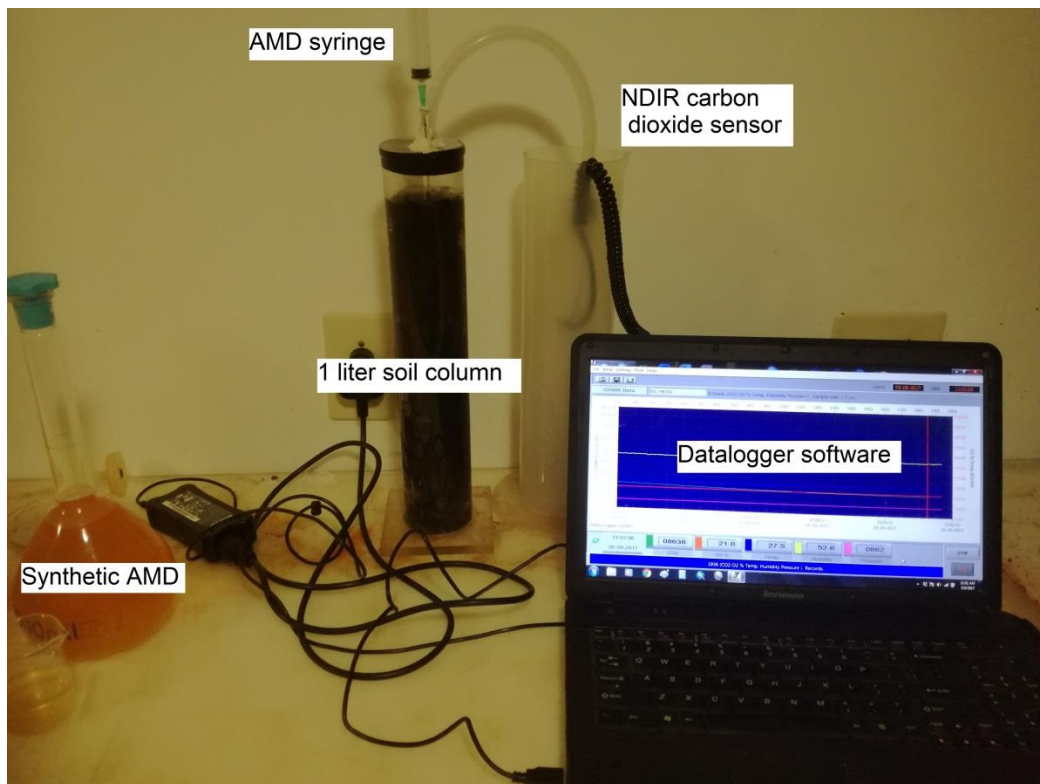


Figure 3.2 Soil column experiment setup

3.4 Results

3.4.1 Organic soil

The results from this experiment aimed to understand whether the addition of AMD into high organic wetland (peat) soils will increase the release of carbon dioxide. Chemical

changes as well as carbon mass balances were also analysed. Low organic soils that did not occur in wetlands also followed the same procedure, in order to distinguish results between peat and the opposite in terms of percentage carbon.

The carbon dioxide emissions as a function of time were plotted against each other to determine the type of reaction taking place.

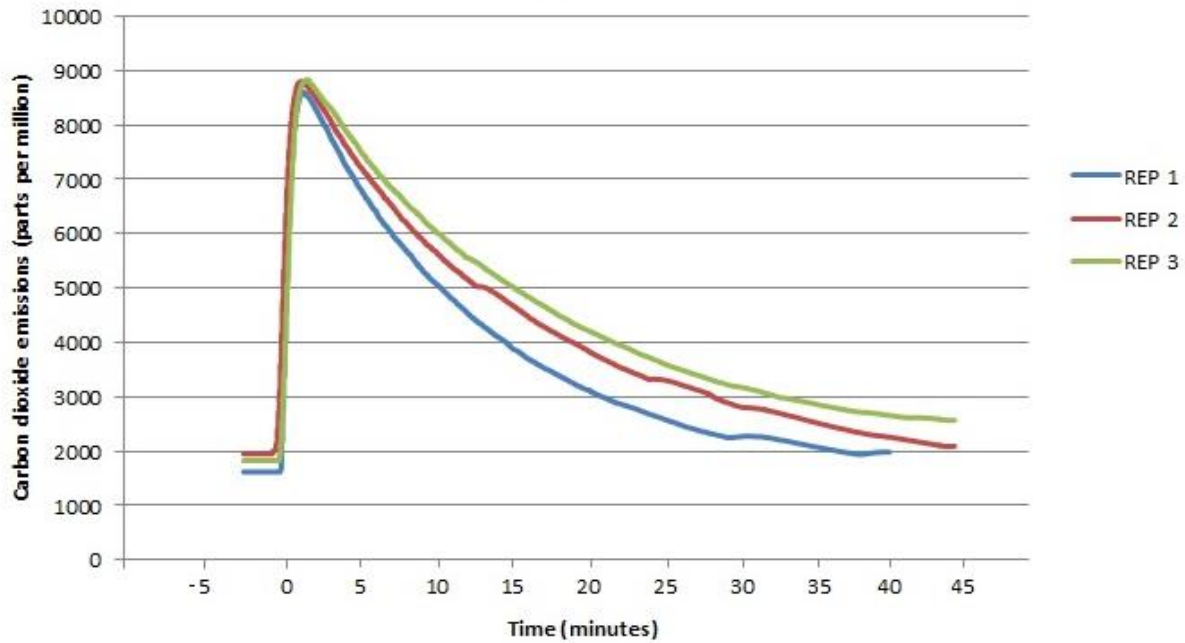


Figure 3.3 Carbon dioxide release in response to AMD for organic soil

Each of three replicates was measured in live time via the datalogger software (see appendix, Figure A15, for an example of a screenshot of live recording on the software). The datalogger software outputs each replicate as an excel spreadsheet where further data analysis can be done in Excel. For each replicate, once a steady state of the carbon dioxide readings has been reached within the soil column, 10 ml of AMD was injected into the soil column at time = 0 (figure 3.3). A rapid increase, almost instantaneous, of carbon dioxide emissions can be seen, where a maximum peak for all three replicates occur at around time = 3 minutes. The microbial flush according to the

“Birch Effect” as seen above (rapid increase in CO₂), is therefore also applicable to saturated soils. The introduction of easily metabolizable nutrients also contributes to the microbial flush. As the carbon dioxide emissions peak till when they reach steady state again at around time = 45 minutes, a second order reaction is taking place. A second order reaction is the relationship between 1/CO₂ versus time. The reaction captures the “overall” kinetics of a very complex system, where a more suitable term would be pseudo-second order.

Three orders of kinetic chemical reactions can happen, namely; zero, first and second order reactions. To test for the order, the coefficient of determination must be calculated for each order. Zero order reactions would be the relationship between CO₂ versus time. Linear regression is used to obtain the important rate constants of kinetic reactions, and also serves as diagnostic “tests” for first or second order reactions. First order reactions would be between ln([CO₂]) vs time, and second order reactions would be between 1/CO₂ versus time. The R² value that is closest to 1 determines the order (Atkins and de Paula 2011).

Table 3.4 Average coefficient of determination (R²) test for each reaction order

Zero order R ²	First order R ²	Second order R ²
0.496	0.969	0.996

From the R² values, the second order reaction has the best linear fit, thus showing that the kinetics of CO₂ release was closer to second order reaction (pseudo-second order) than a first order.

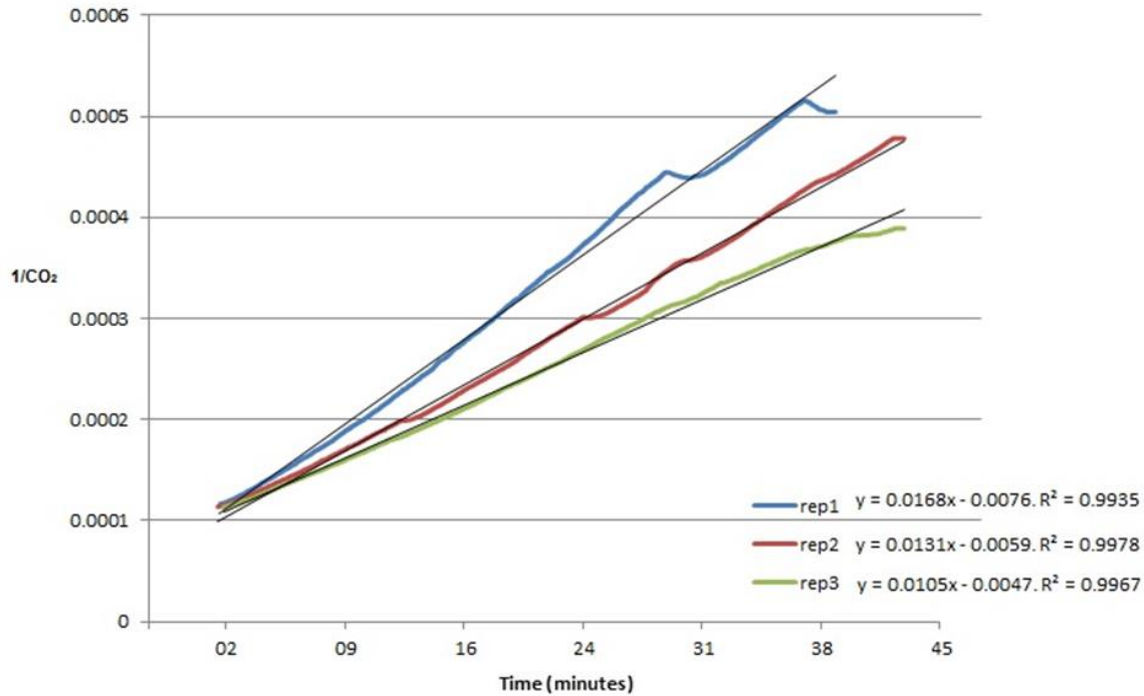


Figure 3.4 Second order reaction (1/CO₂ vs time) for organic soil

Table 3.5 Second order average values for organic soil

Linear equation	$y = 0.013x + 0.0067$
Second order reaction equation	$1/[CO_2] = kt + 1/[CO_2]_0$
<i>k</i> (CO₂.min⁻¹)	0.013

In a second order reaction, CO₂ approaches zero more slowly after the addition of AMD than in a first-order reaction, even with the same initial rate. The half-life of a second order reaction depends, however on the initial CO₂ concentration (unlike in a first order reaction). This means, from an environmental point of view, that the rate of CO₂ decrease (from maximum emissions) after the addition of AMD, will continue in lower concentrations for longer periods of time than in first order reactions. This is because the half-life of the second order reaction is longer when the CO₂ concentrations are low (Grobbelaar *et al* 2004).

3.4.2 Mineral soil

The same methodology was used to observe the initial response of the mineral soil to AMD.

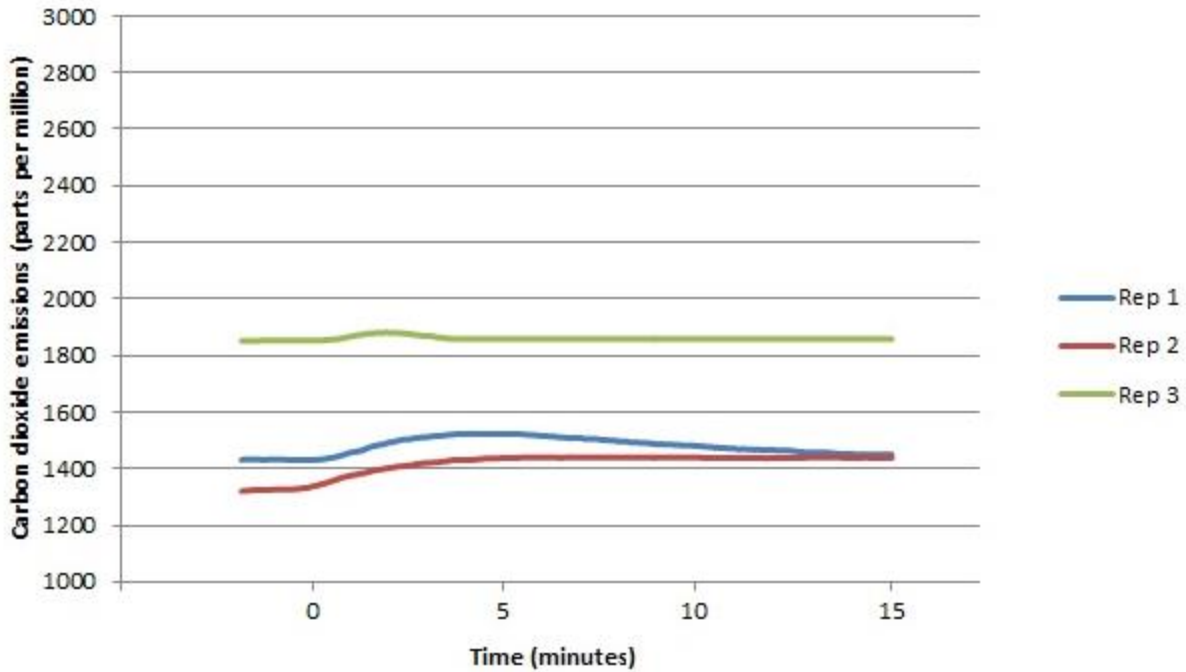


Figure 3.5 Carbon dioxide release in response to AMD for mineral soil

The initial response of the mineral soil to the AMD is clearly less than the organic soil. At time=0 (this is when the AMD was added), the carbon dioxide emissions increased slightly, before returning slightly to above initial carbon dioxide emissions. The coefficient of determination was calculated for each reaction order; this will indicate which reaction order took place.

Table 3.6 Average coefficient of determination (R^2) test for each reaction order

Zero order R^2	First order R^2	Second order R^2
0.2157	0.909	0.910

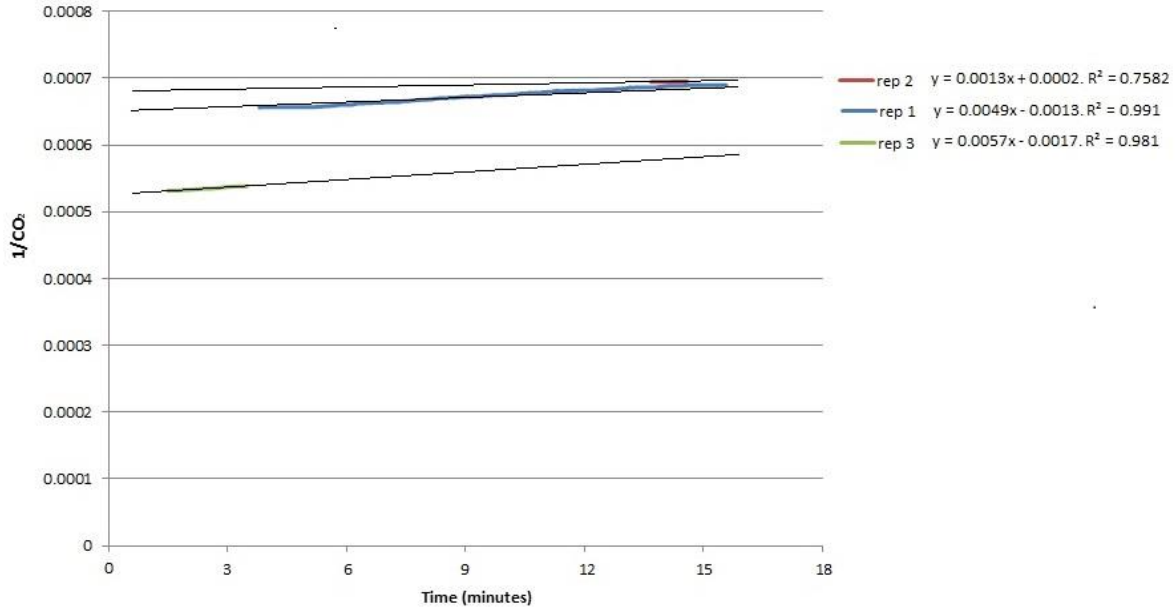


Figure 3.6 Second order reaction (1/CO₂ vs time) for mineral soils

From the R² values, the second order reaction produced the best fit, with a R² value of 0.910. The first order reaction was almost identical, with an R² of 0.909. This means that the reaction from maximum carbon dioxide emissions to steady state is a second order reaction, the same as was observed for the organic soils.

Table 3.7 Second order average values for mineral soil

Linear equation	$y = 0.00397x - 0.00107$
Second order reaction equation	$1/[CO_2] = kt + 1/[CO_2]_0$
<i>k</i> (CO₂.min⁻¹)	0.00397

3.5 Chemical data analysis and carbon mass

The pH, Electrical Conductivity, redox potential, % Organic carbon as well as carbon dioxide measurements were taken before and after the addition of the AMD into the two different soil types.

Table 3.8 Average data for organic/mineral soils before and after addition of AMD

	pH	EC ($\mu\text{s}/\text{cm}$)	Redox potential (mV)	% carbon	CO ₂ Maximum (ppm)
Organic soil					
Before	6.84	403	-184	19.65	1801
After	6.11	826	-34	19.04	8746
% change	10.7% decrease ▼	105% increase ▲	81.6% increase ▲	3.1% decrease ▼	385.6% increase ▲
Mineral soil					
Before	6.43	86.4	286	0.808	1534
After	5.63	526	372	0.786	1615
% change	12.4% decrease ▼	508% increase ▲	30.0% increase ▲	2.72% decrease ▼	5.28% increase ▲

Table 3.9 Significance of differences (p-values)

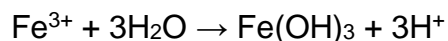
	pH	EC ($\mu\text{s}/\text{cm}$)	Redox potential (mV)	% carbon	CO ₂ Maximum (ppm)
Organic soil					
p-values	0.0000206**	0.0000155**	0.00136**	0.0539	0.0000529**
Mineral soil					
p-values	0.0000175**	0.0000104**	0.000315**	0.751	0.969

*= Significant difference ($\alpha=0.05$)

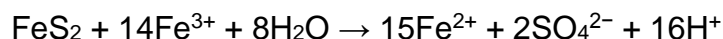
** = Highly significant difference ($\alpha=0.01$)

The p-values calculated using a student t-test indicates that the changes were highly significant for pH, EC, CO₂ increase and redox potential for both the organic and mineral soil.

It can be seen that the addition of the AMD caused a slight increase in the pH of the soil, an increase in the electrical conductivity (EC), a slight decrease in the percentage carbon in the soil and an increase in carbon dioxide emissions after re-equilibrium. An important observation was that the carbon dioxide emissions after adding AMD had increased, although not enough to be statistically significant. As explained previously, the reaction was a second order reaction, and CO₂ decrease (from maximum emissions) after the addition of AMD, will continue in lower concentrations for longer periods of time. At the same time the carbon percentage of the soil had decreased (Table 3.8). The decrease in pH can also be attributed to the presence of iron precipitates, as well as the organic material oxidation. At low pH values, ferric iron precipitates as Fe(OH)₃ if oxidation occurred, leaving trace amounts of Fe³⁺ in solution while simultaneously lowering the soil pH. It is important to note that the AMD solution was purged with Argon gas to displace the dissolved oxygen. The following reaction explains the oxidation of ferric iron to ferrous iron (Akcil and Koldas 2006):



Any trace amounts of Fe³⁺ that were not oxidised, can further oxidise extra FeS₂.



The significant increase in the Electrical Conductivity (EC) is directly a result of the high levels of salts, particularly the sulphates. The increase in carbon dioxide emissions for the organic soil was shown to be highly significant after the addition of AMD. It has been suggested that an increase in EC can lead to a change in microbial activity. (Adviento-

Borbe *et al* 2006). The mineralization of the organic matter is also assumed to have contributed to the increased salinity. The increase in salinity and EC has also been suggested to lead to increased greenhouse gas emissions, such as CO₂ and CH₄ (Xijun *et al* 2017), since gas solubility in solution decreases with increasing salinity. Dissolved organic carbon (DOC) has been shown to be the primary source for CO₂ emissions rather than soil organic carbon (SOC). The focus of this study was on the carbon dioxide emissions, although greenhouse gasses such as CH₄ and N₂O were assumed to be present. The redox potential of -34 mV in the organic soil indicates that the system cannot produce methane anymore. According to literature, the formation of CH₄ was shown to be more complex than CO₂ (Xijun *et al* 2017). The important factors worth noting in the production of greenhouse gasses include redox conditions, sulphate and iron (III) reducers and the anaerobic microorganisms (competing methanogens). It is also worth noting that the significant difference (p-value) for the decrease in % carbon in the organic soil after the addition of AMD was 0.0539, which is close to the 0.05 alpha level. This tells us that the increase in carbon dioxide emissions can also be related to the decrease (consumption) in soil organic carbon, although not proven to be statistically significant. The increase in CO₂ emissions (from steady state to maximum levels) for the organic soil proved to be highly significant, where the mineral soils showed no significant increase. This shows that the addition of AMD into a high organic content wetland will cause significantly elevated CO₂ emissions.

Both soils showed a general increase in their level of oxidation (redox potential measurements). From a macroscopic point of view, the soil system responded by releasing a large amount of CO₂ in its attempt to reach an equilibrium again.

Inductively coupled plasma optical emission spectrometry (ICP-OES) was used to analyse certain elements before and after the addition of AMD. The values that were analysed included the major ions (Fe, Mn, Al, Mg, Na, Ca, K). The trace ions (B, Cu and Zn) were not reported as the values were low, and the significance of the trace ions were assumed to be negligible.

Table 3.10 ICP results for the major ions for the organic and mineral soil.

	Fe	Mn	Al	K	Ca	Mg	Na
Organic soil	(mg/l)						
Before	167	18.1	6.92	12.9	470	145	17.5
After	157	27.4	10.4	11.6	513	160	24.4
Mineral soil							
Before	20.4	56.3	17.98	17.0	79.3	24.8	0.86
After	27.2	57.1	22.4	19.3	89.12	20.8	2.79

Table 3.11 Statistical inference of concentration changes of major ions

	Fe (mg/l)	Mn (mg/l)	Al (mg/l)	K (mg/l)	Ca (mg/l)	Mg (mg/l)	Na (mg/l)
Organic soil							
p-values	0.102	0.0474*	0.0362*	0.736	0.00864**	0.00590**	0.075
Mineral soil							
p-values	0.228	0.781	0.0405*	0.223	0.0875	0.261	0.0828

*= Significant difference ($\alpha=0.05$)

** = Highly significant difference ($\alpha=0.01$)

For the organic soil, statistically significant differences occurred for the changes in manganese and aluminium concentrations after the addition of AMD. Highly significant differences occurred in the calcium and magnesium levels after the addition of AMD. For the mineral soil, statistically significant differences were only found for the changes in aluminium. These changes can be due to the low pH of the AMD, high concentrations of iron, aluminium and manganese. Elevated aluminium levels were observed in both organic and mineral soils as significant differences were detected after the addition of AMD. Dissolved aluminium has a negative effect on water quality and ecology of watercourses, with the Al^{3+} ion likely to be the most toxic form (Waters and Webster-Brown 2013).

Microbial activity is an important part of redox chemistry in wetlands. Microbial bacteria such as the *acidiphilium spp.* can live and thrive in acidic media, such as AMD. When pH is increased under anoxic conditions, through the addition of AMD for example, *acidiphilium spp.* microbes can redissolve ferric iron minerals that have been precipitated (Baker and Banfield 2003). *Acidiphilium* species (dominantly *Acidiphilium cryptum*) have the ability to reduce Fe^{3+} under aerobic conditions, whilst producing elevated levels of CO_2 emissions (Kusel *et al* 1999), (Kupka 2005). For the purpose of this study, the focus was to investigate soil responses to AMD, it is acknowledged all the chemical reactions discussed were possibly mediated in various ways by microbial activity.

Highly significant differences were observed for the increase in Ca^{2+} in the organic soil. Calcium dissolution, as well as the presence of calcium carbonates in the organic soil, is also likely to be the cause of elevated CO_2 levels. The reaction between acidic AMD and naturally occurring calcium carbonates is a neutralisation reaction, with CO_2 being the product. The summarized reaction between the AMD and calcium carbonate is as follows (Fusi *et al* 2012):



The reaction between carbonates and AMD is becoming an increasing geo-hazard on reclaimed mine land, where AMD reacts with a neutralising agent (often carbonate material) causing elevated CO_2 levels (Awuah-Offei *et al* 2016).

In order to understand the major source of carbon dioxide emissions from the previous experiment, AMD was added to a saturated calcium carbonate ($CaCO_3$) to determine the amount of CO_2 released as well as to calculate the rate constant. Similarities between rate constants for the calcium carbonate solution and the soils used previously will provide indications as to the reaction between AMD and carbonates present in the soil, especially for the organic soil. The same procedure as was used for the soils was used on the saturated $CaCO_3$ solution, again adding 10ml to the solution. The result is shown as the inverse of the carbon dioxide emissions produced plotted against time.

The reaction (from maximum emissions) was again a second order reaction, as determined by the R² value.

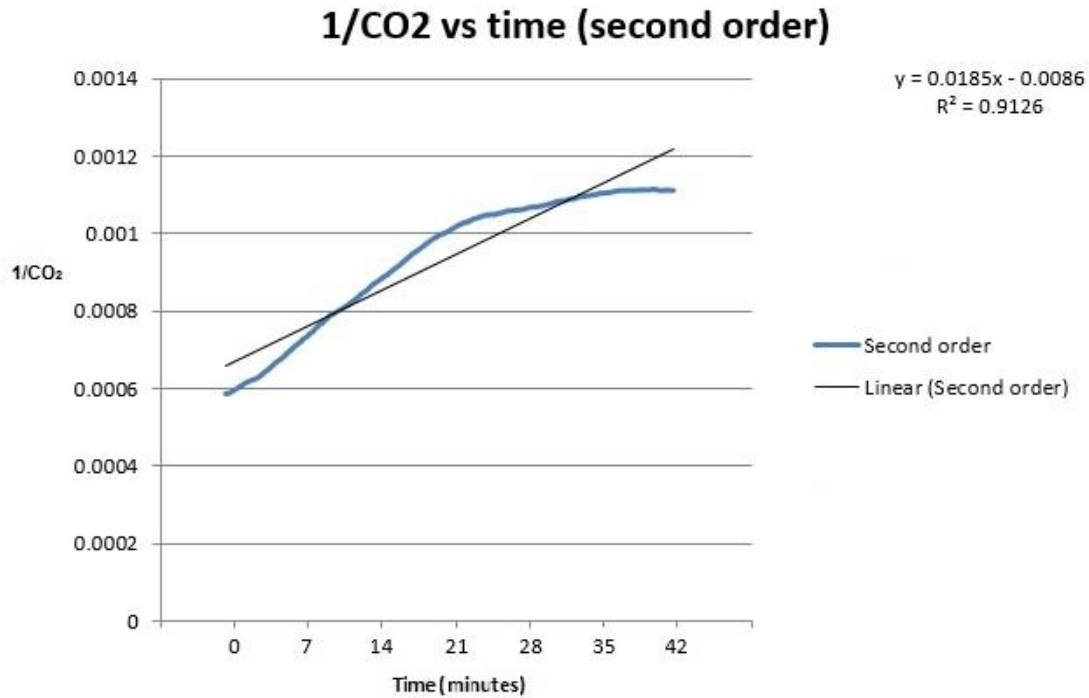


Figure 3.7: Second order reaction (1/CO₂ vs time) for saturated CaCO₃

Table 3.12 CaCO₃ reaction

Linear equation	$y = 0.018x + 0.0086$
Second order reaction equation	$1/[CO_2] = kt + 1/[CO_2]_0$
<i>k</i> (CO₂.min⁻¹)	0.018
Alkalinity before (mg/L as CaCO₃)	320 mg/l
Alkalinity after (mg/L as CaCO₃)	130 mg/l
pH before addition of AMD	8.3
pH after addition of AMD	6.2

The rate constant (k) for the CaCO_3 experiment was 0.018, where the rate constant for the organic soil experiment was 0.013. The rate constant for the mineral soil experiment was 0.00397. The similarities between the rate constants of the organic soil experiment and the CaCO_3 experiment suggests that it could have contributed to the amount of CO_2 measured. The increase in CO_2 could partly be due to the neutralization reaction between the acid and the carbonates.

3.5.1 Carbon mass balances

The calculation of the carbon present (stored) in the soil and the amount of carbon released after the addition of AMD will quantify the amount of carbon that was converted to carbon dioxide. The field measurement of carbon dioxide gave a reading parts per million (ppm) of carbon dioxide. The MIC thermo-hygro CO_2 meter measures the carbon dioxide pressure and temperature. An example of the mass of carbon dioxide released is shown, per the Ideal Gas Law.

- Temperature: 25 degrees Celsius equals 298.15 K
- Pressure: 847 hPa equals 84700 Pa
- Mass of 1 mol of carbon dioxide equals 44.01 g
- Gas constant equals 8.31441
- 351 ppm (volume) $\text{CO}_2 = 351 \times 10^{-6} \text{ m}^3 \text{ CO}_2/1\text{m}^3 \text{ air}$

The mass of carbon dioxide per volume therefore becomes:

Mass of CO_2 in grams = $\frac{(44.01)(84700)(351 \times 10^{-6})}{(8.31441)(298.15)} = 0.527 \text{ g/m}^3$. The volume of the column headspace is then calculated as 0.00029 m^3 . Therefore $0.527 \text{ g/m}^3 \times 0.00029 \text{ m}^3 = \underline{0.000153 \text{ g}}$ of carbon.

The amount of carbon stored in the soil is calculated via the Walkley-Black method. The mass of carbon can be calculated by the % C and the mass used in the procedure. The full dataset can be found in the Appendix.

Table 3.13 Average carbon mass before and after

	C in soil (g)	C released as CO₂ (g)	% C Change
Organic soil			1.99 ▼
Before AMD	0.0194	0.000218	
After AMD	0.0190	0.00106	
Mineral soil			6.56 ▼
Before AMD	0.00421	0.000186	
After AMD	0.00393	0.000195	

Table 3.13 shows that the total amount of CO₂ released was more than the amount of carbon lost in the soil. This confirms that carbonates and microbial respiration play a large role in the release of CO₂ when AMD is introduced into the soil system, and the amount of CO₂ released is not a direct result of the %C loss in the soil, as not all carbon oxidized will be CO₂ (some would have been transformed to dissolved organic carbon). Carbonates are inorganic sources of carbon, and are not calculated as %C in the Walkley-Black method, but rather as Total Organic Carbon (TOC) in other methods (Schumacher 2002). The same outcome was seen in the mineral soil, after the addition of AMD, the soil %C decreased whilst the amount of CO₂ released increased. It is also important to acknowledge that methane (CH₄) dynamics were not studied, methane oxidation is also a major source of CO₂ production, although methane oxidation was assumed to be a minor contributor for the measured redox potentials. For this experiment, however, the focus is only on CO₂. The increased levels of Dissolved Organic Carbon (DOC) can potentially have negative consequences on the mobility of heavy metals in the soil. The organic acids that exist in the DOC can act as a chelating agent, resulting in increased mobilization of heavy metals in the soil (Sherene 2009).

3.6 Significance of results

From the results, it can be concluded that soils with high levels of organic matter and thus a high carbon percentage, pose a greater risk to increased carbon dioxide

emissions if acid mine drainage is released into them. In Chapter two, Wetland C was classified as an organic wetland. The drastic changes seen in Chapter three can therefore be applied to the organic wetlands on a larger scale. These high carbon percentage soils are particularly common in wetland systems, most notable the permanent zone of the wetland. Discharging acid mine drainage into wetland systems can cause changes to redox chemistry, microbial activity, pH and EC, as well as elevated levels of CO₂ production. The greater Emalahleni coal mining region contains significant amounts of wetlands and river systems that are already under threat, such as channeled valley bottom wetlands, depressional pans, flat wetlands, seepage wetlands, valley head seeps as well as unchannelled valley bottom wetlands. Figure 3.8 proposes areas of high risk wetland areas, should acid mine drainage enter the system. The wetland data is per the National Freshwater Ecosystem Priority Areas (NFEPA) according to the efforts of the Water Research Commission and the South African National Biodiversity Institute (SANBI) (Driver *et al* 2011).

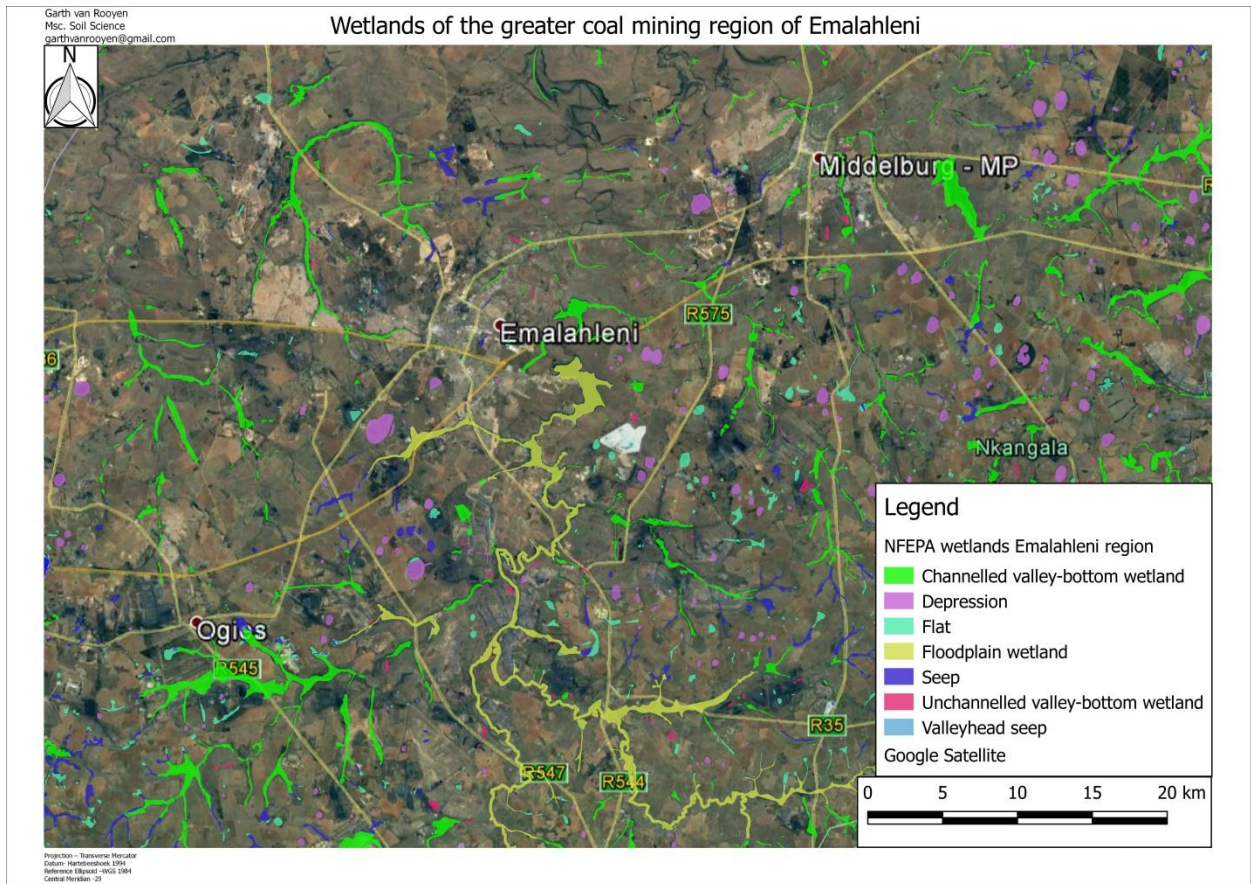


Figure 3.8 High risk areas susceptible to acid mine drainage effects in the greater Emalahleni area

CHAPTER FOUR: Synthesis

The aim of the study in Chapter two was to develop a field method for measuring and quantifying CO₂ emissions using a hand-held meter. Following the field method was a field study consisting of three wetlands in the Mpumalanga Highveld. Wetland A was a wetland affected by industrial activity, Wetland B was a rehabilitated wetland, and Wetland C was an organic wetland not directly affected by industrial activity. All the mineral wetlands exhibited a distinctive CO₂ release pattern, where the organic wetland showed an inverse relationship to that of the mineral wetlands. All wetlands showed a CO₂ release pattern with soil forms. Conclusions that were drawn from this study were that statistically, the redox potential appears to be the driving force behind the amount of CO₂ released in the permanent zone of a wetland. The Organic wetland is a highly-reduced system, which proved to be very effective in accumulating organic carbon. The redox conditions inhibit C(0) from oxidation and volatilisation to C(+4), thus resulting in a higher organic carbon content. The conclusion from this chapter led to chapter three, where AMD was introduced into two soil systems: low organic carbon soil and a high organic carbon soil (core collected at Wetland C).

These two soils represent the opposite ends of the wetland spectrum: high carbon permanent zone soil, and outer low carbon terrestrial zone soil. Addition of AMD onto these soils resulted in an initial release of CO₂. The total amount of CO₂ released was more than the amount of carbon lost in the soil, and the amount of CO₂ released is not a direct result of the % C loss in the soil, as not all carbon was oxidized to CO₂, with a significant portion of the carbon presumably being transformed to dissolved organic carbon. An increase in the mobility of heavy metals present in wetland soils is also a possible concern. The organic acids that exist in the Dissolved Organic Carbon (DOC) fraction can act as a chelating agent, thus possibly resulting in increased mobilization of heavy metals in the soil.

The carbon balance of an ecosystem is controlled by two dominant factors: carbon loss through respiration, and carbon gain through photosynthesis. These processes decide whether the system acts as a source or sink of carbon. Disrupting the carbon balance can alter the “source” or “sink” component of the ecosystem.

Changes in the soil before and after the addition of AMD were highly significant with respect to pH, EC, CO₂ increase and redox potential for both the organic and mineral soil. Upon the addition of AMD, the organic soil increased its original CO₂ emissions by 385.6%, with the mineral soil increasing by 5.28%. The “Birch Effect” was proven to be relevant in saturated soils, rather than only in unsaturated soils. This ultimately concludes that soils with high levels of organic matter, and thus a high carbon percentage, pose a greater risk to increased carbon dioxide emissions if AMD is released into them. These high carbon percentage soils are particularly common in wetland systems, most notably the permanent zone of the wetland.

The introduction of AMD into wetlands proved to enhance the “sink” component, disrupting the carbon balance and at the same time enhancing atmospheric CO₂ concentrations.

Suggestions for future research:

- Include more wetlands of different hydrogeomorphic types (pan, seepage, peat, floodplain, depression wetlands)
- Use several AMD types (eg. high Fe/Mn concentration AMD etc.)
- Prolonged exposure of the soil to AMD
- Effect of temperature and saturation on carbon respiration in organic soils
- Study the effects of microbial activity on soil respiration for varying soil types

REFERENCES

- Adviento-Borbe MAA, Doran JW, Drijber RA, Dobermann A. 2006. Soil Electrical Conductivity and Water Content Affect Nitrous Oxide and Carbon Dioxide Emissions in Intensively Managed Soils. *Journal of Environmental Quality*. Volume 35: 1999-2010.
- Aerts R, Ludwig F. 1997. Water-table changes and nutritional status affect trace gas emissions from laboratory columns of peatland soils. *Soil Biology Biochemistry* 29: 1691–1698
- Akcil A, Koldas S. 2006. Acid Mine Drainage (AMD): causes, treatments and case studies. *Journal of Cleaner Production*. Volume 14: 1139-1145
- Amthor JS, Dale VH, Edwards NT, Garten CT, Gunderson CA, Hanson PJ, Huston MA, King AW, Luxmoore RJ, McLaughlin SB, Marland G, Mulholland PJ, Norby RJ, O'Neill EG, O'Neill RV, Post WM, Shriner DS, Todd DE, Tschaplinski TJ, Turner RS, Tuskan GA, Wullschlegel SD. 1998. Terrestrial ecosystem responses to global change: a research strategy. Oak Ridge National Laboratory. *ORNL Technical Memorandum 1998/27*.
- Andriess JP. 1988. Nature and Management of Tropical Peat Soils. *FAO Soils Bulletin* 59: 1–178
- Annandale JG, Jovanovic NZ, Pretorius JJB, Lorentz SA, Rethman NFG, Tanner PD. 2001. Gypsiferous mine water use in irrigation on rehabilitated open-cast mine land: Crop Production, soil water and salt balance. *Ecological engineering* (17: 153-164)
- Aqion. 2106. The open carbonate system. [ONLINE]. Available at: <http://www.aqion.de/site/161>. [Accessed 16 August 2016]
- Arias-Navarro C, Díaz-Pinés E, Kiese R, Rosenstock RS, Rufino MC, Stern D, Neufeldt H, Verchot LS, Butterbach-Bahl K. 2013. Gas pooling: A sampling technique to

overcome spatial heterogeneity of soil carbon dioxide and nitrous oxide fluxes. *Soil Biology Biochemistry* 67: 20-23

Astiani D, Mujiman, Hatta M, Hanisah, Fifian Firda. 2015. Soil CO₂ respiration along annual crops or land-cover type gradients on West Kalimantan degraded peatland forest. *Procedia Environmental Sciences* (28: 132-141)

Atkins P, de Paula Julio. 2011. *Physical Chemistry for the Life Sciences. 2nd edition. Pg 224-234*

Awuah-Offei K, Mathiba M, Baldassare FJ. 2016. Identifying the Presence of AMD-Derived Soil CO₂ in Field Investigations Using Isotope Ratios. *Minerals* (18: 2-12)

Baker BJ, Banfield JF. 2003. Microbial communities in acid mine drainage. *FEMS Microbiology Ecology* (44:139–152)

Bano N, Moran MA, Hodson RE. 1997. Bacterial utilization of dissolved humic substances from a freshwater swamp. *Aquatic Microbial Ecology* (12: 233–238)

Bridgham SD, Richardson CJ. 1992. Mechanisms controlling soil respiration (CO₂ and CH₄) in southern peatlands. *Soil biology and biochemistry* (24 (11): 1089-1099)

Carbonell-Bojollo RM, Repullo-Ruibérriz de Torres MA, Rodríguez-Lizana A, Ordóñez-Fernández R. 2012. Influence of Soil and Climate Conditions on CO₂ Emissions from Agricultural Soils. *Water Air Soil Pollution* (223: 3425–3435)

Chemistry for biologists. 2016. [ONLINE]. Available at: <http://www.rsc.org/Education/Teachers/Resources/cfb/Photosynthesis.htm>. [accessed 16 August 2016]

City of Tshwane. 2015. Rietvlei Nature Reserve. [ONLINE]. Available at: <http://www.tshwane.gov.za/sites/Tourism/NatureConservation/Pages/Rietvlei-Nature-Reserve.aspx> . [Accessed 11 November 2017]

- Collier SM, Ruark MD, Oates LG, Jokela WE, Dell CJ. 2014. Measurement of greenhouse gas flux from agricultural soils using static chambers. *Journal of visualized experiments* (90: 52110)
- Collins ME, Kuehl RJ. 2001. Organic matter accumulation in organic soils. In: Richardson JL, Vepraskas MJ (eds) *Wetland soils. Genesis, hydrology, landscapes, and classification: (137–162)*
- Conrad R, Frenzel, P. 2002. Flooded soils. *Encyclopedia of Environmental Microbiology: (1316–1333)*
- Costanza R, d'Arge R, de Groot R, Farber S, Grasso M, Hannon B, Limburg K, Naeem S, O'Neill RV, Paruelo J, Raskin RG, Sutton P, van den Belt M. 1997. The value of the world's ecosystem services and natural capital. *Nature* (387, p. 253)
- de Klerk AR, Oberholster PJ, Chamier J, Cho M, Crafford J, de Klerk LP, Harris K, le Roux W, Schaefer L, Truter JC, van Deventer H. 2015. Assessment of the ecological integrity of the Zaalklapspruit wetland in Mpumalanga (South Africa) before and after rehabilitation. *Water Research Commission. pg 16*
- Denman KL, Brasseur G, Chidthaisong A. 2007. Couplings between changes in the climate system and biogeochemistry. Cambridge: *Cambridge University Press*
- Dini J. 2004. Restoring wetlands and healing a nation: South Africa's Working for Wetlands programme. *National Wetlands Newsletter. (26 vol 3: Pg 7)*
- Domville SJ, Li MG, Sollner LD, Nesbitt, W. 1994. Weathering behavior of mine tailings and waste rock: A surface investigation. *Proceedings of the International Land Reclamation and Mine Drainage Conference. (Vol 1: 167-176)*
- Driver A, Nel JL, Snaddon K, Murray K, Roux DJ, Hill L, Swartz ER, Manuel J, Funke N. 2011. Implementation Manual for freshwater Ecosystem Priority Areas. *Water Research Commission. WRC report No. 1801/1/11. Pg 18*

- DWAF (Department of Water and Forestry). 2005. A practical field procedure for identification and delineation of wetlands and riparian areas. *National Water Act Edition 1: 5-19*
- DWAF (Department of Water Affairs and Forestry). 1996. South African Water Quality Guidelines. *Volume 7: Aquatic Ecosystems. (Pg 108-110)*
- Fiedler S, Sommer M. 2004. Water and Redox Conditions in Wetland Soils-Their Influence on Pedogenic Oxides and Morphology. *Soil Science Society of America (68: 326-335)*
- Freeman C, Ostle NJ, Fenner N, Kang H. 2004. A regulatory role for phenol oxidase during decomposition in peatlands. *Soil Biology and Biochemistry (36: 1663–1667)*
- Fusi L. Monti A. Primicerio M. 2012. Determining calcium carbonate neutralization kinetics from experimental laboratory data. *J Math Chem (50: 2492–2511)*
- Geoscience. 2017. 1:100 000 Geological Data. [ONLINE]. Available at: <http://www.geoscience.org.za/index.php/publication/downloadable-material>. [Accessed 5 June 2017]
- Gorham E, Underwood JK, Janssens JA, Freedman B, Maass W, Waller DH, Ogden JG 1998. The chemistry of streams in southwestern and central Nova Scotia, with particular reference to catchment vegetation and the influence of dissolved organic carbon primarily from wetlands. *Wetlands (18: 115–132)*
- Grobbelaar R, Usher B, Cruywagen IM, de Necker E, Hodgson FDI. 2004. Long-term impact of intermine flow from collieries in the Mpumalanga area. *WRC Report No1056/1/04. Water Research Commission, Pretoria.*
- Grundling PL, Grobler R. 2005. Peatlands and Mires of South Africa. *Stapfia 85, zugleich Kataloge der Oö', Landesmuseen Neue Serie (35: 379-396)*
- Guillén, MD, Manzanos MAJ. 2002. Study of the volatile composition of an aqueous oak smoke preparation. *Food Chemistry (79: 283-292)*

- Han L, Sun K, Jin J, Xing B. 2016. Some concepts of soil organic carbon characteristics and mineral interaction from a review of literature. *Soil Biology & Biochemistry* (94: 107-121)
- Hensel PF, Day JW Jr, Pont D .1999. Wetland vertical accretion and soil elevation change in the Rhône River delta, France: the importance of riverine flooding. *Journal of Coastal Research* (15: 668–681)
- Herrero J, Weindorf DC, Castañeda C. 2015. Two Fixed Ratio Dilutions for Soil Salinity Monitoring in Hypersaline Wetlands. *PLoS one* 10(5): e0126493
- Hou AX, Chen GX, Wang ZP, Cleemput OV, Patrick WH .2000. Methane and nitrous oxide emissions from a rice field in relation to soil redox and microbiological processes. *Soil Science Society of America Journal* (64: 2180–2186)
- Inglet PW, Reddy KR, Corstanje R. 2005. Anaerobic soils. University of florida. *Elsevier*. Pg 1-7
- Iriana W, Tonokura K, Kawasaki M, Inoue G, Kusin K, Limin HS. 2016. Measurement of carbon dioxide flux from tropical peatland in Indonesia using the nocturnal temperature-inversion trap method. *Environmental Research Letters: Vol 11* (9)
- Jardine CN, Boardman B, Osman A. 2002. Methane UK: Chapter 2: Climate science of methane. Environmental Change Institute, *Univeristy of Oxford* pg 15
- Jarvis PG, Rey A, Petsikos C, Rayment M, Pereira JS, Banza J, David JS, Miglietta F, Valentini R. 2007. Drying and wetting of soils stimulates decomposition and carbon dioxide emission: the “Birch Effect”. *Tree Physiol* (27 (2007), pp. 929-940)
- Jerman V, Metje M, Mandic-Mulec I, Frenzel P. 2009. Wetland restoration and methanogenesis: the activity of microbial populations and competition for substrates at different temperatures. *Biogeosciences* (6: 1127-1138)
- Jovanovic NZ, Barnard RO, Rethman NFG, Annandale JG. 1998. Crops can be irrigated with lime-treated acid mine drainage. *Water South Africa* (24: 113-121)

- Kafri U, Foster MBJ. 1989. Hydrogeology of the Malmani dolomite in the Klip River and Natsalspruit basins, South Africa. *Environmental Geology and Water Sciences* (13:2 pg 153-166)
- Kayranli B, Scholz M, Mustafa A. 2010. Carbon storage and fluxes within freshwater wetlands: a critical review. *Wetlands* (30:111–124)
- Kotze DC, Klug JR, Hughes JC, Breen CM. 1996. Improved criteria for classifying hydromorphic soils in South Africa. *South African Journal of Plant and Soil* (13: 3-7)
- Kupka D. 2005. Bacterial reduction of ferric iron and co-respiration of O₂ and Fe³⁺ at various oxygen concentrations. *Acta Montanistica Slovaca* (10: 178-185)
- Kusel K, Dorsch T, Acker G, Stackebrandt E. 1999. Microbial Reduction of Fe(III) in Acidic Sediments: Isolation of *Acidiphilium cryptum* JF-5 Capable of Coupling the Reduction of Fe(III) to the Oxidation of Glucose. *applied and environmental microbiology* (65: 3633–3640)
- Lannbroek HJ. 2009. Methane emission from natural wetlands: interplay between emergent macrophytes and soil microbial processes. A mini-review. *Annal of Botany* (105: 1-14)
- Liu X, Ruecker A, Song B, Conner WH, Chow AT. 2017. Effects of salinity and wet–dry treatments on C and N dynamics in coastal-forested wetland soils: Implications of sea level rise. Clemson University: *Forestry & Environmental Conservation*. (Pg 2-6)
- Mastalerz M, Drobniak A, Hower JC, O’Keefe JMK. 2011. Coal and Peat Fires: A Global Perspective. Volume 1: Coal–Geology and Combustion. (Pg 47-62)
- McCarthy TS, Pretorius K. 2009. Abstracts of the International Mine Water conference. Pretoria, South Africa. (pg 56-64)
- Meowweather. 2017. Witbank rainfall data. [ONLINE]. Available at: <http://www.meowweather.com/history/South%20Africa/na/-25.8666667/29.2333333/Witbank.html>. [Accessed 5 June 2017].

- Metje M, Frenzel P. 2005. Effect of Temperature on Aerobic Ethanol Oxidation and Methanogenesis in Acidic Peat from a Northern Wetland. *Applied and Environmental Microbiology* (71: 8191-8200)
- Mitsch WJ, Gosselink JG .2007. Wetlands, 4th edn. Wiley, New York
- Moore TR, Dalva M. 1993. The influence of temperature and water table position on carbon dioxide and methane emissions from laboratory columns of peatland soils. *Journal of soil science* (44: 651-664)
- Moreno-Mateos D, Power ME, Comín FA, Yockteng R. 2012. Structural and Functional Loss in Restored Wetland Ecosystems. *PLOS Biology* (10(1): e1001247)
- National Water Act, Act 36. 26 August 1998. *Government Gazette*. Vol 398. No. 19182
- Olson L, Ye S, Yu X, Wei M, Krauss KW, Brix H. 2015. Factors influencing CO₂ and CH₄ emissions from coastal wetlands in the Liaohe Delta, Northeast China. *Biogeosciences* (12: 4965-4977)
- Pezeshki SR, DeLaune RD. 2012. Soil Oxidation-Reduction in Wetlands and its Impact on Plant Functioning. *Biology* (1(2): pg 196-221)
- Ponnamperuma FN. 1972. The chemistry of submerged soils. *Advanced Agronomy* (24: 29-96)
- Ramsar Convention on Wetlands. 2013. Its History and Development.
- Reddy KR, D'Angelo EM, Harris WG. 2000. Biogeochemistry of wetlands. *Handbook of soil science*. (pg 89-119)
- Sattazahn B. 2012. Static gas chamber. [ONLINE]. Available at: <http://csereu.engg.ksu.edu/S12/bsattaz/>. [Accessed 16 august 2016]
- Schlesinger WH .1997. An analysis of global change. Academic, Harcourt Brace, San Diego, CA, USA

- Scholz M. 2011. Wetland systems: Stormwater Management Control. *Springer: ISSN 1865-3529*
- Schumacher B. 2002. Methods for the Determination of Total Organic Carbon (TOC) in Soils and Sediments. United States Environmental Protection Agency. *Ecological Risk Assessment Support Center (1282: 4-15)*
- Seitz J, Tong C. 2013. NDIR CO₂ gas detection system. Texas instruments. *SNA207. (Pg1-7)*
- Setia R. Marschner P. Baldock J. Chittleborough D. 2010. Is CO₂ evolution in saline soils affected by an osmotic effect and calcium carbonate?. *Biol. Fertil Soils. (46: 781-792)*
- Sherene T. 2009. Effect of Dissolved Organic Carbon (DOC) on Heavy Metal Mobility in Soils. *Nature Environment and Pollution Technology (8 (4): pg 817-821)*
- Six J, Paustian K, Elliot ET, Combrink C. 2000. Soil Structure and Organic Matter: Distribution of Aggregate-Size Classes and Aggregate-Associated Carbon. *Soil Science Society of America Journal (64: 681–689)*
- Soil Classification Working Group. 2018. Soil Classification. A Natural and anthropogenic system for South Africa. Soil Science Society of South Africa
- Soil Quality. 2011. Respiration. [ONLINE]. Available at: <http://soilquality.org/indicators/respiration.html>. [Accessed 16 August 2016]
- South African National Biodiversity Institute. 2014. Rehabilitation Plan for the Highveld Wetland Project. Prepared by Margaret Lowies, Aurecon South Africa (Pty) Ltd as part of the planning phase for the Working for Wetlands Rehabilitation Programme. SANBI Report No. 109664/8819. *pg 31*
- Sparks DL. 2003. Environmental Soil Chemistry 2nd edition. (*pg 245-255*)

- Sutton T, Dassau O, Sutton M. A Gentle Introduction in GIS: Spatial Analysis (Interpolation). Spatial Planning & Information, Department of Land Affairs, Eastern Cape.
- Unger S, Maguas C, Pereira JS, David T, Werner C. 2010. The influence of precipitation pulses on soil respiration – Assessing the “Birch effect” by stable carbon isotopes. *Soil Biology and Biochemistry* (42(10): 1800-1810)
- Van der Valk AG. 2012. The biology of freshwater wetlands. (pg 20)
- Vepraskas MJ, Christopher BC. 2016. Wetland soils: Genesis, Hydrology, Landscapes, and Classification. *Second edition: (121-124)*
- Vermeulen PD, Usher BH, van Tonder GJ. 2008. Determination of the impact of coal mine water irrigation on groundwater resources. *Water Research Commission: 1507/1/08: 10-11*
- Waddington JM, Rotenberg PA, Warren FJ. 2001. Peat CO₂ production in a natural and cutover peatland: implications for restoration. *Biogeochemistry* (54: 115–130)
- Waring BG, Powers JS. 2016. Unraveling the mechanisms underlying pulse dynamics of soil respiration in tropical dry forests. *Environmental Research Letters* 11: (105005)
- Waters AS, Webster-Brown JG. 2013. Assessing aluminium toxicity in streams affected by acid mine drainage. *Water and Science Technology* (67: 1764-1769)
- Whalen SC. 2005. Biogeochemistry of methane exchange between natural wetlands and the atmosphere. *Environmental Engineering Science* (22: 73–94)
- Xijun L, Ruecker A, Song B, Xing J, Conner WH, Chow HT. 2017. Effects of Salinity and Wet–dry Treatments on C and N Dynamics in Coastal-Forested Wetland Soils: Implications of Sea Level Rise. *Forestry & Environmental Conservation* (9: 3-27)



Zweifel UL .1999. Factors controlling accumulation of labile dissolved organic carbon in the Gulf of Riga. *Estuarine, Coastal and Shelf Science* (48: 357–370)

APPENDIX



Figure A1: Transition between yellow brown apedal B horizon and soft plinthic horizon



Figure A2: Mottling within the soft plinthic horizon



Figure A3: *Schoenoplectus sp.* and *Typha Capensis*

Table A1: Data for Rietvlei, different wetland zones

Sample point	Description	Soil form	Wetland zone
1	<ul style="list-style-type: none"> • B horizon: 10YR 3/4 • No mottles 	Clovelly	Terrestrial
2	<ul style="list-style-type: none"> • High clay • A horizon :5Y 2.5/1, 5% mottles • B horizon >10% mottles 	Westleigh	Seasonal
3	<ul style="list-style-type: none"> • Orthic A horizon, 5Y 2.5/1. 5 % mottles • G horizon: gley1 2.5/N 	Katspruit	seasonal/permanent
4	<ul style="list-style-type: none"> • Orthic A: 10YR 3/4 • Soft plinthic B >10% mottles 	Westleigh	Seasonal
5	<ul style="list-style-type: none"> • Orthic A: 10YR 2/2, 1% mottles • Yellow brown apedal B, 10YR 3/4, 2-5% mottles • Soft plinthic horizon >10% mottles 	Avalon	Temporary
6	<ul style="list-style-type: none"> • Orthic A, 1% mottles • Yellow brown apedal B 	Avalon	Temporary

	10YR 3/4		
7	<ul style="list-style-type: none"> • Orthic A: 10YR 3/4 • Soft plinthic B >10% mottles 	Westleigh	Seasonal
8	<ul style="list-style-type: none"> • Orthic A horizon, 5Y 2.5/1. 5 % mottles • G horizon: gley1 2.5/N 	Katspruit	Permanent
9	<ul style="list-style-type: none"> • Orthic A: 10YR 3/4 • Soft plinthic B >10% mottles 	Westleigh	Seasonal
10	<ul style="list-style-type: none"> • Orthic A • Yellow brown apedal B, 10YR 4/4 • No mottles 	Clovelly	Terrestrial
11	<ul style="list-style-type: none"> • Orthic A, 1% mottles • Yellow brown apedal B 10YR 3/4 	Avalon	Temporary
12	<ul style="list-style-type: none"> • Orthic A, 1% mottles • Yellow brown apedal B 10YR 3/4 	Avalon	Temporary
13	<ul style="list-style-type: none"> • Orthic A horizon, 5Y 2.5/1. 5 % mottles • G horizon: gley1 2.5/N 	Katspruit	Permanent
14	<ul style="list-style-type: none"> • Orthic A: 10YR 3/4 • Soft plinthic B >10% mottles 	Westleigh	Seasonal
15	<ul style="list-style-type: none"> • Orthic A, 1% mottles • Yellow brown apedal B 10YR 3/4 	Avalon	Temporary
16	<ul style="list-style-type: none"> • Orthic A, 3% mottles • Yellow brown apedal B, 10YR 3/4, 2-5% mottles • Soft plinthic >10% mottles 	Avalon	Temporary
17	<ul style="list-style-type: none"> • Orthic A, 5Y 2.5/1 • G horizon: gley 1 2.5/N 	Katspruit	Permanent
18	<ul style="list-style-type: none"> • Orthic A, no mottles • G horizon: gley1 2.5/N 	Katspruit	Permanent
19	<ul style="list-style-type: none"> • Orthic A • Soft plinthic B >10% mottles 	Westleigh	Seasonal
20	<ul style="list-style-type: none"> • Orthic A, 1% mottles • Yellow brown apedal B 10YR 3/4 	Avalon	Temporary

21	<ul style="list-style-type: none"> • Orthic A • Yellow brown apedal B, 10YR 4/4 • No mottles 	Clovelly	Terrestrial
22	<ul style="list-style-type: none"> • Orthic A, 1% mottles • Yellow brown apedal B 10YR 3/4 	Avalon	Temporary
23	<ul style="list-style-type: none"> • Orthic A horizon, 5Y 2.5/1. 5 % mottles • G horizon: gley1 2.5/N 	Katspruit	Permanent
24	<ul style="list-style-type: none"> • Orthic A: 10YR 3/4 • Soft plinthic B >10% mottles 	Westleigh	Seasonal
25	<ul style="list-style-type: none"> • Orthic A, 1% mottles • Yellow brown apedal B 10YR 3/4 	Avalon	Temporary
26	<ul style="list-style-type: none"> • Orthic A • Yellow brown apedal B, 10YR 4/4 • No mottles 	Clovelly	Terrestrial
27	<ul style="list-style-type: none"> • Orthic A, 1% mottles • Yellow brown apedal B 10YR 3/4 	Avalon	Temporary
28	<ul style="list-style-type: none"> • Orthic A: 10YR 3/4 • Soft plinthic B >10% mottles 	Westleigh	Seasonal
29	<ul style="list-style-type: none"> • Orthic A: 10YR 3/4 • Soft plinthic B >10% mottles 	Westleigh	Seasonal
30	<ul style="list-style-type: none"> • Orthic A, 1% mottles • Yellow brown apedal B 10YR 3/4 	Avalon	Temporary
31	<ul style="list-style-type: none"> • Orthic A • Yellow brown apedal B, 10YR 4/4 • No mottles 	Clovelly	Terrestrial
32	<ul style="list-style-type: none"> • Orthic A: 10YR 3/4 • Soft plinthic B >10% mottles 	Westleigh	Seasonal
33	<ul style="list-style-type: none"> • Orthic A horizon, 10YR 2/1. 5 % mottles • G horizon: gley1 2.5/N 	Katspruit	Permanent
34	<ul style="list-style-type: none"> • Orthic A, 1% mottles • Yellow brown apedal B 	Avalon	Temporary

	10YR 3/4		
35	<ul style="list-style-type: none"> Orthic A Yellow brown apedal B, 10YR 4/4 No mottles 	Clovelly	Terrestrial
36	<ul style="list-style-type: none"> Orthic A, no mottles Yellow brown apedal B, no mottles, 10YR 4/4 	Clovelly	Terrestrial
37	<ul style="list-style-type: none"> Orthic A Soft plinthic B >10% mottles 	Westleigh	Seasonal
38	<ul style="list-style-type: none"> Stream 	Katspruit	Permanent
39	<ul style="list-style-type: none"> Orthic A, 10YR 2/1 Soft plinthic >10% mottles 	Westleigh	Seasonal
40	<ul style="list-style-type: none"> Orthic A Yellow brown apedal B, 10YR 4/4 No mottles 	Clovelly	Terrestrial

*Note: pH is a logarithmic scale, so averages must be converted to [H+] first, averaged, then converted back into pH, which is $-\log[H^+]$, which gives the true average.

pH at 25 degrees Celsius for Temporary zone

Sample number	A horizon	B horizon
6	5.17	5.23
11	5.34	5.22
15	5.24	4.92
16	5.17	5.34
34	5.67	6.11
True average	5.28	5.23

pH at 25 degrees Celsius for Seasonal zone

Sample number	A horizon	B horizon
12	5.76	6.18
29	5.82	6.01
33	7.51	7.52
24	7.97	7.84
7	6.83	6.66

True average	6.16	6.42
--------------	------	------

pH at 25 degrees Celsius for Permanent zone

Sample number	A horizon	G horizon
8	6.54	6.83
13	6.09	6.12
18	6.10	5.67
23	5.57	4.93
38	6.09	6.58
True average	5.97	5.52

Electrical Conductivity (EC) at 25 degrees Celsius for Temporary zone

Sample number	A horizon ($\mu\text{s/cm}$)	B horizon ($\mu\text{s/cm}$)
6	124	88.4
11	83	50
15	38.8	70.7
16	76.9	62.9
34	91.7	55.9
Average	82.88	65.58

Electrical Conductivity (EC) at 25 degrees Celsius for Seasonal zone

Sample number	A horizon ($\mu\text{s/cm}$)	B horizon ($\mu\text{s/cm}$)
12	113.9	52.1
29	74.8	45.2
33	276	127
24	226	128
7	105	50.3
Average	159.14	80.52

Electrical Conductivity (EC) at 25 degrees Celsius for Permanent zone

Sample number	A horizon ($\mu\text{s/cm}$)	G horizon ($\mu\text{s/cm}$)
8	119.5	65.2
13	182	50.3
18	142.4	44.7

23	113.4	42.8
38	167	62.6
Average	144.86	53.12

Table A2: Data for grams per cubic meter of carbon dioxide and carbon release from Rietvlei

Sample number	g/m ³ of CO ₂	g/m ³ of Carbon
1	0.923	0.251
2	1.724	0.470
3	2.071	0.565
4	1.431	0.390
5	0.783	0.213
6	1.053	0.287
7	1.737	0.474
8	1.916	0.522
9	1.514	0.413
10	0.845	0.230
11	0.981	0.267
12	1.983	0.541
13	1.607	0.438
14	1.798	0.490
15	1.371	0.374
16	0.670	0.182
17	0.934	0.255
18	1.878	0.512
19	1.867	0.509
20	0.824	0.224
21	0.727	0.198
22	0.995	0.271
23	2.780	0.758
24	2.153	0.587
25	1.335	0.36
26	0.792	0.216
27	0.978	0.267
28	1.429	0.390
29	1.170	0.319
30	0.944	0.257

31	0.689	0.188
32	1.743	0.475
33	2.181	0.5953
34	1.328	0.362
35	0.876	0.239
36	0.782	0.213
37	1.439	0.392
38	1.869	0.510
39	0.678	0.185
40	1.088	0.297
Atmospheric	0.516	0.140

Figure A4: Ideal Gas Law

Example:

- Atmosphere at 351ppm carbon dioxide
- Pressure at 847 hPa
- Temperature at 31.7 degrees Celsius

Ideal Gas law: $PV=nRT$

Where P=pressure, V=volume, n=number of moles, R=gas constant and T=temperature in Kelvin.

- Temperature: 31.7 degrees Celsius equals 304.85 K
- Pressure: 847 hPa equals 84700 Pa
- Mass of 1 mol of carbon dioxide equals 44.01
- Gas constant equals 8.31441
- 351 ppm (volume) $CO_2 = 351 \times 10^{-6} \text{ m}^3 \text{ CO}_2/1\text{m}^3 \text{ air}$

The mass of carbon dioxide per volume therefore becomes:

$$\text{Mass of } CO_2 \text{ in grams} = (44.01)(84700)(351 \times 10^{-6}) / (8.31441)(304.85) = \underline{0.516 \text{ g/m}^3}$$



Figure A5: Visible surface cracks in the vertic horizon



Figure A6: Slickensides in the vertic horizon



Figure A7: Wetland in foreground with Evraz Highveld steel in the background



Figure A8: White effluent being discharged directly into Wetland A



Figure A9: White precipitate (gypsum) from the Zaalklapspruit wetland



Figure A10: Concrete structure within the permanent zone of Wetland B



Figure A11: Gasses escaping through the water once disturbed



Figure A12: Hydrous Ferric oxide precipitates in the surface water downstream from mine

Figure A13: Walkley-Black method for percentage carbon.

- Weigh soil (0.5g for mineral soil and 0.1g for organic soil) into 500ml Erlenmeyer flask
- Work in a fume hood
- Add 10ml 0.167 M $K_2Cr_2O_7$ (98.16g of $K_2Cr_2O_7$ made into a two liter solution made up to the mark with deionised H_2O)
- Add 20ml concentrated H_2SO_4 (95-97%)
- Heat up to 150 degrees celsius for one hour on hot plate to ensure complete oxidation of organic material
- Allow solution to cool for 30 minutes
- Add 150ml deionised H_2O
- Add 10ml concentrated H_2PO_4 (85% Orthophosphoric acid)
- Allow solution to stand for 30 minutes
- Add 1ml carbon indicator ($Ba(C_{12}H_{10}NO_3S)_2$ - Barium diphenylamine sulphonate)
- Titrate with Fe-solution (196 grams of ammonium iron II sulphate mixed with 5ml of H_2SO_4 made into one litre solution with the remaining solution being deionised H_2O) until solution becomes green
- Note the volume of Fe-solution titrated

Example of Walkley-Black calculations after titration:

- Mass of soil: 0.1g
- Blank titration: 18.1ml
- Volume of Fe-solution titrated: 6.7ml

M factor: $(0.167M K_2Cr_2O_7 * 10^6) / 18.1 = 0.55359116$

% carbon: $((18.1-6.7)*0.55359116*0.3)/0.1 = \mathbf{18.932 \% C}$

Table A3: Chemical data for acid mine drainage from undisclosed colliery

DATE_MEAS	EC	FE	MN	PH	B	CL-	MG	NA	AL	CA	SO4	NH4	K	NO3	TDS	PO4	TEMP	F
2016-03-07	468.62	1259.685	58.12	2.58	0.06	2.52	162.38	5.88	178.298	230.82	4218	12.83	6.1476	0	6968	0.67	25.1	0
2016-02-10	473.78	368.4975	103.4	2.54	0.45	3.46	205.9	5.49	333.655	209.56	3697	13.95	8.5807	0.63	4204	0.31	23.1	0.01
2016-01-19	421.08	157.6585	69.3	2.66	0.08	2.8	175.85	5.09	175.379	237.16	3650	10.22	10.4187	0.67	5352	0.3	23.8	0.02
2015-12-03	479.7	300.3	106.79	2.64	0.11	3.16	208.68	6.61	127.682	261.77	4210	13.69	8.4351	0.2	6718	0.3	23.5	0.01
2015-11-04	478.02	277.0725	102.4	2.66	0.1	2.78	209.59	5.3	193.2695	347.76	5272	10.43	12.1766	0.09	6360	0.43	24.2	0.01
2015-10-13	540.14	208.469	99.25	2.58	0.07	2.47	216.04	5.27	225.41	336.44	4520	13.55	10.274	0.86	7006	0.3	27	0.02
2015-09-07	443.53	196.1308	94.5	2.62	0	2.7	189.37	4.89	171.7838	302.71	4164	11.13	13.0296	0.29	5291	0.23	24.3	0.03
2015-08-12	421.85	332.9125	84.89	2.78	0.15	3.49	183.99	5.42	180.7675	353.88	4897	15.41	11.5611	0	5856	0.67	22.8	0.01
2015-07-06	452.05	102.207	102.21	2.75	0.15	3.71	219.9	6.77	261.354	297.34	4647	11.48	10.6712	0.13	6697	1.38	21.1	0
2015-06-03	393.23	225.3155	80.7	2.68	0.1	4.25	176.76	7.38	141.6413	313.87	4263	13.35	15.1498	0	4985	0.61	21	0.01
2015-05-07	427.57	285.372	60.08	2.65	0.16	8.84	207.68	6.43	200.032	258.7	4323	17.76	10.0712	0.22	6433	0.58	23.9	0.01
2015-04-07	416.84	256.713	50.38	2.51	0.17	3.86	106.21	5.91	222.2025	179.85	4140	26.57	9.6744	1.14	5281	0.27	24.8	0.01
2015-03-02	507.18	286.2513	56.1	2.52	0.16	4.45	122.07	8.16	184.5288	266.63	4434	37.51	10.5655	0.18	5782	0.63	26.6	0.01
2015-02-03	513.21	255.302	76.06	2.48	0.14	3.39	144.79	6.89	250.6874	244.23	4383	17.84	10.6105	0.08	6386	0.19	25.8	0.01
2015-01-06	462.21	207.848	44.35	2.42	0.11	5.56	85.68	4.71	227.702	149.64	3940	31.1	8.8842	0.36	5401	0.2	27.7	0.01
2014-12-03	429.32	222.954	67.6	2.59	0.12	7.25	155.7	6.34	134.5176	244.89	3170	16.35	13.9987	1.18	4250	0	24.8	0.01
2014-11-05	127.87	451.394	55.92	6.32	0.25	6.68	123.59	7.75	199.5142	267.44	3412	40.95	14.4027	0.66	6465	0.41	25	0.01
2014-10-01	442.24	402.525	53.91	2.52	0	4.36	108.53	6.97	242.641	234.23	4735	45.41	9.6578	0.93	5839	0	22.4	0
2014-08-06	495.16	423.098	73.9	2.69	0.31	3.95	174.47	8.53	235.208	343.78	4910	34.69	12.3192	0.1	6988	0.36	23.1	0.01
2014-07-02	469.19	552.2488	64.09	2.64	0.32	5.11	166.07	7.88	260.6263	268.48	5484	4.81	11.5136	0.09	7105	0.4	18.6	0.01
2014-06-17	558.31	447.45	86.2	2.42	0.25	4.25	188.12	11.03	245.712	320.44	4988	30.65	11.4166	0	7033	1.26	20.7	0.01
2014-05-19	501.2	367.19	92.56	2.39	0.21	3.88	181.34	10.45	235.962	327.09	4711	18.3	12.7181	0	6131	0.45	19.7	0.01
2014-03-17	403.47	196.712	74.32	2.55	0.09	4.84	137.76	15.5	175.297	206.08	2521	8.6	12.2466	0.39	3565	0.24	22.3	0.01
2013-11-06	498.64	280	90	2.31	0.07	3.4	129.72	12.38	187	212.63	3393	10.07	8.13	0.17	5626	0.3	24.8	0
2013-10-14	505.98	337.934	0.34	2.53	0.13	2.69	188.23	19.12	189.5954	254.03	4250	13.85	55.024	0.11	4250	1	22	0.01
2013-09-16	450.67	276.504	65.32	2.42	0.12	3.78	115.9	10.41	201.031	212.52	3890	16.37	7.9513	0	5581	0.38	22.5	0.01
2013-08-07	352.66	187.257	38.58	2.38	0.09	2.62	70.1	8.11	157.843	118.34	2816.5	13.18	5.733	0.13	4477	0	22.5	0.02
2013-07-15	401.38	298.339	66.55	2.53	0.11	4.7	88.91	14.69	254.7528	169.24	3690	16.81	4.4992	0.29	5703	0.66	20	0.02
2013-06-05	357.85	288.9655	99	2.58	0.1	2.19	122.82	15.46	178.646	189.22	3800	13.81	4.9549	0.14	5290	0.49	18.7	0.01
2013-05-13	426.76	415.235	112.11	2.43	0.12	2.81	138.83	16.45	210.993	230.64	3530	15.44	5.0965	0.28	5998	1	22.6	0.01
2013-04-24	377.21	146.8045	97.96	2.34	0.05	3.8	142.24	23.44	112.491	327.84	3570	13.8	5.4666	0.31	4757	0.15	21.8	0.02
2013-03-27	435.44	227.599	107.87	2.38	0.09	2.43	131.34	12.63	183.902	214.47	2920	13.59	5.0994	-0.13	5465	0.43	21.4	0.02
2013-02-11	418.12	407.7365	162.59	2.47	0.11	3.19	96.27	13.79	186.447	119.59	2690	21.54	5.5226	1	5279	0.45	24.88	0.02
2013-01-14	402.52	266.427	160.49	2.57	0.1	3.36	179.4	18.56	187.343	290.13	2610	13.07	5.4667	0.05	6350	0.26	22.65	0.1
2012-12-10	404.51	290.4105	82.61	2.5	0.1	4.4	133.18	15.42	193.222	215.1	3490	17.17	3.7563	-0.66	6570	0.53	24.29	0.03
2012-11-13	391.34	321.862	63.36	2.45	0.19	5.44	111.29	14.02	215.238	186.18	3200	20.45	3.0886	0.26	6011	0.44	21.67	0.03
2012-10-09	414.01	306.3613	100.04	2.53	0.25	2.95	153.13	11.75	192.3335	252.92	2640	16.54	4.6228	0.14	4275	1.2	24.32	0.03
2012-09-11	450.28	261.06	70.42	2.5	0	3	148.13	9.73	159.647	223.55	2670	21.2	4.4674	0.21	4247	0.7	26.68	0.04
2012-08-07	429.85	234.411	84.92	2.45	0.11	2.46	164.9	11.88	175.039	254.61	2800	20.61	4.4004	-0.19	5515	0.42	23.43	0.04
2012-07-09	333.62	422.8605	80.44	2.62	0.19	3.14	118.48	14.23	217.059	203.37	3290	19.6	4.5976	0.03	4227	0.34	21.55	0
2012-06-11	306.6	184.4643	52.82	2.41	0.14	2.99	95.66	11.44	195.9495	162.98	2700	16.79	4.7178	0.04	4752	0.42	21.95	0.02
2012-05-08	320.06	166.0508	41.99	2.56	0.18	2.92	84.64	12.14	151.4125	144.08	2130	16.51	4.1173	0.9	4046	0.35	21.41	0.01
2012-04-11	311.18	434.5458	37.62	2.4	0.27	3.42	77.82	12.35	177.4505	140.58	2890	14.65	4.2411	4.6	5115	0.62	23.89	0
2012-03-19	275.43	180.833	45.61	2.46	0.15	4.69	93.09	11.32	116.7715	147.88	1570	15.6	4.4193	0.08	3726	0.7	20.77	1.14
2012-02-09	292.69	252.2845	71.33	2.7	0.14	1.53	133.27	9.7	162.709	201.03	2190	22.79	3.8339	0.69	5121	0.74	21.5	0.01
2012-01-09	387.68	309.4308	75.63	2.76		2.32	195.17	15.71	135.2955	288.17	2765		5.0536		5962		24.34	
2011-12-08	327.26	289.3595	71.68	2.54		4.87	116.21	13.91	151.6515	194.11	2045		5.5489		4522		23.66	
2011-11-09	253.18	150.0683	36.85	2.87		2.52	79.69	9.57	101.033	127.44	2875		3.168		2963		21.9	
2011-10-10	366.46	355.994	71.58	2.75		2.41	131.93	11.97	144.703	229.93	2525		5.8643		3377		19.96	
2011-08-10	431.09	349.4027	97.72	2.51		3.92	234.59	14.69	161.5605	296.36	3335		7.721		6481		18.3	
2011-07-06	465.55	615.3687	95.16	2.69		3.1	218.15	12.97	254.3935	270.38	5005		5.8875		8071		18	
2011-05-12	446.52	326.476	136.91	2.66		4.26	344.85	14.26	106.913	354.71	2985		10.1152		6841		23.56	
2011-04-14	538.72	732.617	87.47	2.55		3.52	202.81	14.28	301.75	267.81	3840		5.02		9033		22.38	
2011-03-09	442.05	346.3195	82.47	2.4		3.4	165.23	17.9	201.585	239.55	4080		3.14		6461		23.2	
2011-02-10	339.04	175.2695	48.22	2.54		2.63	94.76	15.9	136.89	241.37	1670		3.075		4222		23.19	
2010-10-11	240.21	140.28	37.48	2.65		3.55	77.48	8.46	117.27	130.15	2890		3.08		2838		21.47	
2010-08-12	137.73	99.6633	17.39	3.01		2.06	40.45	4.18	36.0602	51.37	770.695		2.6236		1279		22.7	
2010-07-08	216.65	133.022	10.88	4.1		6.47	36.9	10.36	85.2777	105.01	1067		3.2193		1350		20.52	
2010-05-18	290.2	215.947	35.28	2.79		2.85	80.09	17.66	120.5769	237.34	2245		2.8798		3754		21.5	
2010-04-08	221.95	165.3448	32.4	2.74		2.4	71.84	13.54	68.0602	132.89	1352.35		4.0718		2479		22.73	
2010-03-01	390.06	410.19	46.28	2.63		3.45	96.14	17.23	176.06	159	2865		3.97		5312		22.8	
2010-01-04	0.1	251.914	53.38	4.7		3.93	119.6	15.03	81.2428	147.51	1440.9		5.7234		3271		23.63	
2009-06-23	324.52	492.8455	27.34	2.67		31.07	65.47	34.7	162.2635	143.01	7100		5.0742		4426		22.54	
2008-12-05	928.96	1657.83	35.03	2.06		49.78	62.7	48.54										

Figure A14. Synthetic acid mine drainage calculations

Only the major ions were considered when making the synthetic acid mine drainage. The chemical compounds that were used are listed below.

Chemicals used for synthetic acid mine water:

Element or ion	Chemicals used
Fe (II)	FeSO ₄ .7H ₂ O
Mn (II)	MnSO ₄ .4H ₂ O
Ca (II)	CaCl ₂ .2H ₂ O
Mg (II)	MgSO ₄ .7H ₂ O
Na (I)	Na ₂ SO ₄
Al (III)	Al ₂ (SO ₄) ₃
Ca (II)	CaSO ₄ .2H ₂ O
SO ₄ ²⁻	(NH ₄) ₂ SO ₄

A 1000 milliliter volumetric flask was used to make up the synthetic acid mine drainage.

The volumetric flask contained 800 milliliters of deionised water in it prior to adding the compounds, this allowed each added compound to dissolve. Once all the ions have been calculated and all the correct masses have been added to the 1000ml volumetric flask, The desired pH needed to be created. This was done by adding 0.5 M sulphuric acid. One milliliter (1ml) of sulphuric acid was added to the volumetric flask, and deionised water was used to bring the synthetic AMD to the 1000 milliliter mark. The amount of sulphuric acid added was based on the $C_1V_1=C_2V_2$ equation. A pH of 3.30 was used (an approximate proton concentration of $10^{-3.3}$ M), which translates to a logarithmic value of 0.0005 M concentration of H₂SO₄. The rearranged equation thus becomes $1000\text{ml} \times 0.0005 / 0.5 = 1\text{ml}$. The pH of 3.30 was expected to drop as the salts were added to the solution. The final pH of the synthetic AMD was 2.00, whilst the

electrical conductivity (EC) was 4.063 mS/cm. The synthetic acid mine drainage was purged with Argon gas (Ar) for eight minutes. The reason for purging with Ar was to slow down the oxidation of ferrous iron to ferric iron, as well as to isolate the acidity effect of the AMD. An ICP-OES analysis was done after mixing together the synthetic AMD solution in order to analyse the solution. The full calculations for all the ions can be seen below:

Final answers rounded to 3 decimals.

Ion: Fe

- Desired Fe concentration: 288.965 mg/l, or 0.288965 g/l
- Compound used: FeSO_4
- 2 Fe present in compound formula, therefore it becomes $0.288965/2 = 0.14445$ g/l.
- 0.14445 g/l divided by atomic mass of Fe (55.845) = 0.002587
- 0.002587 multiplied by total molar mass of FeSO_4 (151,908) = 0.39g
- Therefore 0.39 grams of FeSO_4 must be added to a 1000ml volumetric flask to make up a concentration of 288.965 mg/l.

Ion: Mn

- Desired Mn concentration: 99 mg/l, or 0.099 g/l
- Compound used: $\text{MnSO}_4 \cdot 4\text{H}_2\text{O}$
- 0.099 g/l divided by atomic mass of Mn (54.938) = 0.0018
- 0.0018 multiplied by total molar mass of $\text{MnSO}_4 \cdot 4\text{H}_2\text{O}$ (223.0618) = 0.401
- Therefore 0.401 grams of $\text{MnSO}_4 \cdot 4\text{H}_2\text{O}$ must be added to a 1000ml volumetric flask to make up a concentration of 99 mg/l.

Ion: Cl^-

- Desired Cl^- concentration: 2.19 mg/l, or 0.00219 g/l
- Compound used: $\text{CaCl}_2 \cdot 2\text{H}_2\text{O}$
- 2 Cl^- present in compound formula, therefore it becomes $0.00219/2 = 0.001095$ g/l.

- 0.001095 g/l divided by atomic mass of Cl (35.453) = 0.0000308
- 0.0000308 multiplied by total molar mass of $\text{CaCl}_2 \cdot 2\text{H}_2\text{O}$ (147.0146) = 0.00454g
- Therefore 0.005 grams of $\text{CaCl}_2 \cdot 2\text{H}_2\text{O}$ must be added to a 1000ml volumetric flask to make up a concentration of 2.19 mg/l .

Ion: Mg

- Desired Mg concentration: 122.82 mg/l , or 0.12282 g/l
- Compound used: $\text{MgSO}_4 \cdot 7\text{H}_2\text{O}$
- 0.12282 g/l divided by atomic mass of Mg (24.305) = 0.005053
- 0.005053 multiplied by total molar mass of $\text{MgSO}_4 \cdot 7\text{H}_2\text{O}$ (246.4746) = 1.245g
- Therefore 1.245 grams of $\text{MgSO}_4 \cdot 7\text{H}_2\text{O}$ must be added to a 1000ml volumetric flask to make up a concentration of 122.82 mg/l .

Ion: Na

- Desired Na concentration: 15.46 mg/l , or 0.01546 g/l
- Compound used: Na_2SO_4
- 2 Na present in compound formula, therefore it becomes $0.01546/2 = 0.00773\text{g/l}$.
- 0.00773 g/l divided by atomic mass of Na (22.989) = 0.000336
- 0.000336 multiplied by total molar mass of Na_2SO_4 (142.039) = 0.0477g
- Therefore 0.048 grams of Na_2SO_4 must be added to a 1000ml volumetric flask to make up a concentration of 15.46 mg/l .

Ion: Al

- Desired Al concentration: 178.646 mg/l , or 0.178646 g/l
- Compound used: $\text{Al}_2(\text{SO}_4)_3 \cdot 18\text{H}_2\text{O}$
- 2 Al present in compound formula, therefore it becomes $0.178646/2 = 0.0893 \text{ g/l}$.
- 0.0893 g/l divided by atomic mass of Al (26.981) = 0.00331
- 0.00331 multiplied by total molar mass of $\text{Al}_2(\text{SO}_4)_3 \cdot 18\text{H}_2\text{O}$ (666.4259) = 2.2056g
- Therefore 2.206 grams of $\text{Al}_2(\text{SO}_4)_3 \cdot 18\text{H}_2\text{O}$ must be added to a 1000ml volumetric flask to make up a concentration of 178.646 mg/l .

Ion: Ca

- Desired Ca concentration: 189.22 mg/l, or 0.18922 g/l
- Compound used: $\text{CaSO}_4 \cdot 2\text{H}_2\text{O}$
- 0.18922 g/l divided by atomic mass of Ca (40.078) = 0.00472g
- 0.00472 multiplied by total molar mass of $\text{CaSO}_4 \cdot 2\text{H}_2\text{O}$ (172.1712) = 0.813g
- Therefore 0.813 grams of $\text{CaSO}_4 \cdot 2\text{H}_2\text{O}$ must be added to a 1000ml volumetric flask to make up a concentration of 189.22 mg/l.

Ion: NH_4

- Desired NH_4 concentration: 13.81 mg/l, or 0.01381 g/l
- Compound used: $(\text{NH}_4)_2\text{SO}_4$
- 2 NH_4 present in compound formula, therefore it becomes $0.01381/2 = 0.006905$ g/l.
- 0.006905 g/l divided by molar mass of NH_4 (18.009) = 0.000383
- 0.000383 multiplied by total molar mass of $(\text{NH}_4)_2\text{SO}_4$ (132.138) = 0.0507g
- Therefore 0.051 grams of $(\text{NH}_4)_2\text{SO}_4$ must be added to a 1000ml volumetric flask to make up a concentration of 13.81 mg/l.

Ion: K

- Desired K concentration: 4.9549 mg/l, or 0.0049549 g/l
- Compound used: K_2SO_4
- 2 K present in compound formula, therefore it becomes $0.0049549/2 = 0.002477$ g/l.
- 0.002477 g/l divided by molar mass of K (39.0983) = 0.00006336
- 0.00006336 multiplied by total molar mass of K_2SO_4 (174.2576) = 0.011g
- Therefore 0.011 grams of K_2SO_4 must be added to a 1000ml volumetric flask to make up a concentration of 4.9549 mg/l.

Figure A15: Example of the results from the datalogger software



Table A4: Field data for Chapter 2

Field data for Wetland A

Sample number	CO ₂ release	pH	Redox	EC
1	796	6.2	207	1454
2	668	6.34	178	3289
3	899	5.92	105	3860
4	698	5.47	156	3178
5	590	6.64	316	1034
6	540	6.26	284	1543
7	792	5.72	163	3082
8	728	5.38	112	4238
9	613	6.08	159	2329
10	944	6.89	193	1342

11	492	6.41	201	1402
12	618	5.98	185	2623
13	1204	5.01	127	4936
14	548	5.8	139	3435
15	461	6.76	302	1987
16	796	6.95	286	1023
17	799	5.78	204	1936
18	929	5.31	118	3930
19	451	5.63	141	2855
20	473	6.05	199	2065

Field data for Wetland B

Sample number	CO ₂ (ppm)	pH	Redox (mV)	EC (µs/cm)
1	834	6.76	204	702
2	2589	6.42	103	1304
3	827	5.8	-88	2386
4	2231	6.28	-42	2108
5	943	6.22	-67	1868
6	995	6.13	60	593
7	474	6.06	94	987
8	490	5.73	-20	2321
9	952	5.98	-168	1504
10	1710	7.1	21	1007
11	1813	6.82	82	926
12	1632	6.39	109	963
13	1850	6.02	-139	1736
14	584	6.45	-28	1165
15	1037	6.91	3	1342

16	984	5.75	-20	2827
17	684	6.17	36	1443
18	1294	5.48	-37	2001
19	1439	5.94	-76	1332
20	974	6.94	17	863

Field data for Wetland C

Sample number	CO₂ (ppm)	pH	Redox (mV)	EC (µs/cm)
1	1428	6.78	-120	206
2	1293	6.84	-145	345
3	1486	6.82	-273	408
4	646	6.32	-243	406
5	760	6.34	-174	412
6	683	6.86	-184	404
7	567	6.13	-326	407
8	1235	6.42	-256	421
9	1410	6.66	-147	339
10	1637	6.98	-179	187
11	2350	6.89	-23	97
12	3048	6.49	-69	401
13	1194	6.87	-129	403
14	580	6.45	-204	405
15	673	6.98	-137	414
16	1032	6.87	-103	410
17	770	6.56	-172	400
18	1080	6.47	-164	409
19	1373	6.58	-92	327
20	1278	6.42	-14	89